

Master Thesis
TVVR 21/5003

Effectiveness of Barrier Well by Pumping Ratio Control for Saltwater Intrusion: Lab- Scale Experiments and Numerical Modeling

Shinichi Ozaki



Division of Water Resources Engineering
Department of Building and Environmental Technology
Lund University

Effectiveness of Barrier Well by Pumping Ratio Control for Saltwater Intrusion: Lab- Scale Experiments and Numerical Modeling

By:
Shinichi Ozaki

Master Thesis

Division of Water Resources Engineering
Department of Building & Environmental Technology
Lund University
Box 118
221 00 Lund, Sweden

Water Resources Engineering

TVVR-21/5003

ISSN 1101-9824

Lund 2021

www.tvrl.th.se

Master Thesis
Division of Water Resources Engineering
Department of Building & Environmental Technology
Lund University

English title: Effectiveness of Barrier Well by Pumping Ratio Control
for Saltwater Intrusion: Lab-Scale Experiments and
Numerical Modelling
Author(s): Shinichi Ozaki
Supervisor: Ronny Berndtsson
Examiner: Magnus Persson
Language: English
Year: 2021
Keywords: Saltwater intrusion; Barrier well; Pumping ratio control;
Production well; Salinity-affected coastal aquifer;
Critical groundwater pumping ratio

Acknowledgments

This paper is a product of my academic experiences and lessons throughout my master course at the Department of Urban and Environmental Engineering, Faculty of Engineering, Kyushu University and the Division of Water Resources, Lund University. The successful completion of this dissertation would not have happened without the kind support of many individuals who deserve to be acknowledged and recognized for their invaluable help.

I am deeply grateful to my supervisor Associate Professor Yoshinari Hiroshiro for giving me a significant support and plenty of advice. I got a lot of knowledge about groundwater from him and could not have finished this research without his guidance.

From Lund University, my supervisor Professor Ronny Berndtsson helped me a lot about my master thesis. He gave me many advices for this research and academic writing in English. He cared about me even after I came back to Japan. I really appreciate his help.

I am also grateful to my examiner Professor Magnus Larson for giving me a grateful support for my master thesis. Without his support, I could not finish my master thesis.

Keisuke Konishi and Edangodage Duminda Pradeep Perera gave me invaluable advice about solute transport model. Without their help, the numerical model could not be completed.

I would like to express my sincere gratitude to Yuya Fujita and Christel Abi Aki for lab-scale experiments. With their insights about experimental results, the numerical model was developed.

I would also thank Tatsuya Nagino for giving me grateful idea about a numerical model. His help developed the model and my master thesis.

Finally, I would like to appreciate my family and friends for helping everything in Kyushu University and Lund University.

Abstract

Saltwater intrusion is the most challenging problem in coastal regions. To prevent saltwater intrusion, saltwater pumping from a barrier well is widely applied, which is a direct abstraction of intruded saltwater from a coastal aquifer. Owing to its easy installation, many studies have been carried out. However, quantitative relationships between barrier and inland production well have not been revealed. Therefore, in this study, basic lab-scale experiments were conducted to examine the effectiveness of a barrier well on the possible pumping amount of a production well. In the lab-scale experiments, pumping ratio between barrier and production wells was changed from 0.9 to 2.6. As a result, the critical pumping ratio of 1.9 was obtained. Moreover, a two-dimensional numerical model was created to analyze the experimental results. As a result of simulation, the barrier well extracted highly concentrated saltwater when the pumping ratio was less than the critical ratio, which had a large effect to prevent saltwater intrusion. Therefore, it is concluded that there is a critical pumping ratio between barrier and production well. Moreover, barrier well can prevent saltwater intrusion by extracting highly concentrated saltwater as long as the pumping ratio is kept less than the critical ratio.

Table of Contents

| | |
|---|----|
| 1. Background | 1 |
| 1.1. Saltwater intrusion..... | 1 |
| 1.2. Objectives..... | 4 |
| 2. Saltwater Intrusion | 7 |
| 2.1 Saltwater intrusion..... | 7 |
| 2.2 Effect of external factors (excessive pumping and global warming) | 8 |
| 2.3 Countermeasures for saltwater intrusion | 8 |
| 2.3.1. Conventional methods | 8 |
| 2.3.2. Physical barrier | 9 |
| 2.3.3. Hydraulic barrier..... | 11 |
| 2.4 Previous studies of saltwater pumping | 14 |
| 3. Laboratory experiments..... | 17 |
| 3.1 Experimental device | 17 |
| 3.2 Experimental materials | 19 |
| 3.2.1 Freshwater density | 19 |
| 3.2.2 Saltwater density..... | 19 |
| 3.3 Hydrological parameters | 21 |
| 3.3.1 Estimation of hydraulic conductivity..... | 21 |
| 3.4 Experimental process..... | 22 |
| 3.5 Experimental condition | 24 |
| 4. Results of laboratory experiments..... | 27 |
| 4.1. Step 1: Saltwater wedge formation..... | 27 |
| 4.2. Step 2: Water intake from barrier well (well A) | 29 |
| 4.3. Step 3: Water intake from barrier well and production well (well A&B)..... | 32 |
| 4.4. Step 4: Turning off well B and retreat process of saltwater..... | 35 |
| 4.5. Step 5: Retreat process of saltwater intrusion without pumping | 37 |
| 5. Methodology | 41 |
| 5.1. Analysis conditions..... | 41 |

| | |
|--|----|
| 5.2. Conceptual model | 41 |
| 5.3. Mathematical model | 41 |
| 5.3.1. Groundwater flow equation | 42 |
| 5.3.2. Two-dimensional solute transport equation for advection and dispersion..... | 46 |
| 5.3.3 Mathematical solution | 48 |
| 5.3.4. Stability of calculation..... | 55 |
| 5.4 Numerical model | 55 |
| 6. Results and discussion..... | 59 |
| 6.1. Model conditions | 59 |
| 6.2. Sensitivity analysis | 59 |
| 6.3. Results of step 1..... | 60 |
| 6.4. Results of step 2..... | 62 |
| 6.5. Results of step 3..... | 63 |
| 6.6. Results of step 4..... | 66 |
| 6.7. Results of step 5..... | 67 |
| 6.8. Discussion..... | 67 |
| 7. Conclusions | 73 |
| References | 75 |
| Appendix | 71 |

1. Background

1.1. Saltwater intrusion

Groundwater is the most important freshwater resource in the world. Most of the water on the earth are occupied by seawater, which exceeds 97% of total water volume (Beth et al., 2016). In other words, only 3% of water on the earth are stored on land areas as freshwater. In addition, more than 75% of freshwater are stored as ice caps and glaciers, which is not usually available as freshwater (Fetter, 2011). Thus, only a few percentages of water on the earth are available to human activities as freshwater. Within this small percentage, groundwater plays a primary role as the largest freshwater resource. Moreover, groundwater has many beneficial characteristics to human activities. Generally, the temperature of groundwater is stable through the whole year and its quality is relatively high comparing to surface water. In addition, the access to groundwater is commonly free, which means that, if there is an extraction well, water can be pumped and supplied to human activities freely. Even when the water supply system is broken in a disaster situation, groundwater can be used for humans. Thanks to these beneficial characteristics, groundwater has been used for various human activities in terms of drinking, industrial and agricultural purposes.

However, groundwater has limitations for human activities in some cases. One problem is the distribution of groundwater in the global and local perspectives. The distribution of groundwater is varying depending on region, leading uneven access to potable water around the world or even in a local region. In arid and semi-arid coastal areas, the access to freshwater is especially of primary concern for human activities due to lack of surface water and rainfall. Another problem is a depletion of groundwater. In recent years, a population explosion has occurred, which is related to the increasing demand for freshwater. Although the development of pumping technologies enables to supply a certain amount of groundwater to meet the increasing population, this leads to excessive pumping, followed by rapid depletion of groundwater resources. In arid and semi-arid regions, the amount of pumped groundwater is larger than the natural recharge, thus, the impact of excessive pumping is significant. Decrease of groundwater induces various environmental problems. Reduction of groundwater level leads to less interaction between groundwater and surface water, following the reduction of water in streams and lakes. Moreover, there may be a large risk of land subsidence due to the loss of support of groundwater in the soil. Furthermore, in coastal regions, saltwater intrusion is one of the most severe problems caused by the depletion of groundwater, which induces salinization of the coastal aquifer and deteriorates the water quality in the coastal regions. Saltwater intrusion has significant impacts on groundwater related to human lives around the coastal regions.

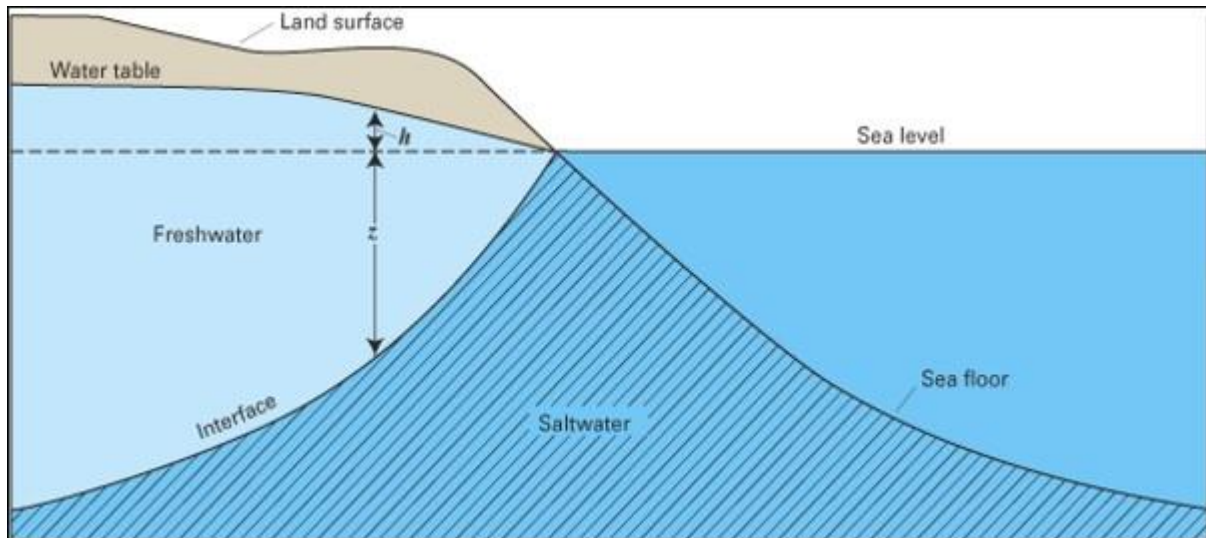


Figure 1.1. Simplified illustration of salt-freshwater interface in the coastal aquifer (Barlow, 2003)

Saltwater intrusion is a lateral encroachment of seawater towards the coastal aquifers caused by the density difference between salt and freshwater. In the coastal aquifer, the denser saltwater is underlying the freshwater and the interface between salt and freshwater is formed as shown in Figure 1.1. Under natural conditions, the seaward flow of freshwater prevents saltwater movement towards the inland and the salt-fresh water interface is in a steady state. However, saltwater intrusion will advance further towards the inland once the equilibrium of salt and freshwater interface is disturbed owing to several factors including groundwater depletion caused by excessive pumping and the rise of seawater level. As saltwater intrusion further advances towards the inland, groundwater and intruded saltwater in the coastal aquifer will be mixed and salinization of groundwater will occur, which highly impacts on the groundwater use. Normally, groundwater is extracted from wells, thus salinization of pumping wells is a critical problem to human activities in coastal regions.

Many coastal areas have suffered from saltwater intrusion. Figure 1.2 shows the distribution of saltwater intrusion areas and global population density (Costall et al., 2018). As shown in the figure, saltwater intrusion has been reported in many regions along the coast, which are associated with high population density regions. It is considered that the growing population is leading to increasing demand of potable water, which induces an excessive pumping following a lack of groundwater resources and then advances the saltwater intrusion further into the inland.

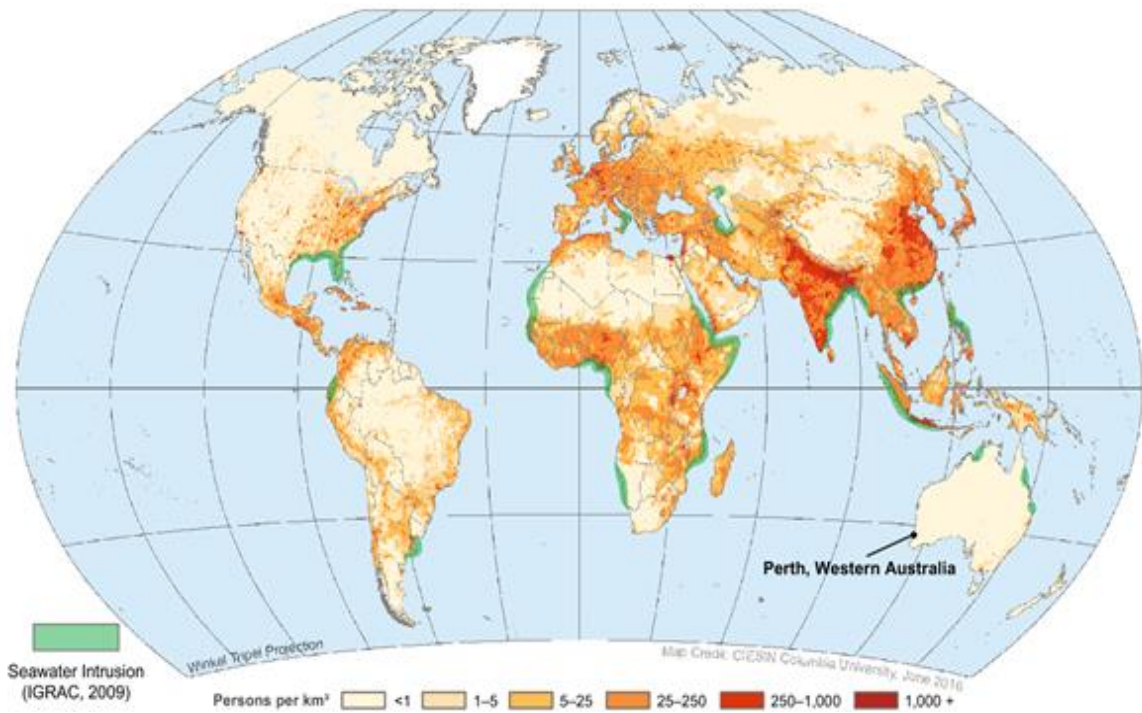


Figure 1.2. Distribution of global population density and seawater intrusion regions (Costall et al., 2018)

In addition, global warming in recent years links to the rise of seawater level, which advances saltwater intrusion further towards the inland. As predicted by the IPCC's fifth assessment report (IPCC, 2013), sea level will rise by an 82 cm between 2006 and 2100 in the worst scenario (Figure 1.3). This will lead to a rise in the level of salt-freshwater interface, which will advance saltwater intrusion further towards the inland.

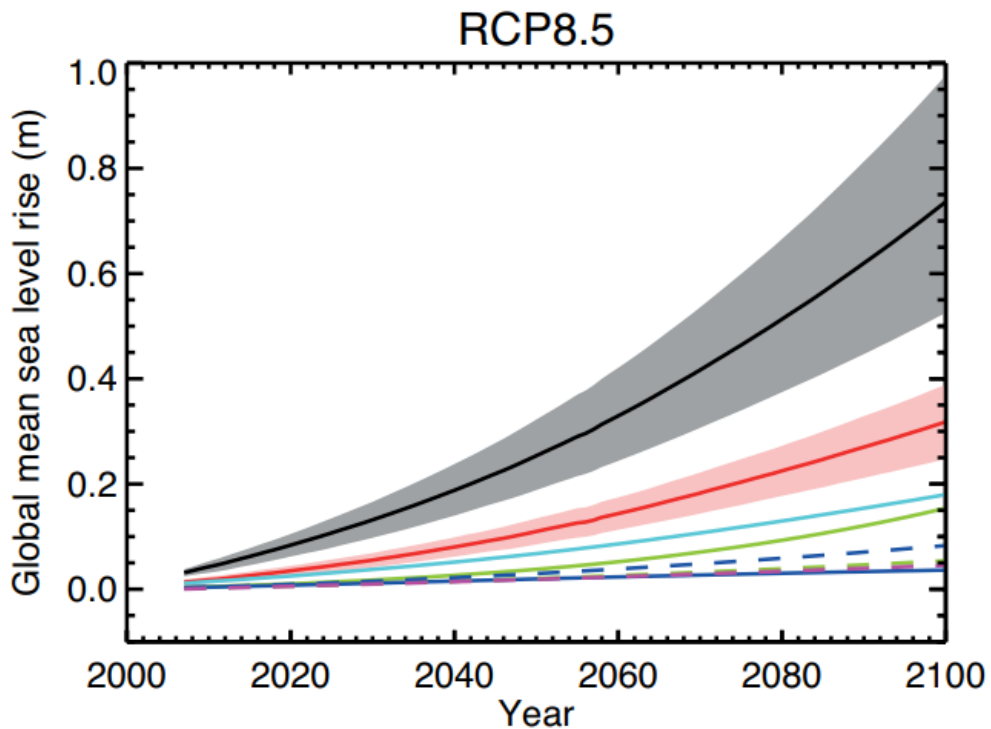


Figure 1.3. Expected global mean sea level rise in the scenario of RCP8.5 (IPCC, 2013)

To prevent saltwater intrusion, various countermeasures have been developed. Hussain et al. (2019) categorized these countermeasures into three different groups: conventional methods, physical barriers, and hydraulic barriers. Among these countermeasures, the hydraulic barrier is the most popular method, in particular saltwater pumping is applied widely in coastal regions. In this method, brackish or saline water is continuously pumped through barrier wells located near the coast as shown in Figure 1.4. The extracted water can be directly discharged into the sea or used as a water source for desalination plants. In addition to utilizing existing wells, this method is widely applicable to coastal aquifers, even in urban areas where the land is restricted. Owing to these advantages, saltwater pumping has been studied and the effectiveness of this method to prevent or retreat saltwater intrusion has been confirmed.

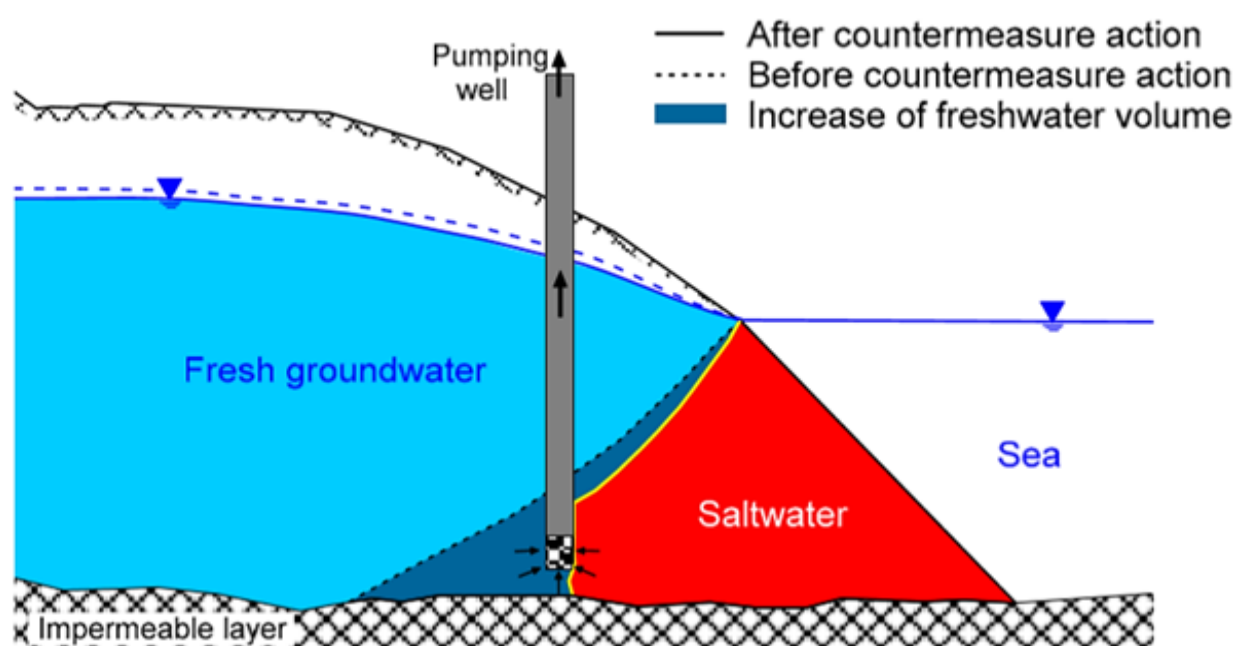


Figure 1.4. Conceptual image of saltwater pumping (Hussain et al., 2019)

1.2. Objectives

As mentioned above, saltwater pumping is considered as an effective method against saltwater intrusion in coastal regions. Many studies have been carried out and the effect of the barrier well on saltwater intrusion has been well investigated mainly by numerical analysis using hypothetical models. However, most of them have focused only on the behavior of saltwater intrusion, and few studies have investigated the effect of the barrier well on the pumping amount from the inland production well. Therefore, quantitative relationships between the barrier well and the production well have not been revealed. When using a barrier well in a coastal area, it is important to study the effectiveness of the barrier well against the possible pumping amount of freshwater from the inland production well. It is considered that if the effectiveness of the barrier well is clarified, saltwater intrusion may become controllable by water ratio manipulation between the barrier and the production well, which can be implemented in any salinized coastal area with multiple wells to solve salinization problems. Therefore, a fundamental study that

considers the effectiveness of the barrier well in relation to possible water intake from production wells is necessary. In this study, a basic lab-scale experiment was conducted to examine the effectiveness of saltwater pumping by a barrier well on the possible freshwater intake from an inland production well. Furthermore, a two-dimensional numerical model based on the advection dispersion equation was created to analyze the results of the lab-scale experiment.

2. Saltwater Intrusion

This chapter explains the fundamental theory of saltwater intrusion and the effect of external factors on saltwater intrusion. Then, solutions for saltwater intrusion are categorized into three types and described. Finally, previous studies on saltwater pumping are described and some problems of these previous studies are discussed. The objective of this chapter is to describe basic concepts for saltwater intrusion and discuss previous studies.

2.1 Saltwater intrusion

Saltwater intrusion is a major problem that degrades the groundwater quality in coastal regions, where the need for potable water is relatively high due to the lack of other freshwater resources. Groundwater salinization, which is caused by saltwater intrusion, is categorized as a special type of pollution that degrades groundwater quality since groundwater will become inadequate for human uses due to mixing of only a few percentages of saltwater with groundwater (Abd-Elhamid et al., 2015). Moreover, salinization of pumping wells is a severe problem for human activities in coastal regions, especially where groundwater is used for drinking water or agriculture by using abstraction wells. In arid and semi-arid regions, where groundwater is the only freshwater source due to little natural recharge, groundwater is more excessively pumped than the natural recharge, leading the further lack of groundwater in the regions (Hussain et al., 2019).

Saltwater intrusion is natural phenomena caused in coastal aquifers, which is a lateral encroachment of saltwater into the aquifers. Saltwater intrusion is caused by the density differences between saltwater and freshwater in coastal aquifers. The steady state between saltwater and freshwater in coastal aquifers is well established by Ghyben and Herzberg. Figure 2.1 shows the steady state of Ghyben-Herzberg principle (Ingham et al., 2006). In the steady-state condition, continuous interaction between saltwater and freshwater occurs, which forms the salt-freshwater interface. Normally, this salt-freshwater interface is in the steady state under natural conditions without any external factors. Under this condition, the groundwater flow in the aquifer is naturally towards the sea, which prevents saltwater and further seawater intrusion. However, once the equilibrium between saltwater and freshwater is disturbed by external factors, saltwater flow will exceed the seaward groundwater flow, leading to advancement of saltwater intrusion further to the inland. It is known that saltwater intrusion may contaminate large areas in the coast, which reaches several kilometers in some cases, and the saline level of groundwater will exceed the standard criteria for drinking and other human uses (Abd-Elhamid et al., 2015).

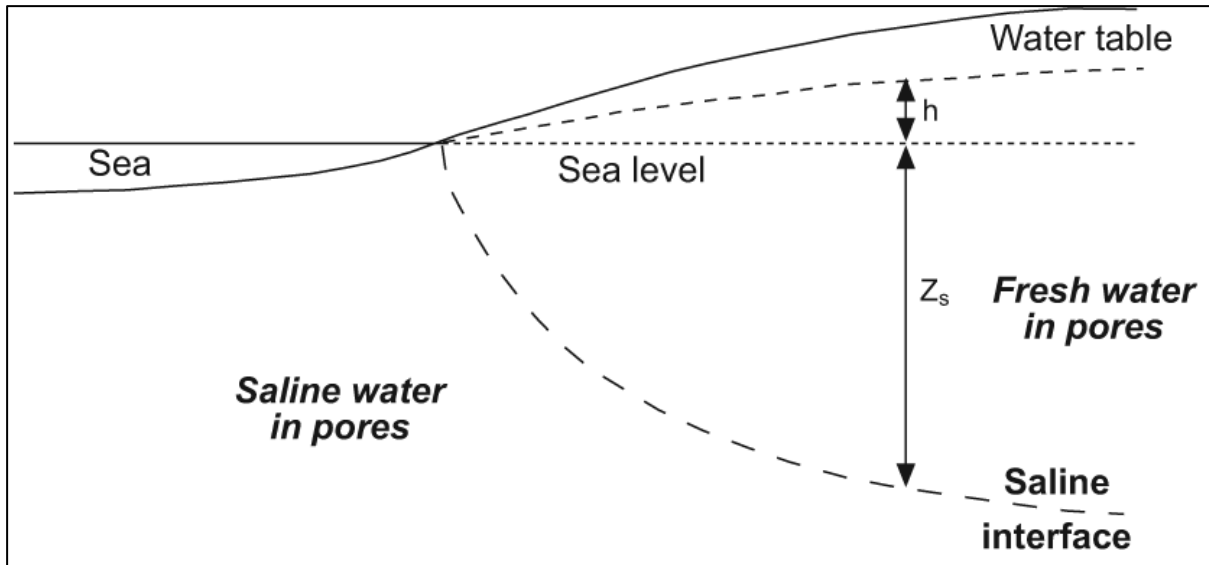


Figure 2.1. Ghyben-Herzberg principle (Ingham et al., 2006)

2.2 Effect of external factors (excessive pumping and global warming)

The shape and degree of the seawater intrusion in a coastal aquifer are depending on several factors. Some of the factors are natural, such as the type of coastal aquifer, geometry, natural recharge rate, and cannot be artificially controlled (Sherif & Singh, 2002). On the other hand, other factors are anthropogenic and could, thus, be managed by human activities. However, these anthropogenic factors have large influences on saltwater intrusion.

Excessive pumping of groundwater is one of the factors that has been accelerated by the development of technologies and increment of the demand for portable water due to global population explosion. Excessive pumping induces the depletion of groundwater level in the aquifer and reverse the water flow in the aquifer towards the inland, leading to further saltwater intrusion towards the inland. Moreover, the rise of seawater level associated with global warming and climate change is regarded as the most influential factor on saltwater intrusion for the future (Werner & Simmons, 2009). Global warming in recent years is linking to the rise of seawater level. It was reported by FAO (1997) that the rise of sea level mitigates the mixing zone of freshwater and saltwater in coastal aquifers towards the further inland. As predicted by the IPCC's fifth assessment report (IPCC, 2013), sea level will rise by more than 95%, with an 82 cm rise between 2006 and 2100 in the worst scenario of RCP 8.5. This will lead to a rise in the level of salt-freshwater interface, which advances groundwater salinization to further the inland.

2.3 Countermeasures for saltwater intrusion

To prevent saltwater intrusion and groundwater salinization, various solutions have been developed, and these solutions are mainly categorized into three different groups: conventional methods, physical barriers, and hydraulic barriers (Hussain et al., 2019). The basic ideas for each countermeasure groups are described in the following parts.

2.3.1. Conventional methods

Main types of conventional methods are reduction of pumping and relocation of pumping wells. With

reducing the abstraction amounts from pumping wells, the pumping rates from wells are literally decreased to meet the condition for preventing or retreating SWI and protect the fresh groundwater in the aquifers. Reduction of pumping is the simplest method to keep the hydraulic equilibrium between saltwater and groundwater in the coastal aquifers and prevent saltwater intrusion, which has been widely used due to its high cost-effectiveness. However, increasing water demand is an obstacle of this method. This method requires alternative options to provide other water sources instead of reduced pumped water to human activities to meet the water demand in the region. In addition, the cost of providing alternative potable water and accessibility to the alternative water sources are other problems to achieve the reduction of pumping. Concrete plans considering these problems are required to carry out this method in the real fields. Thus, this method is regarded as a temporal measure.

Relocation of pumping wells is another measure. In this method, pumping wells located near the coast are relocated to the further inland, which shifts the seaward hydraulic gradient to proper condition to keep the hydraulic balance between saltwater and freshwater, and decrease the excessive losses of groundwater abstracted from the aquifers.

Land availability is the main obstacle of this method since it requires other areas for relocated wells. If other public sectors are managing the new land, this method cannot be applied. In addition, if the contaminated water spreads over large areas, the new wells need to be located keeping a certain distance to the old well position to avoid the contamination of the new wells. Furthermore, the cost of delivering water to the regions where the water is supplied from the old abstraction wells is another limitation of this method. Planning the new distribution of pumping wells must be carefully taken into account and designed to be suitable for controlling saltwater intrusion.

2.3.2. Physical barrier

This method is the application of physical measures. In this part, two main types of physical barrier are described.

(1) Physical subsurface barrier

Figure 2.2 illustrates a physical subsurface barrier. In this method, a cut-off wall is constructed in front of seawater in the coastal aquifer, which physically blocks the seawater intrusion. The cut-off wall is often composed of concrete, grout, bentonite, slurry walls, and sheet piles. Many studies were carried out to examine the effectiveness of physical barrier by experimental and numerical simulations. The condition to make the best performance of this method has been studied widely (Luyun et al., (2011), Abdoulhalik and Ahmed (2017), & Kaleris and Ziogas (2013)). It was reported that the performance of physical barrier was the best when the physical barriers are located at deep position, closer to the coast and in front of the toe location.

Despite of high initial installation and material cost, this method is considered as the most cost-effective strategy due to its low maintenance and repairing costs. However, the installation of the physical barrier in deep aquifers is an expensive process. In addition, saline water remaining behind the physical barrier is an unavoidable problem when the physical barrier is constructed. With steep seaward hydraulic

gradient, this stagnant condition can be fixed by freshwater flow towards the sea through the barrier or below the foundation of barrier. However, with excessive pumping or low hydraulic gradient, this stagnant saline water can be diffused towards the inland, which contaminates freshwater in the aquifer.

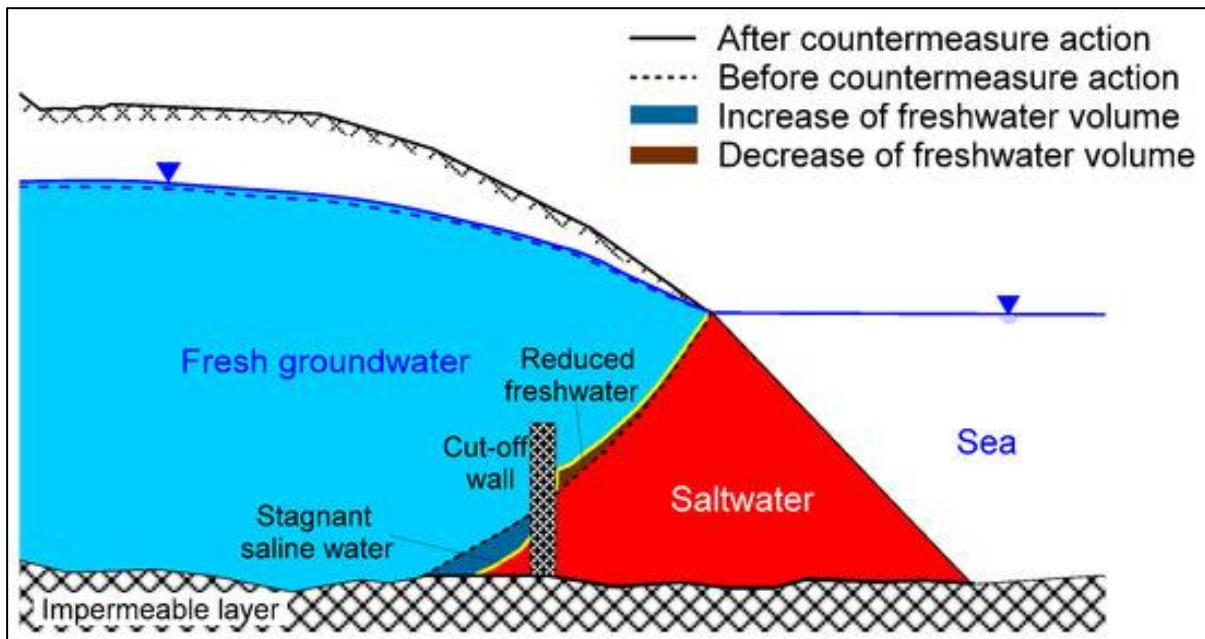


Figure 2.2. A generalized sketch of a cut-off wall

(2) Land reclamation

Land reclamation is another type of physical barrier, which artificially reclaims the coastal lands and extends the coastline towards the sea. As shown in Figure 2.3, reclaimed land is filled with reclamation soils, forming a new zone of fresh groundwater body. Through this reclamation soil, fresh groundwater flows into the sea, which forces reverse flow on saltwater, leading to a delay of seawater intrusion process or the retreat of seawater towards the sea. By increasing the distance from the coast to the production wells, a large zone of freshwater body is formed, and larger amount of water can be stored and used for various activities. This method can be adopted to regions where new land areas are required due to population growth and urbanization. The cost of material for reclamation soils and installation for large areas is the main obstacle of this method. Reclamation materials are required to be carefully chosen and designed to avoid land subsidence since reclaimed materials burdens the pressure on the underlined old soil. Moreover, land reclamation may have negative effects on environmental conditions near the coast. Thus, within this method, the influence on the surrounding environment including marine life, fishing and tourism activities should be carefully taken into account.

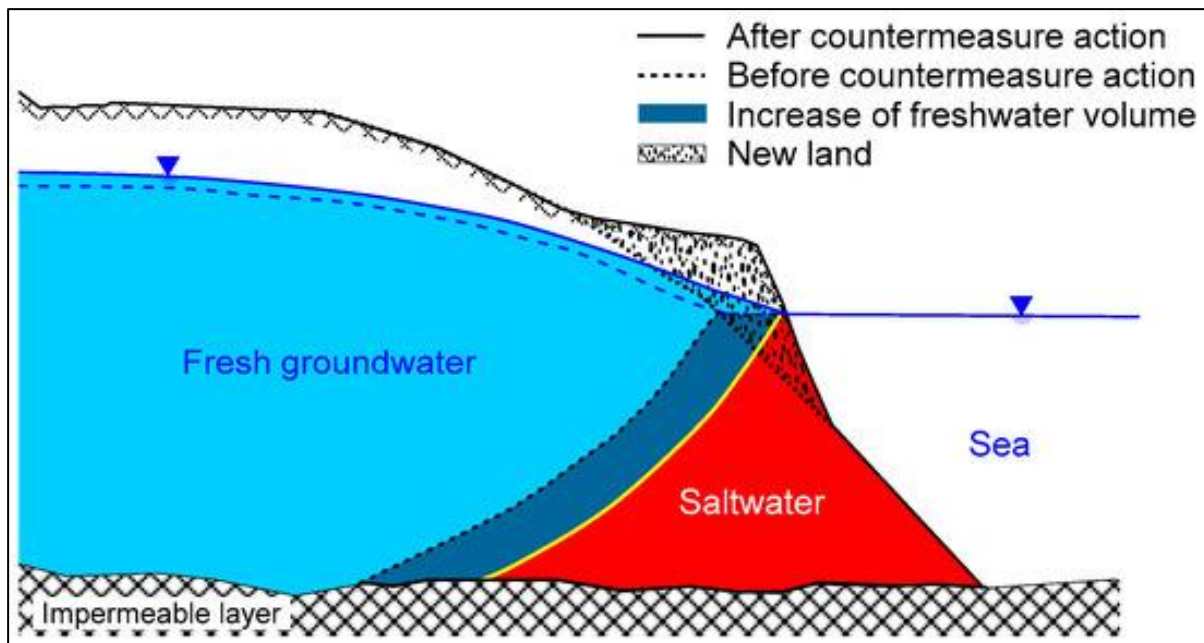


Figure 2.3. A generalized sketch of land reclamation

2.3.3. Hydraulic barrier

Hydraulic barriers are the most popular and used method in the world. Moreover, many studies regarding the hydraulic method have been carried out. Hydraulic barrier is divided into three main types: recharge, abstraction, and combination of different strategies.

(1) Recharge barrier

Figure 2.4 shows the generalized sketch of a recharge well system. Artificial recharge of high-quality water (e.g., surface water, rainwater, extracted groundwater, treated water, or desalinated water) to the aquifer forms the positive or pressure barrier, which increases the groundwater head in the inland and keeps the hydraulic gradient toward the sea. Good quality water can be obtained from surface reservoirs, treated water, or desalinated water. This method can be applied for wide ranges of objectives, such as reducing flood flows, storing freshwater in the aquifers, raising groundwater levels, relieving over-pumping, improving water quality and suppressing the saline water body.

Mahesha (1996) studied the effect of artificial recharge through single and double injection wells. According to Luyun et al. (2011), the efficiency of artificial recharge increases when appropriate recharge rate and well spacing between injection wells are chosen properly. Moreover, for deep recharge systems, installation of a recharge system to the deep zone of the aquifer, has high positive potential to retardant saltwater intrusion. Owing to these advantages, artificial recharge is one of the most popular methods among other strategies. However, the cost of preparing good quality water and delivering it to injection wells without any losses are the main obstacles of this method. Furthermore, in dry seasons or arid regions, the access to such good quality water sources is difficult, which is another problem of this method.

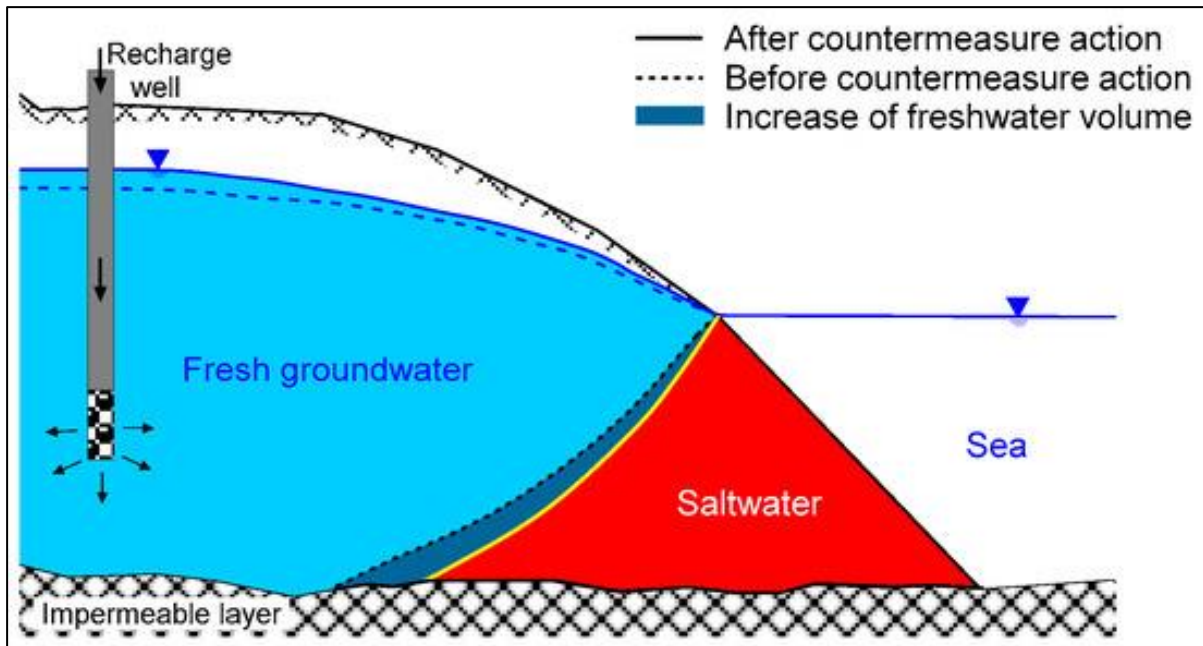


Figure 2.4. A generalized sketch of artificial recharge

(2) Abstraction barrier

Figure 2.5 shows the generalized sketch of an abstraction barrier. In contrast to the recharge barrier, this method is categorized as negative barrier, and called saltwater pumping. The abstraction well, which is called as barrier well, is installed deep in aquifers that continuously extract the brackish or saline water. With this method, old or current pumping wells existing near the coast can be utilized as barrier wells to extract saline water, which indicates that any further costs for constructing new pumping wells may not be required. Moreover, the pumped saline water can be delivered to desalinization plants to be used as water resources, or directly used for other industrial activities in terms of cooling the rejected flow from industrial plants. This method is widely applicable to coastal aquifers, even in urban areas where the land is restricted. Due to its easiness of installation and management, saltwater pumping from the barrier well has been widely assessed and applied to actual coastal regions. At the same time, many studies of this method have been carried out. The specific studies are described in chapter 2.4.

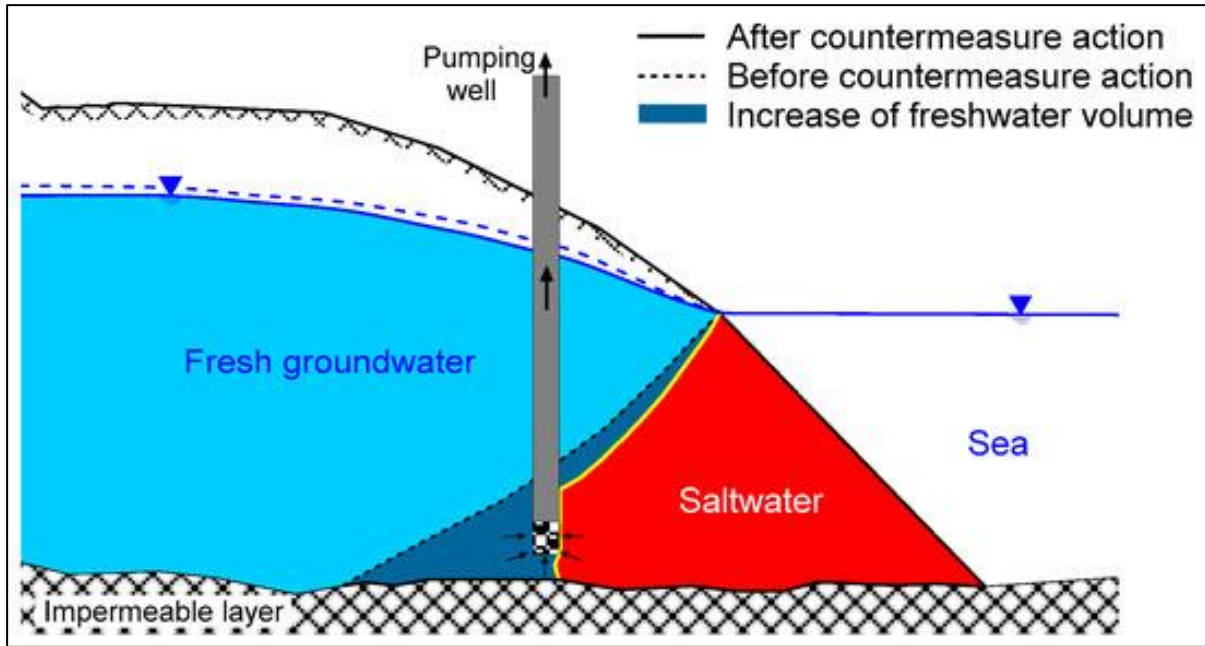


Figure 2.5. A generalized sketch of abstraction barrier

(3) Combination of aforementioned strategies

The combination of strategies mentioned above has the possibility to achieve better control of saltwater intrusion since the merits of individual strategies are combined. For example, the combination of reduction in the pumping rates and recharge barrier is one of the possible combinations in the real field. The combination of artificial recharge and abstraction barrier is another example. As shown in Figure 2.6, the barrier well near the coast abstracts saltwater through the deep zone while the artificial recharge is carried out through the inland well. This combination can achieve more efficiency than individual strategies.

Within various countermeasures, saltwater pumping has obtained certain popularity and been widely applied. Many studies have been carried out to investigate the effectiveness of saltwater pumping through barrier wells. The following chapter describes previous studies regarding the effectiveness of saltwater pumping.

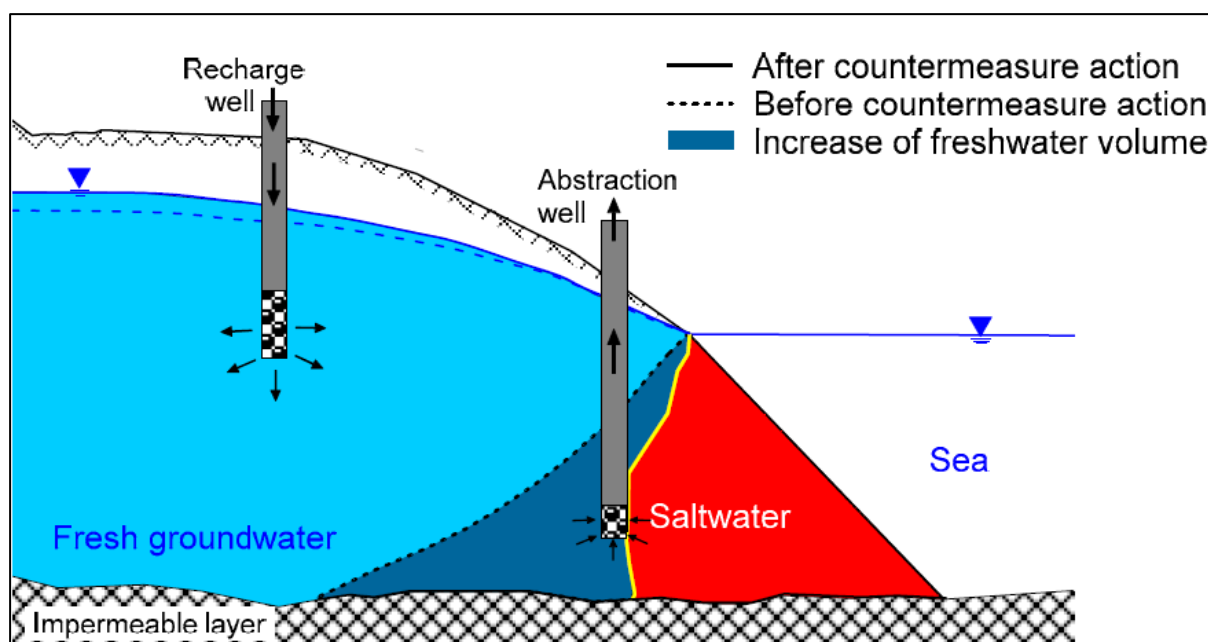


Figure 2.6. A generalized sketch of an abstraction-recharge barrier system

2.4 Previous studies of saltwater pumping

Many studies have been carried out on saltwater pumping since it has many advantages for saltwater intrusion. Sherif and Hamza (2001) evaluated the abstraction of saltwater from the dispersion zone as a measure of saltwater intrusion control using a two-dimensional finite element model. They numerically analyzed the relationship between the saltwater pumping position and saltwater intrusion behavior. The results showed a significant reduction in the length of saltwater intrusion owing to brackish water pumping from the dispersion zone. The quality of the pumped water was improved in cases where the barriers were screened away from the sea or near the upper horizons of the mixing zone. However, this result was associated with the reduction and loss of a portion of freshwater mixed with saltwater in the dispersion zone, which was reported as the major drawback of this method. Pool and Carrera (2010) used a three-dimensional variable density flow model to study the dynamics of a system with double negative barriers. One of the barriers tended to abstract the saline water near the coast, while the other pumped freshwater further to the inland. The concept of this method was to create a low-velocity zone between the two abstraction zones with an almost horizontal hydraulic gradient, which would help to protect and increase the productivity of the inland freshwater well. They demonstrated that this model would have a high efficiency in shallow aquifers, and its efficiency would even increase in the cases where the seawater well pumps the saline water at high rates in a zone close to the sea. It was demonstrated that screening the top of the freshwater well and pumping seawater from the bottom of the aquifer increases the overall performance of the proposed control measure.

Besides these researches, many studies on saltwater pumping have focused on the behavior of saltwater intrusion using hypothetical models and by carrying out numerical analysis. However, few studies have been conducted to investigate the effect of the barrier well on pumping amount from the production well. In the other words, quantitative relationship between the production well and the barrier well has not

been revealed. When using barrier wells in coastal areas, it is important to study the effectiveness of the barrier well against the possible pumping amount of freshwater from the production well, which enables the water ratio control of saltwater intrusion.

Park et al. (2012) used a multidimensional hybrid Lagrangian–Eulerian finite element model to study the effects of different parameters, including the positions, pumping rates, and the number of barrier wells, on the quality of the water pumped from another production well. They investigated the effect of barrier well on the quality of freshwater pumped from the production well with constant pumping rate. As a result, the effectiveness of saltwater extraction was sufficient when the saltwater was extracted from a single well located in the middle between the coastline and pumping well and the extraction rate was equal to 30% of groundwater pumping.

However, the pumping rate of groundwater from the production well was constant in this study and the effect of the amount of pumped water was not taken into account. It is needed to examine whether the amount of pumped water affects the performance of barrier well. Furthermore, this result was considered as a well performance condition, but it did not reveal the critical pumping ratios of the barrier well on the production well. In terms of water ratio control, changing the pumping rate of groundwater depending on the extraction rate of barrier well can be a possible application to reduce the loss of the amount of pumped water utilized for various human activities. Moreover, if there is a critical intake ratio between barrier and production well, the barrier well has a certain effect to prevent or retard saltwater intrusion by keeping the water intake ratio below a critical value. Using water ratio control, the saltwater extraction method can be practiced in any salinized coastal regions with existing wells to solve the saltwater intrusion problem.

Therefore, a fundamental research that considers the effectiveness of the barrier well in relation to possible water intake from the production well is necessary. In this study, a basic lab-scale experiment was conducted to examine the effect of saltwater pumping by the barrier well on the possible freshwater intake from the inland production well by changing the pumping rate. In addition, a two-dimensional numerical model based on a solute transport model was employed to reproduce and analyze the results of lab-scale experiments with barrier and production wells.

3. Laboratory experiments

This chapter describes the experimental setup, detailed method of preparing experimental materials, and the procedure of experiments from step 1 to 5. At the end of this chapter, the experimental conditions are presented.

3.1 Experimental device

The experimental device used was a transparent acrylic water tank with an internal length, height, and width of 122.1, 40.0, and 10.6 cm, respectively (Figure 3.1). It consisted of a freshwater tank at the right, a permeation tank in the center, and a saltwater tank to the left. Storage tanks for saltwater and freshwater were installed on both sides of this device and connected to the saltwater and freshwater tank, respectively. The storage tanks had overflow drainages that can be adjusted at optional heights to control the water head. Saltwater and freshwater heads at saltwater and freshwater tanks were maintained at 30.0 cm and 31.5 cm, respectively, by pumps connected to storage tanks. The central chamber was lined with a 5×5 cm grid to easily measure the positions and shapes of saltwater intrusion.

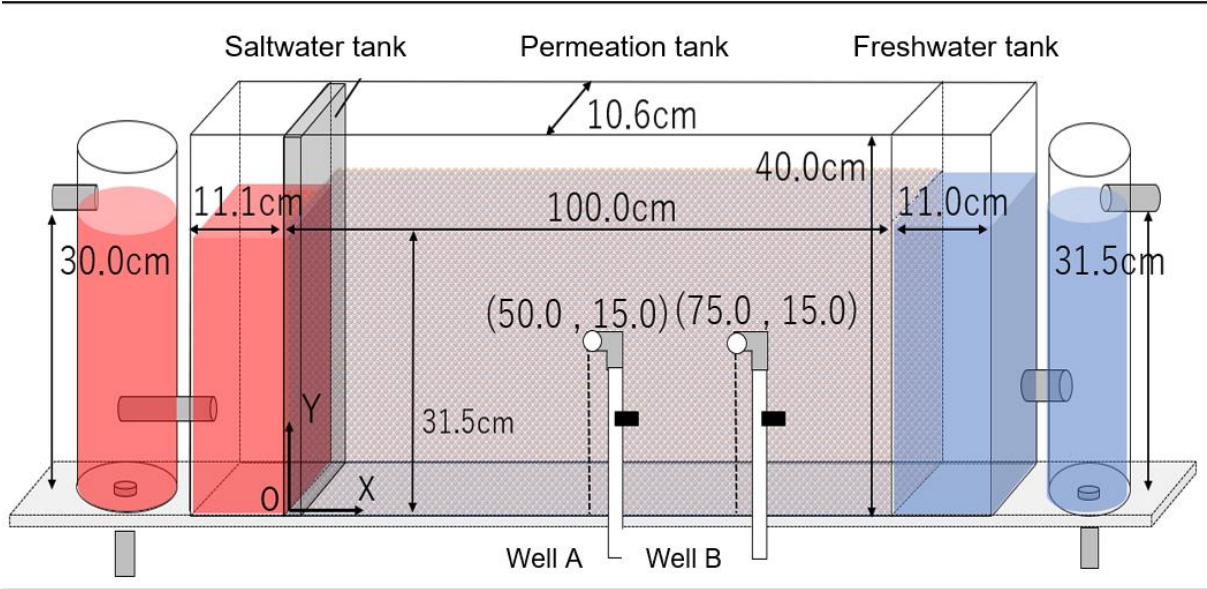


Figure 3.1. Conceptual diagram of the experimental device

The permeation tank was filled with glass beads, ASGB-20 made by AS ONE, which were evenly filled to a height of 31.5 cm under saturated conditions to minimize the entrapment of air in the device. The glass beads represented sand in a sandy coastal unconfined aquifer, which were selected based on their size and porosity. The particle sizes of the glass beads ranged from 0.71 to 1.00 mm, which satisfied the range of coarse sand in the Wentworth grain size classification shown in Table 3.1 (Blair and McPherson, 1999). The porosity of glass beads was estimated as to be 34.8 %, which is within the range of unconsolidated sand in Table 3.2 (Yu et al., 1993).

Table 3.1. Wentworth grain size classification (Blair and McPherson, 1999)

| Millimeters (mm) | Micrometers (μm) | Phi (ϕ) | Wentworth size class |
|------------------|-------------------------------|----------------|----------------------|
| 4096 | | -12.0 | Boulder |
| 256 | | -8.0 | Cobble |
| 64 | | -6.0 | Pebble |
| 4 | | -2.0 | Granule |
| 2.00 | | -1.0 | Very coarse sand |
| 1.00 | | 0.0 | Coarse sand |
| 1/2 | 0.50 | 1.0 | Medium sand |
| 1/4 | 0.25 | 2.0 | Fine sand |
| 1/8 | 0.125 | 3.0 | Very fine sand |
| 1/16 | 0.0625 | 4.0 | Coarse silt |
| 1/32 | 0.031 | 5.0 | Medium silt |
| 1/64 | 0.0156 | 6.0 | Fine silt |
| 1/128 | 0.0078 | 7.0 | Very fine silt |
| 1/256 | 0.0039 | 8.0 | Clay |
| | 0.00006 | 14.0 | |

Table 3.2. The classification of porosity of deposits (Yu et al., 1993)

| Soil Type | Porosity, p_t |
|--------------------------------|-----------------|
| Unconsolidated deposits | |
| Gravel | 0.25 - 0.40 |
| Sand | 0.25 - 0.50 |
| Silt | 0.35 - 0.50 |
| Clay | 0.40 - 0.70 |
| Rocks | |
| Fractured basalt | 0.05 - 0.50 |
| Karst limestone | 0.05 - 0.50 |
| Sandstone | 0.05 - 0.30 |
| Limestone, dolomite | 0.00 - 0.20 |
| Shale | 0.00 - 0.10 |
| Fractured crystalline rock | 0.00 - 0.10 |
| Dense crystalline rock | 0.00 - 0.05 |

In order to prevent the movement of glass beads from the central permeation tank, the central tank was separated from both saltwater and freshwater tanks, respectively, by inserting partitions. These partitions were made by attaching a clear filtration mesh to a thin metal plate with small holes. In addition, a removable acrylic plate was inserted between the saltwater tank and the central permeation tank so that saltwater and freshwater contact can be optionally blocked.

Two wells were installed in the permeation tank: Well A and Well B. Well A represented the barrier well

for pumping saltwater and Well B represented the production well for pumping the fresh groundwater. They were located at 50 cm and 75 cm from the left end of the saltwater tank, respectively, and their heights were the same, 15 cm from the bottom of the permeation tank. Both wells had valves to control the amount of water intake.

3.2 Experimental materials

The freshwater used was from university tap water, and its density was 0.991 g/cm³. Saltwater was prepared by adding commercial salt to tap water to achieve a density of 1.025 g/cm³ that is the same as seawater. In addition, saltwater was dyed red using food coloring to observe the salt-freshwater interface. The detailed measurement for freshwater and saltwater is described below.

3.2.1 Freshwater density

The density of freshwater was estimated using an electrical balance and a graduated cylinder. Tap water used as freshwater was poured into a 50-cc graduated cylinder, and 50 ml was weighted. Once the mass of water was measured, the density was estimated by dividing the volume by the calculated mass. This test was performed three times, and the average value was used as the density of freshwater in this study. Table 3 shows test results and the average value of freshwater density (0.991 g/cm³) that was used for the experiments.

Table 3.3. Test results of freshwater density

| | Take 1 | Take 2 | Take 3 |
|------------------------------------|--------|--------|--------|
| Mass (g/50 ml) | 49.643 | 49.453 | 49.505 |
| Density (g/cm ³) | 0.993 | 0.989 | 0.990 |
| Average value (g/cm ³) | 0.991 | | |

3.2.2 Saltwater density

To prepare the saline solution, the relationship among mass, volume and density was used, which was derived as shown below. At first, the density of the saline solution is expressed in Equation (3.1) (Elizabeth et al., 2008).

$$\rho_{salt} = \frac{m_{mass} + m_w}{V_{salt} + V_w} = \rho_w + \frac{1 - \rho_w A}{\frac{F_{salt}}{\rho_w} - 1 + A} \quad (3.1)$$

where, ρ_{salt} is the saltwater density, ρ_w is the freshwater density, m_{mass} is the salt mass, m_w is the freshwater mass, V_{salt} is the volume of salt, V_w is the volume of freshwater, F_{salt} is the mass fraction of salt, and A is the salt density. Since the solute used in this experiment was NaCl, the salt density can be approximated as (Simion et al., 2015):

$$A \approx -0.40064F^2 + 0.37226F + 0.29067 \quad (3.2)$$

Then, substituting Equation (3.2) into Equation (3.1) and rearranging F , cubic F can be expressed in Equation (3.3):

$$-0.40064\rho_w F^3 + 0.37226\rho_w F^2 + (0.29067\rho_w - 1)F + \left(1 - \frac{\rho_w}{\rho_{salt}}\right) = 0 \quad (3.3)$$

In this experiment, the density of saltwater and freshwater was set to 1.025 g/cm^3 and 0.991 g/cm^3 , respectively. Substituting these values into ρ_s and ρ_w in Equation (3.3) and solving the equation, three real solutions were obtained. Knowing that F is the mass fraction, the range of F value should be $0 < F < 1$, which indicates that the equation has only one valid solution of 0.04563 . Thereby, the required mass percent concentration of salt to achieve 1.025 g/cm^3 of saltwater density was calculated to be 4.56% . With the mass percent concentration of 4.56% , the following process was carried out to create the saline solution. First, an arbitrary amount of tap water was poured into a bucket, and the mass of water was measured using an electrical balance. Using the measured value of water mass, salt mass was calculated to achieve the desired concentration of 4.56% , which was mixed with water until it fully dissolved into water. The volume of the solution was calculated by dividing its mass by its density of 1.025 g/cm^3 . After this process, the saline solution was dyed red so as to observe accurately the process of saltwater intrusion. The colorant formulation was determined by a stain test and the amount was stirred with the saline solution until the color of the solution became deep red. Specific gravity of the colorant was ignored in the experiment since it was negligibly small in comparison with the specific gravity of the saline solution. An example of the prepared colored saline solution is shown in Figure 3.2.

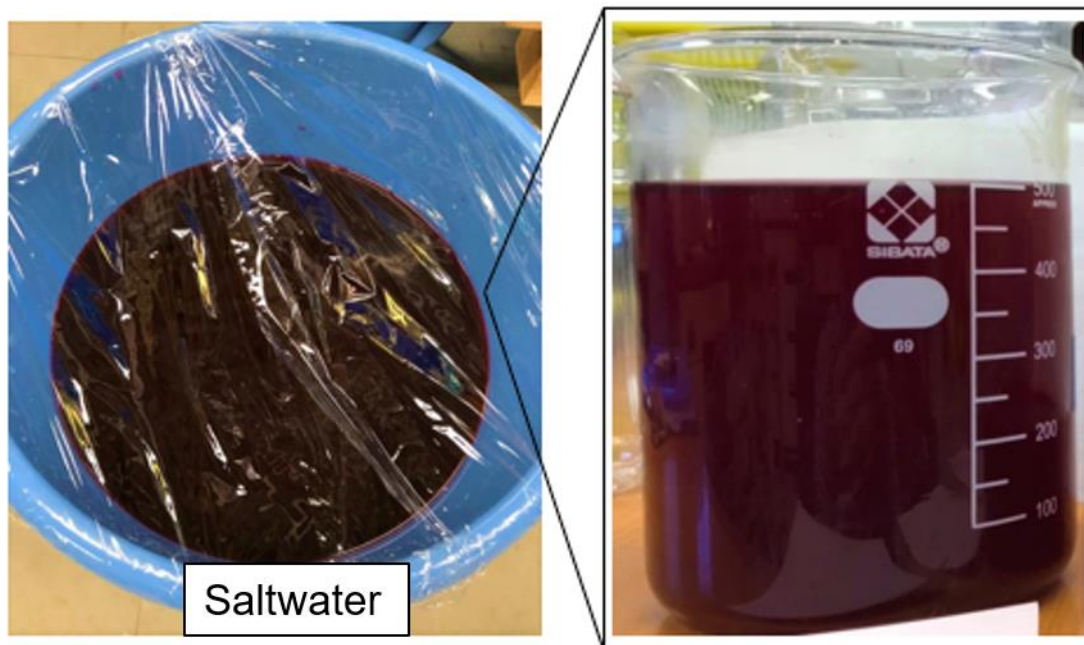


Figure 3.2. An example of colored saline solution

Generally, in an experiment using a colored saline solution, if the flow velocity is significantly small, the diffusion phenomenon dominates the advection phenomenon, that is, the fresh-saltwater interface cannot be observed correctly due to the diffusion of the colorant. However, under the experimental conditions of this study, permeability was relatively high, thus salt and dye concentrations were expected to be approximately the same, which made advection more dominant than diffusion.

Although colored saline solution was harmless, it was well treated when it was disposed of. The colored water was stored, diluted with water by the end of each experiment, and then gradually disposed.

3.3 Hydrological parameters

3.3.1 Estimation of hydraulic conductivity

Hydraulic conductivity or permeability is the ability of soil to transmit fluid through its pores. Hydraulic conductivity was calculated in each experiment using the measured flow rates and the assumption of the Dupuit–Fawer equations (Oscar, 2011). This assumption is based on that the groundwater pressure can be approximated by the hydrostatic pressure distribution when the groundwater level gradient is small, since the groundwater flow direction is almost horizontal, and the flow velocity is relatively small. This assumption can be applied when the permeation layer length, L , is sufficiently larger than the difference between upstream and downstream water level in the permeation layer, dh , as shown in Figure 3.3.

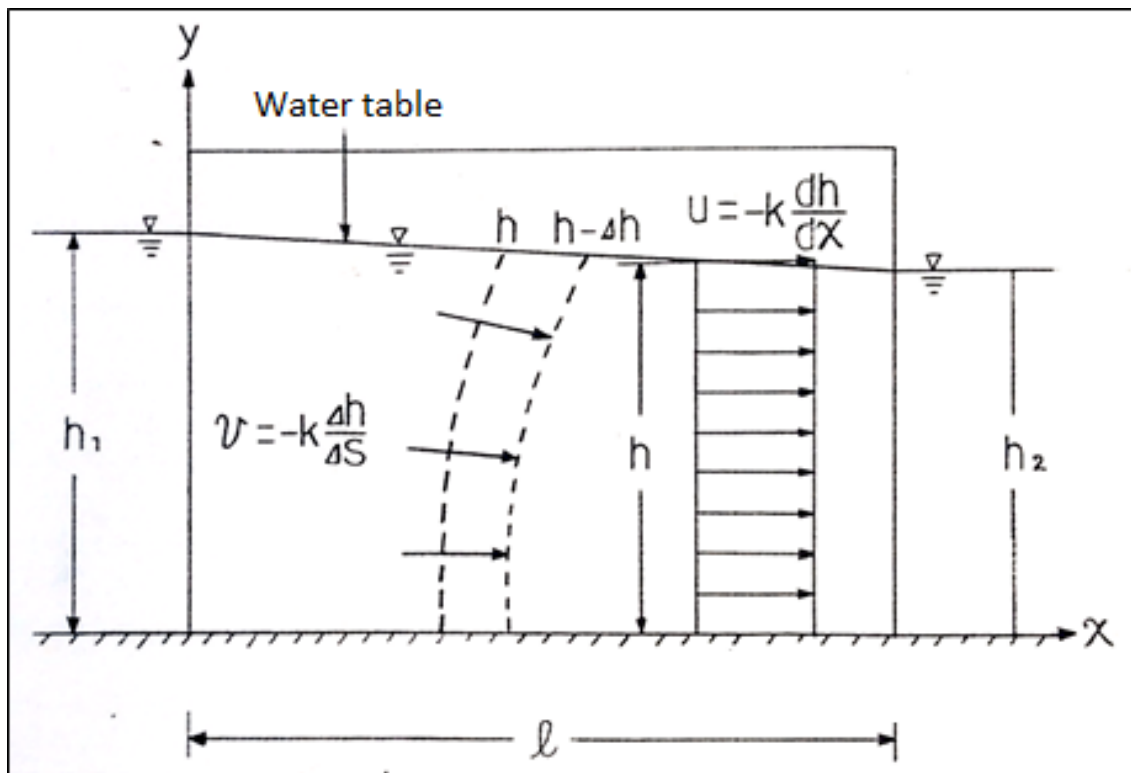


Figure 3.3. The quasi-steady flow by Dupuit-Fawer assumption (Oscar, 2011)

Using the Dupuit-Fawer assumption, the piezometric head is equal to the water depth. Horizontal velocity, u , is expressed using Darcy's equation (3.4) and the unit width flow rate in the permeation layer, q , is expressed as shown in Equation (3.5):

$$u = -k \frac{dh}{dx} \quad (3.4)$$

$$q = uh = -kh \frac{dh}{dx} \quad (3.5)$$

By integrating Equation (3.5) with $h=h_1$ when $x=0$ and $h=h_2$ when $x=L$, Equation (3.6) is obtained.

$$\frac{h_1^2}{2} - \frac{h_2^2}{2} = \frac{q}{k} L \quad (3.6)$$

By rearranging Equation (3.6), Equation (3.7) that calculates the hydraulic conductivity, k , can be obtained.

$$k = \frac{2qL}{h_1^2 - h_2^2} \quad (3.7)$$

where, L is the permeation layer length of 100.0 cm, h_1 is the upstream head of 31.5 cm, and h_2 is the downstream head of 30.0 cm. The unit width flow rate is the average value of the flow rate extruding from the permeation layer in 30 seconds. It was measured three times and divided by the water tank width of 10.6 cm and the time measurement in order to convert it to a unit width flow rate. The estimation results of these calculations for each experiment are shown in Table 3.4.

Table 3.4. The estimation results of hydraulic conductivities for each experiment

| Experiment No. | 1 | 2 | 3 | 4 | 5 | 6 |
|--------------------------------------|----------|----------|----------|----------|----------|----------|
| Flow 1 | 66 | 58 | 56 | 72 | 76 | 70 |
| Flow 2 | 67 | 58 | 56 | 70 | 78 | 74 |
| Flow 3 | 66 | 58 | 58 | 70 | 78 | 76 |
| Width (cm) | 10.6 | 10.6 | 10.6 | 10.6 | 10.6 | 10.6 |
| q (cm²/s) | 0.21 | 0.18 | 0.18 | 0.22 | 0.24 | 0.23 |
| H_f | 31.5 | 31.5 | 31.5 | 31.5 | 31.5 | 31.5 |
| H_s | 30 | 30 | 30 | 30 | 30 | 30 |
| Hydraulic conductivity (cm/s) | 0.45 | 0.40 | 0.39 | 0.48 | 0.53 | 0.50 |

Note that the calculated values of hydraulic conductivity changed through repeated experiments. This difference may be caused by the bulge of the acrylic plates on the front and back sides of the experimental device owing to the settlement of glass beads.

3.4 Experimental process

The experiment consisted of 5 steps shown in Figure 3.4. Before each experiment started, all water tanks, including the saltwater tank, were saturated with freshwater, and then freshwater flow was confirmed to sustain the designed constant head difference. And then, the partition plate was inserted between the saltwater and permeation tank to prevent freshwater flow towards the saltwater tank. Under this condition, freshwater filled in the saltwater tank was fully removed, and the saltwater tank was directly filled with the prepared colored saline solution. The start of each experiment was marked by the removal of the partition plate.

A stopwatch was used to keep track of time. To record the behavior of saltwater intrusion, it was photographed every 10 min using a digital camera, and the position of saltwater toe was recorded using a ruler in 0.5 cm increments. Note that, the first 5 min of every step showed the largest increments, thus it was recorded using a video within these first 5 min. When the steady state was reached in the ongoing step, the next step started. The steady state is a dynamic equilibrium of the fresh-salt water interface due to the difference of their densities. In this laboratory experiment, the steady state was judged when the change of saltwater intrusion toe for 10 minutes was less than 0.5 cm. One experiment continued until

all steps were completed.

Step 1 represents the formation of a saltwater wedge because of the head differences between saltwater and freshwater. In step 2, water was pumped from Well A, and the advancement of the salt-freshwater interface was observed for different water intake amounts. This was followed by step 3, in which water was pumped simultaneously from Well A and Well B. Further advancement of the salt-freshwater interface was observed in the inland at this stage and compared to the respective intake ratios in each experimental trial. Step 4 started when water intake from Well B was turned off and the only pumped water was from Well A, resulting in a retraction of saltwater intrusion back to the position of steady state that was reached in step 2. Step 5 started when Well A was turned off; thus, no more water was pumped in the experimental device. The saltwater intrusion was retracted to the position of steady state in step 1. Full experiment, including all 5 steps, was performed six times with different intake ratios to ensure that comparative considerations can be carried out on test results to consider the positive effect of preventing salinization by pumping saltwater from the barrier well.

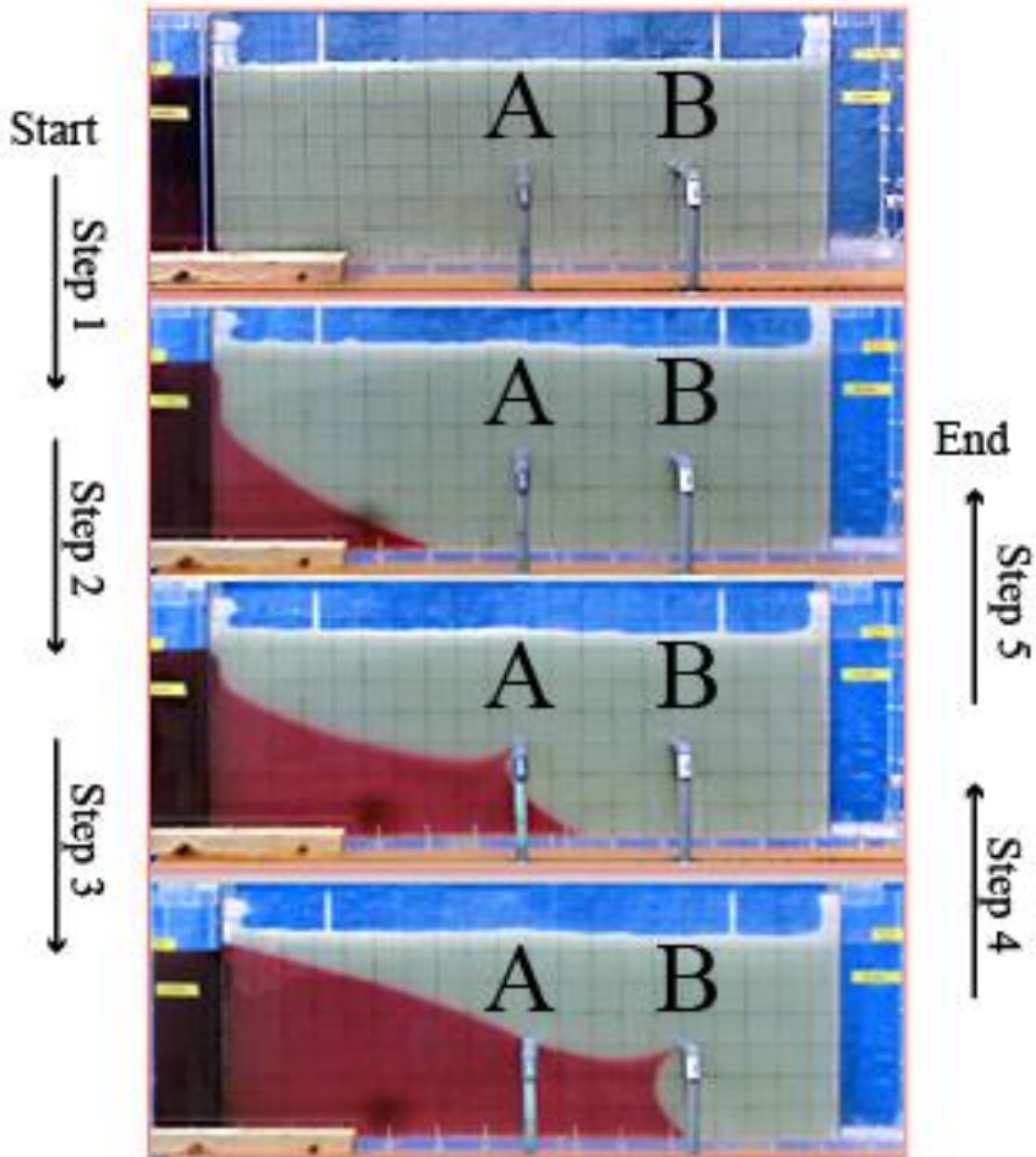


Figure 3.4. Experimental steps

3.5 Experimental condition

Table 5 shows conditions for each experiment. Water intake ratios were varied in each experiment to determine the critical intake ratio between barrier and production wells. The freshwater level in the upstream tank was set to 31.5 cm, and the saltwater level in the downstream saltwater tank was set to 30.0 cm. As a result, the water head difference for the permeation layer length of 100.0 cm was 1.5 cm, resulting in a hydraulic gradient of 0.015. The water temperature in the experiments ranged between 17 and 20 °C. The porosity and hydraulic conductivity were calculated as mentioned above. Water intake ratios were 0.9, 1.2, 1.5, 1.9, 2.0, and 2.6.

Table 3.5. Experimental conditions

| | | | |
|--|-------|---|-----------|
| Freshwater level (cm) | 31.5 | Porosity (%) | 34.8 |
| Saltwater level (cm) | 30.0 | Hydraulic conductivity (cm/s) | 0.39-0.53 |
| Freshwater density (g/cm³) | 0.991 | Water intake from well A (ml/s) | 1.8-3.3 |
| Saltwater density (g/cm³) | 1.025 | Water intake from well B (ml/s) | 1.7-6.1 |
| Water Temperature (°C) | 17-20 | Water intake ratio (Q_B/Q_A) | 0.9-2.6 |

4. Results of laboratory experiments

In this chapter, results of the laboratory experiments are described. It is followed by a discussion of the effect of saltwater pumping in a coastal area to prevent saltwater intrusion and attempts to quantify a critical pumping ratio of the production well. The hydraulic conductivity and water intake amount in each experiment are shown in Table 4.1. The arrow shown in the water intake at well A in experiment 2 indicates a change of water intake from 3.3 ml/s in step 1 and 2 to 2.9 ml/s after step 3 in order to manage the pumping ratio as to 1.2. In experiment 6, two water intake conditions are shown since the water intake from the well B was increased in step 3 as a secondary test to confirm the critical intake ratio.

Table 4.1. Hydraulic conductivity and water intake in each experiment

| | | | | | | | |
|---|------|---------|------|------|------|------|-----|
| Hydraulic conductivity (cm/s) | 0.45 | 0.40 | 0.39 | 0.48 | 0.53 | 0.50 | |
| Water intake at point A; Q_A (ml/s) | 1.8 | 3.3→2.9 | 2.7 | 2.2 | 2.5 | 2.7 | 2.7 |
| Water intake at point B; Q_B (ml/s) | 1.7 | 3.5 | 5.3 | 5.7 | 3.8 | 5.2 | 6.1 |
| Water intake ratio; Q_B/Q_A | 0.9 | 1.2 | 2.0 | 2.6 | 1.5 | 1.9 | 2.3 |

4.1. Step 1: Saltwater wedge formation

An example of saltwater intrusion at the steady state in step 1 is shown in Figure 4.1. The results of the saltwater wedge formation process in step 1 are shown in Table 4.2 listing hydraulic conductivity, elapsed time in minutes to reach steady-state conditions, and intrusion length of saltwater. As a result, the saltwater wedge entering from the saltwater tank reached the steady-state condition at positions between 31.0 cm and 41.0 cm from the saltwater tank. The time required to reach the steady-state conditions was measured to be within 90 to 150 minutes. These results show that the larger the hydraulic conductivity, the faster the steady-state condition was reached. Moreover, the steady-state condition was attained 60 minutes earlier when the hydraulic conductivity was 0.53 cm/s than when it was 0.39 cm/s. Figure 4.2 shows the changes of saltwater intrusion length overtime depending on varying hydraulic conductivity. The slope of the graph represents the intrusion rate. This rate was considerably higher in the first duration, and then gradually decreased to the steady-state condition.

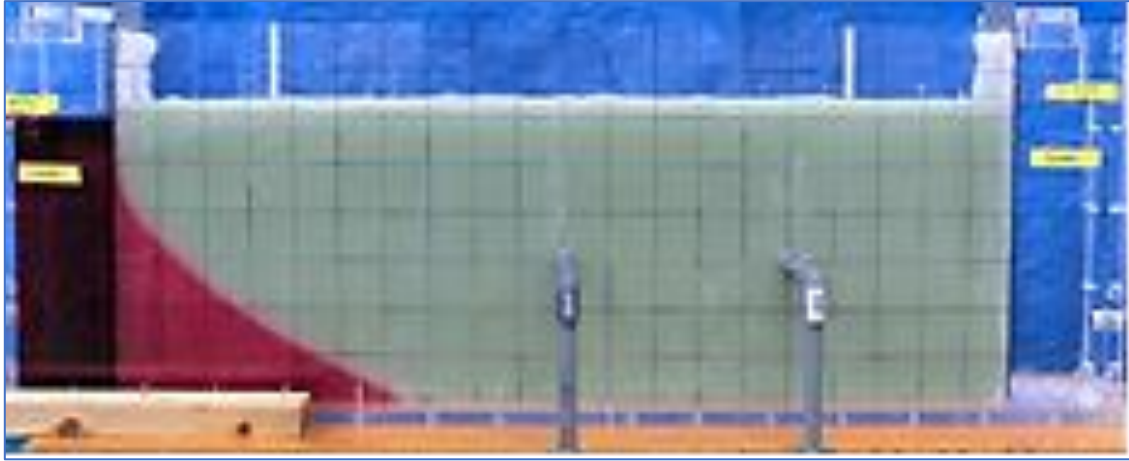


Figure 4.1. Example of saltwater intrusion for experiment number 1

Table 4.2. Results of step 1

| | | | | | | |
|------------------------------------|------|------|------|------|------|------|
| Hydraulic Conductivity (cm/s) | 0.53 | 0.50 | 0.48 | 0.45 | 0.40 | 0.39 |
| Time to reach steady state (min) | 90 | 100 | 110 | 130 | 150 | 150 |
| Intrusion length of saltwater (cm) | 35.0 | 33.0 | 35.0 | 32.5 | 31.0 | 41.0 |

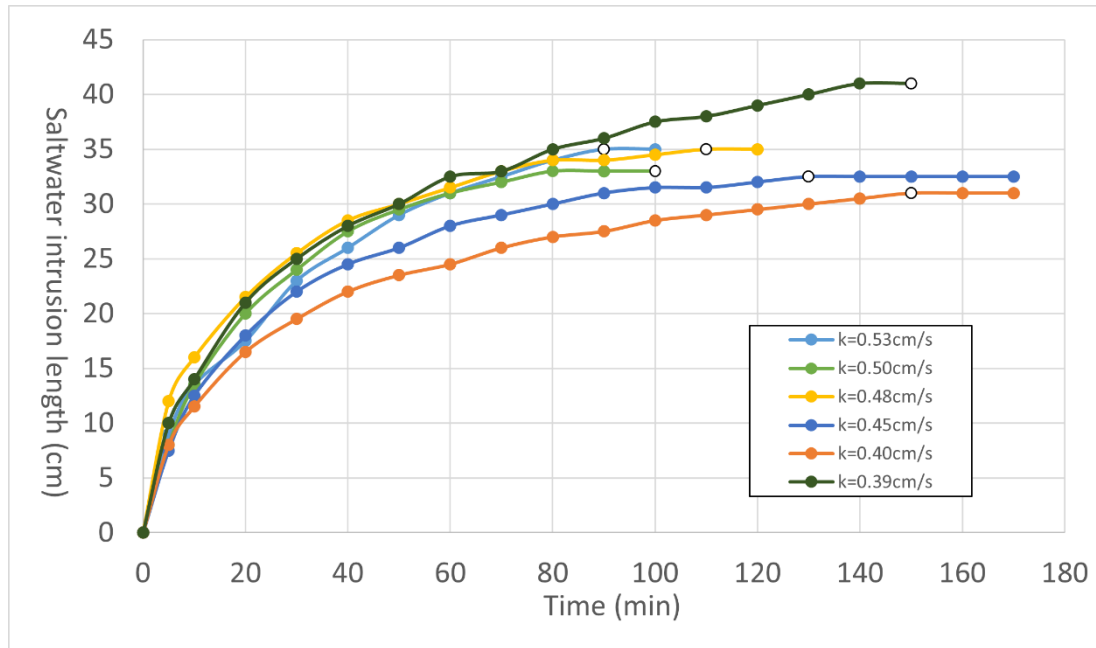


Figure 4.2. Changes in saltwater intrusion length over time in step 1

To verify the adequacy of the intrusion length, theoretical lengths of saltwater intrusion were calculated using Glover's equation (Glover, 1959), which is expressed by Equation (4.1) and depicted in Figure 4.3.

$$h_{fs}^2 = \frac{2Q_f \delta_{sf} x}{K} + \left(\frac{\beta \delta_{sf} Q_f}{K} \right)^2 \quad (4.1)$$

where, h_{fs} is the depth of salt-freshwater boundary, Q_f is the flow rate in aquifer per unit length of shoreline, β is a coefficient ($=1$), K is the hydraulic conductivity, x is the coordinate distances from

shoreline, and δ_{sf} is the coefficient of density difference ($= 29.15$), which is calculated by the following Equation (4.2):

$$\delta_{sf} = \frac{\rho_f}{\rho_s - \rho_f} \quad (4.2)$$

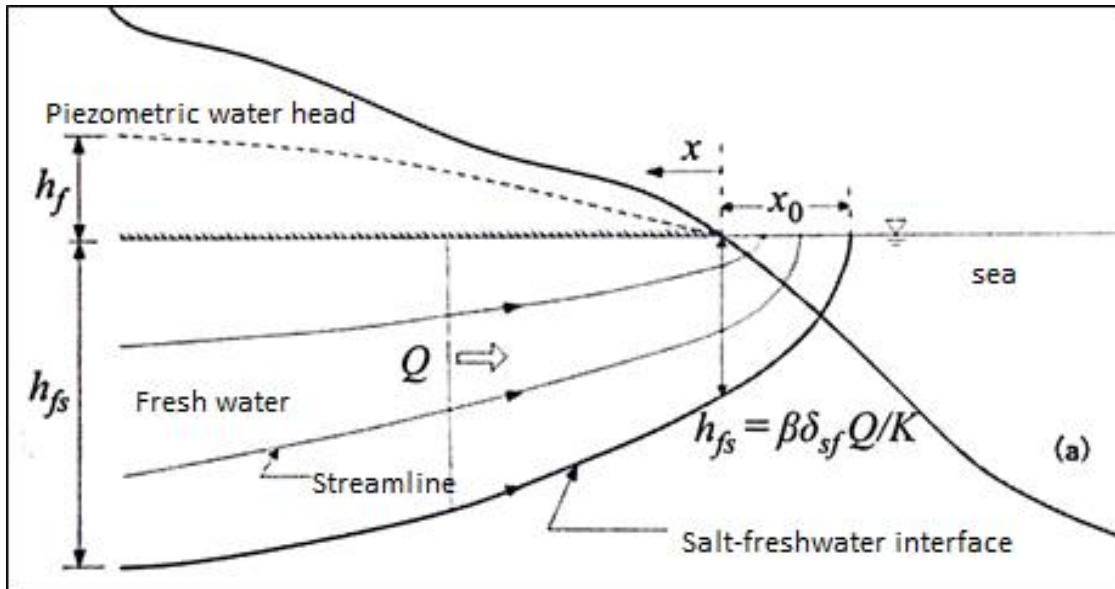


Figure 4.3. Salt-freshwater interface for Glover's equation (Glover, 1959)

Using this equation, theoretical values of intrusion length for each experiment were estimated to be equal to 30.18 cm. The observed values are larger than the theoretical. The error of density measurement of saltwater and freshwater in the preparation process is considered as one of the factors causing this difference between observed and theoretical values. In addition, the experimental device was somewhat inclined, which is considered as another reason.

4.2. Step 2: Water intake from barrier well (well A)

The results of the water intake from well A in step 2 are shown in Table 4.3, listing the amount of water intake from well A (Q_A), the intrusion length of saltwater at the steady state, and elapsed time.

Table 4.3. Results of step 2

| Intake from well A; Q_A (ml/s) | 3.3 | 2.7 | 2.7 | 2.5 | 2.2 | 1.8 |
|------------------------------------|------|------|------|------|------|------|
| Intrusion length of saltwater (cm) | 58.5 | 59.0 | 59.5 | 61.0 | 59.0 | 59.0 |
| Time to reach steady state (min) | 100 | 110 | 90 | 130 | 130 | 240 |

As pumping from well A started at well A, it was observed that saltwater invaded further towards the freshwater zone from its initial equilibrium reached in step 1. The steady state in step 2 was observed at positions between 58.5 to 61.0 cm from the saltwater tank. The toe of saltwater intrusion was measured at approximately 10 cm inland from well A that was located at 50.0 cm from the saltwater tank.

Excluding the experiment of $Q_A=2.7$ ml/s, a proportional trend was observed through five experiments, that is, the higher the water intake from well A, the faster the steady state was reached. In the experiment of $Q_A=2.7$ ml/s, the steady state was achieved faster than other experiments. It is considered as a reason

of this result that the intrusion length in step 1 was 41.0 cm, which was larger and closer to the well A than in other cases. On the other hand, the elapsed time in the case of $Q_A=1.8$ ml/s was considerably longer than in other cases. It is considered that pumping amount of well A was too small to influence saltwater intrusion.

In terms of intrusion length, the following trend was observed within the range of $Q_A=2.5$ to 3.3 ml/s; the larger intake amount shortened the intrusion length. This infers that a barrier well has an effect of blocking saltwater intrusion when it pumps larger amount of water. Figure 4.4 shows the changes in saltwater intrusion length over time. The slope of the graph represents the intrusion rate of saltwater. It shows that the intrusion rate was high when the water intake from well A was large. Note that, in the experiment of $Q_A=2.5$ ml/s, the saltwater intrusion length temporally retreated between 50 and 70 minutes. This was considered to be correlated to an increase of water level in freshwater tank by approximately 5 cm, which was observed around 60 minutes. This changed hydraulic gradient, leading to the retreat of saltwater.

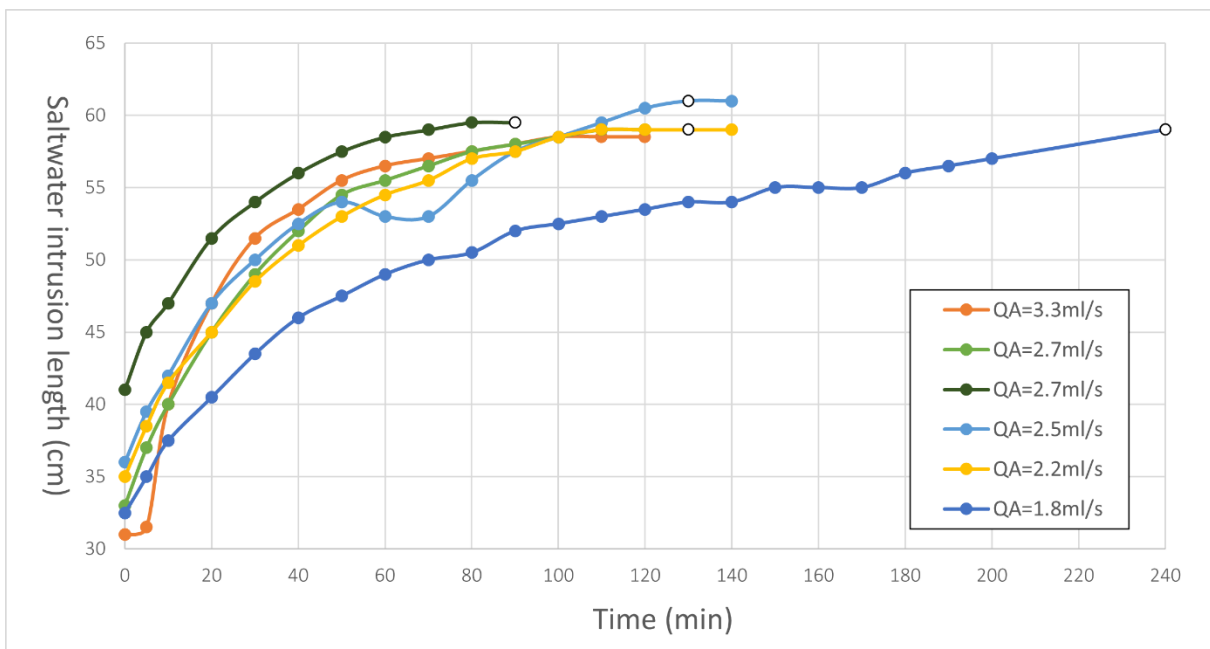


Figure 4.4. Changes in saltwater intrusion length over time in step 2

In addition, the upconing phenomenon was observed in this step. Upconing is upward movement of saltwater towards the freshwater zone in an aquifer due to the reduction of hydraulic pressure by pumping water from the freshwater zone (David, 1991). This phenomenon was analyzed by comparing photographs of each experiment. Note that, the case of $Q_A=2.7$ ml/s was excluded from this comparison for the same reason as mentioned above. This comparison mainly focused on the behavior of saltwater intrusion with upconing phenomenon, which was divided into three stages due to its shape. First stage was immediately after pumping started, when the saltwater wedge changed and started upconing towards the well A. The second stage started when upconing saltwater reached well A, and the third stage started when the steady state was achieved.

Figure 4.5 shows photographs of first stage in five experiments. A sharp rise of saltwater was observed

when the toe of saltwater wedge reached the vicinity below the well A. Moreover, it is considered that the required time to reach the first stage is depending on the pumping amount of well A. Photographs of the second stage is shown in Figure 4.6. In the second stage, saltwater, which started rising in the first stage, sharply reached the well A. As well as the first stage, the larger amount of intake from well A results in the faster achievement of steady state. The shape of the saltwater curve reaching well A was sharp and convex. Figure 4.7 shows the photographs of the third stage. After this stage started, the change of the saltwater wedge shape was not observed, which indicates a steady state. At this stage, the pumped water from well A had deep red color signifying high concentrations of saltwater. The same trend as first and second stages was observed in this stage.

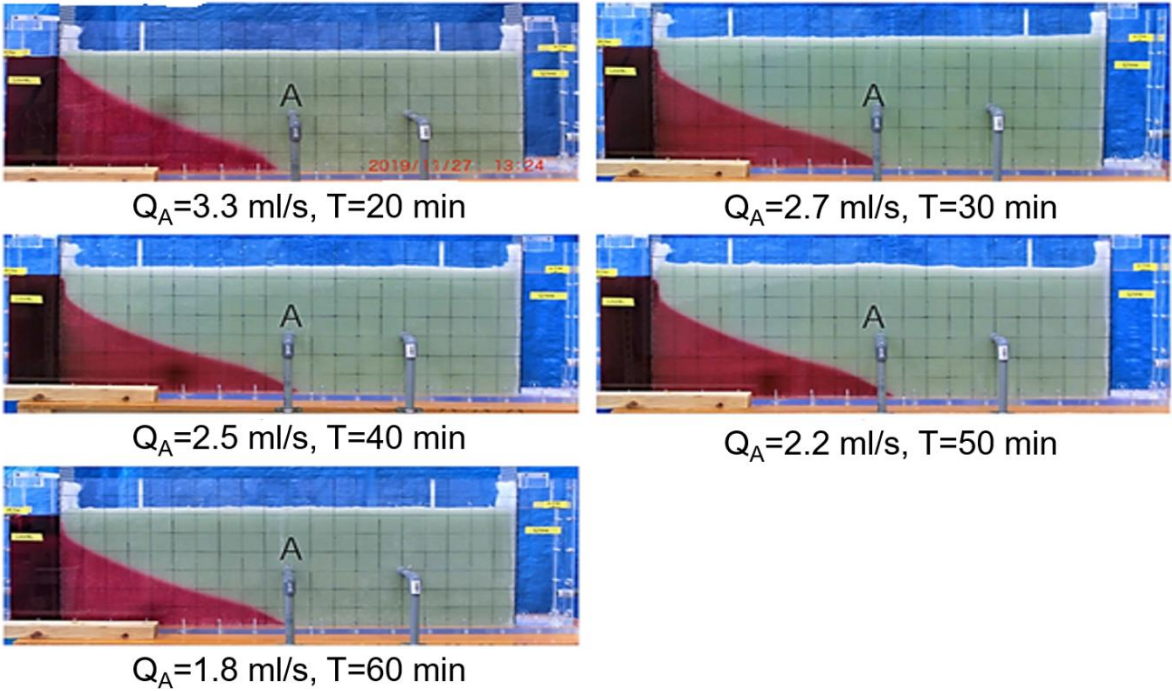


Figure 4.5. First stage of upconing

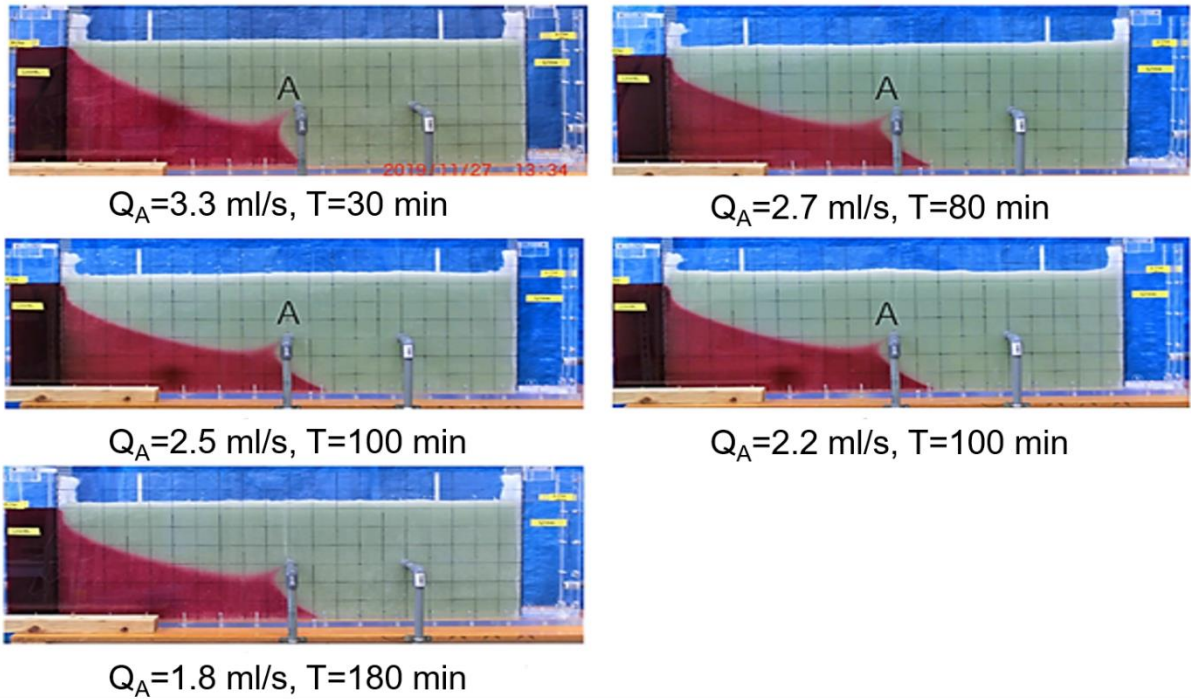


Figure 4.6. Second stage of upconing

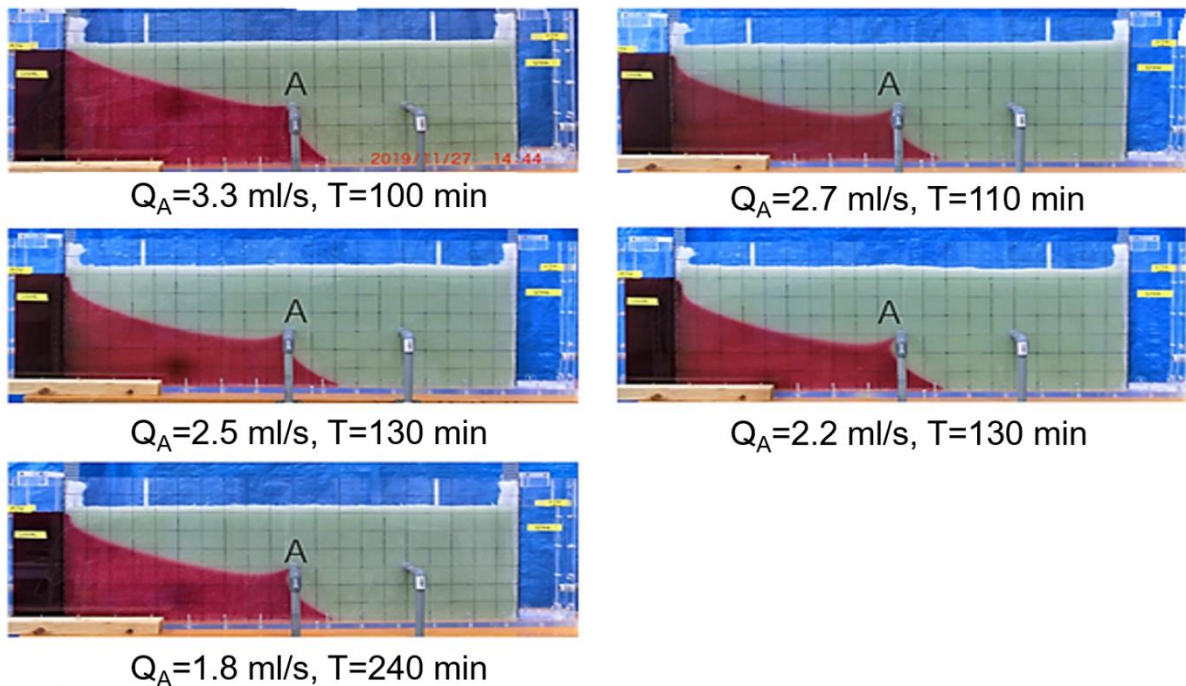


Figure 4.7. Third stage of upconing

4.3. Step 3: Water intake from barrier well and production well (well A&B)

The results of simultaneous pumping from well A and B in step 3 are shown in Table 4.4. When well B started pumping, the saltwater wedge moved from its previous steady state to further inland and resided its toe at a position between 64.5 cm and 75.0 cm. It took between 70 and 130 minutes to reach the steady state of step 3.

Table 4.4. Results of step 3.

| Intake Ratio; Q_B/Q_A | 0.9 | 1.2 | 1.5 | 1.9 | 2.0 | 2.6 |
|---|------------|------------|------------|------------|------------|------------|
| Intrusion length of saltwater (cm) | 67.0 | 64.5 | 72.0 | 73.0 | 74.0 | 75.0 |
| Time to reach steady state (min) | 90 | 70 | 80 | 110 | 130 | 70 |
| Presence of saltwater in well B | × | × | × | × | ○ | ○ |

Salinization of well B was judged by observing the upconing of saltwater to the well B. In addition, the watercolor pumped from well B was observed at the same time as a proof of salinization of well B. As a result, salinization of well B was only observed when the intake ratio of well B to well A was equal or greater than 2.0. Since it took the longest time to achieve the steady state at ratios 1.9 and 2.0, it is considered that the ratio between 1.9 to 2.0 is a critical intake ratio under this experimental condition.

Figure 4.8 shows a comparison of steady-state conditions for all intake ratios. For ratios exceeding 1.2, it was observed that, even after settling of the toe, the salt-freshwater interface kept moving left and upwards towards well B until it reached steady state and settled into its dynamic equilibrium. When the water intake ratio was between 1.5 and 1.9, although the salt-freshwater interface kept moving right and upwards towards well B, the upconing entering well B was not observed. In contrast, it was clearly observed that saltwater reached well B in experiments with intake ratio of 2.0 or exceeding 2.0. In these conditions, the area occupied by saltwater downstream well A was larger than other conditions.

To confirm whether the intake ratio at which saltwater reaches the well B was exactly 2.0, a secondary test was performed with intake ratio of 1.9. In this case, the steady state was achieved without salinization of well B. After the steady state was achieved under this condition, the water intake from well B was increased so that the intake ratio became 2.3. After this increase, saltwater reached well B, which indicates that the critical intake ratio under this experimental condition was 1.9. In other words, well B can pump freshwater without salinization of the well if the water intake ratio is equal to or less than 1.9. It was presumed that, if water is abstracted only from the inland production well, this well has a high risk of salinization. However, when the intake ratio is 1.9 or less, a barrier well has an ability of blocking saltwater intrusion and the production well can be used without salinization.

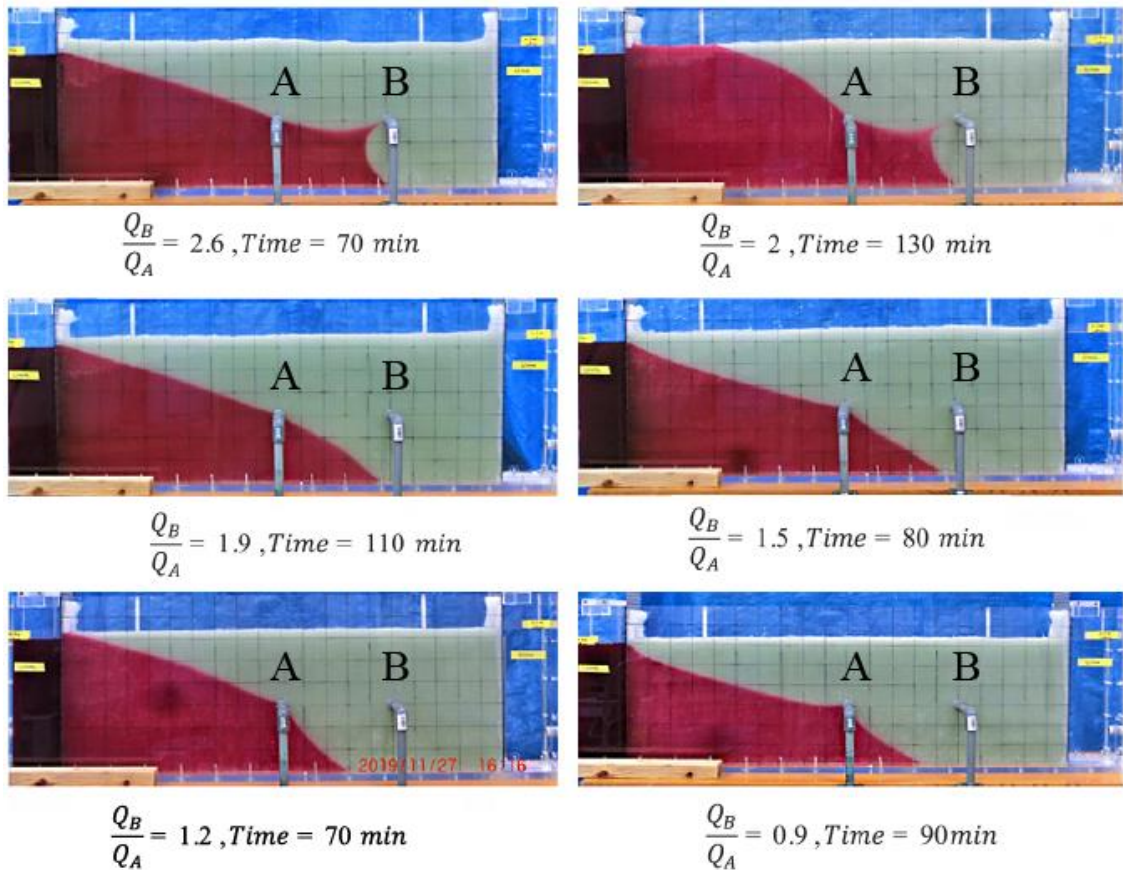


Figure 4.8. Comparison of steady state at different intake ratios.

Figure 4.9 shows the changes in saltwater intrusion length over time in step 3. In this graph, the toe position with intake ratios of 0.9 and 1.2 at the steady state was about 65 cm. Knowing that well B is located 75 cm away from the saltwater tank, saltwater intrusion under these intake ratios did not reach the vicinity of well B. Therefore, the barrier well has a positive effect to prevent saltwater intrusion at far away from the vicinity of the production well, when the pumping rate of the inland production well is almost the same as the pumping rate of the barrier well. Moreover, the salinization of the inland production well is prevented even when the pumping amount of the production well is almost double that of the barrier well.

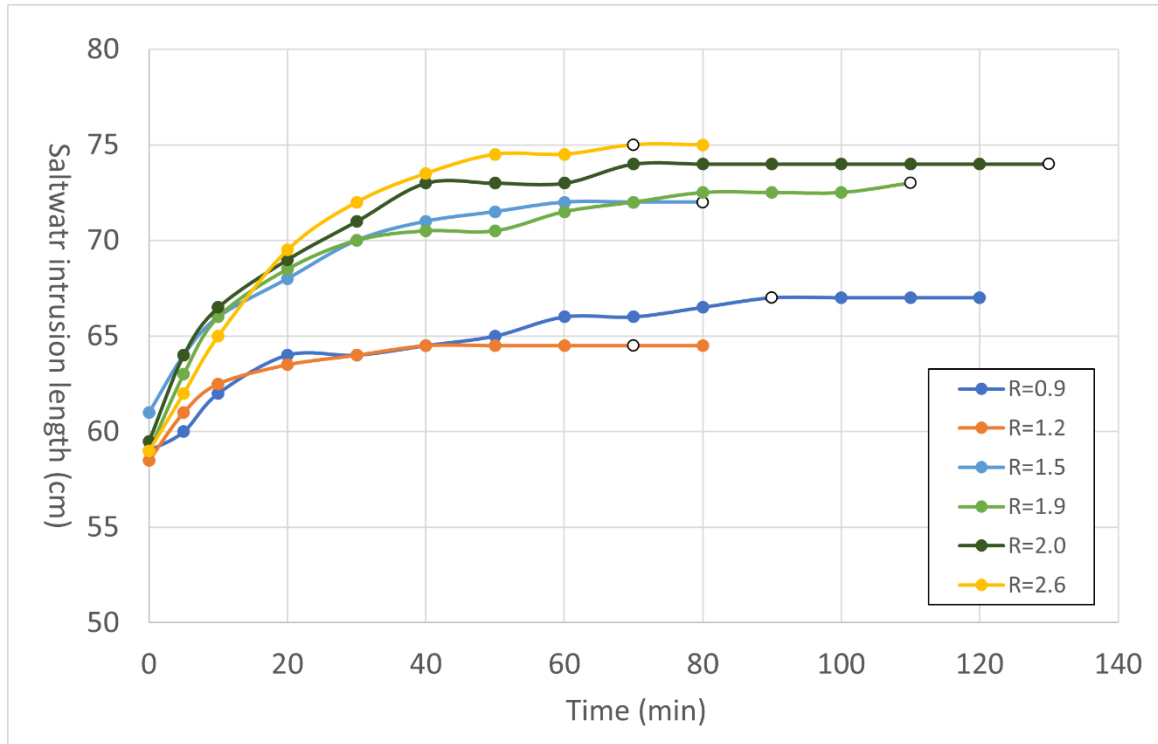


Figure 4.9. Changes in saltwater intrusion length of step 3

4.4. Step 4: Turning off well B and retreat process of saltwater

The behavior of saltwater after turning off pumping from the well B was observed and the results were qualitatively considered by comparing the retreat process recorded by photographs. The retreat process was divided into 2 stages: stage 1 being the reversal of upconing into the well B and stage 2 being the return to the steady state observed at the end of step 2. Figure 4.10 shows stage 1 in which the upconing was reversed directly after turning off the water intake from the well B. Knowing that the upconing process in step 3 required 30 to 60 minutes, the reversal of the upconing was relatively fast. Regarding the stage 2, the obtained steady state was similar to that in step 2. The photographs of these stages showing saltwater intrusion areas and curves were compared in Figure 4.11. As shown in Figure 4.11, Positions, shapes, and areas of saltwater in both steps are identical in all experiments, even in the case that salinization of the well B was observed. Therefore, it is considered that a barrier well has the ability to retreat saltwater intrusion to its initial state and the original equilibrium can be stored, even after over-pumping and salinization of an inland production well.

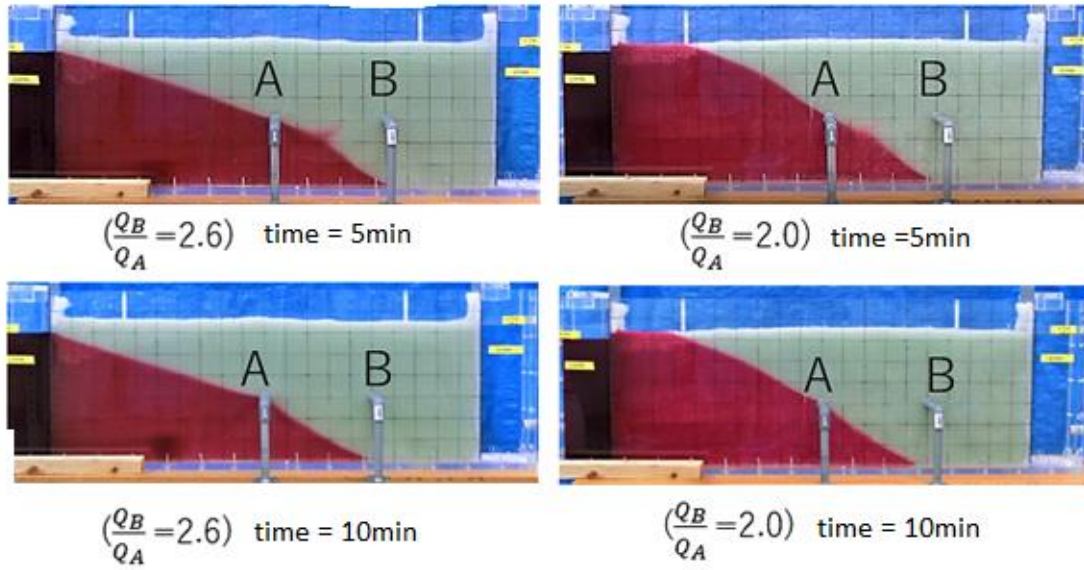


Figure 4.10. Stage 1 in step 4

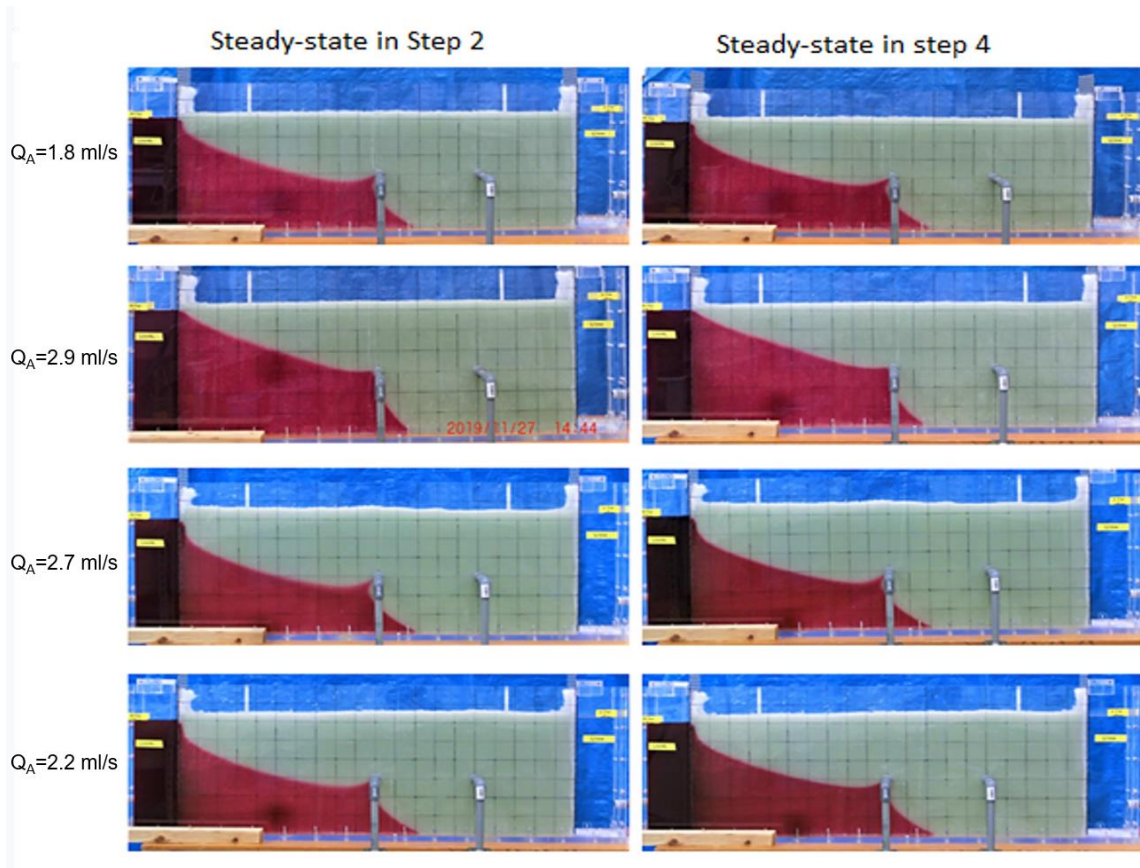


Figure 4.11. Comparison of saltwater intrusion area in step 2 and step 4

In addition, intrusion time recorded in step 3 and retreat time recorded in step 4 are shown in Table 4.5 with each intake ratio. Note that, the experiment with a water intake ratio of 1.9 was disregarded in this step since, as mentioned above, the water intake ratio in this specific experiment was changed to 2.3 in order to check the critical ratio in step 3. Although retreat time was varied in each case, the retreat to

initial steady state in step 2 was obtained in every cases.

Table 4.5. Comparison of the time needed to reach the steady state in step 3 and 4

| Intake Ratio; Q_B/Q_A | 0.9 | 1.2 | 1.5 | 2.0 | 2.6 |
|---|------------|------------|------------|------------|------------|
| Step 3; intrusion time (min) | 90 | 70 | 80 | 130 | 70 |
| Step 4; retreat time (min) | 120 | 40 | 80 | 100 | 80 |

Table 4.6 shows the relationship between the intake amount from well A and the retreat time recorded in step 4 at intake ratios of 0.9, 1.2, and 1.5, at which saltwater did not reach well B. With large intake amount from well A, the retreat time was clearly shortened. Therefore, it is assumed that saltwater retreat time can be shortened by high intake amount from a barrier well.

Table 4.6. Relationship between intake from well A and the retreat time

| Intake Ratio; Q_B/Q_A | 1.2 | 1.5 | 0.9 |
|--|------------|------------|------------|
| Water intake from well A; Q_A (ml/s) | 2.9 | 2.5 | 1.8 |
| Step 4; retreat time (min) | 40 | 80 | 120 |

4.5. Step 5: Retreat process of saltwater intrusion without pumping

For convenience, this step was only performed in the cases of $R=1.5$, 1.9, and 2.6. Intrusion time recorded in step 2 and retreat time in step 5 with varying intake amounts from the well A are compared as shown in Table 4.7. As a result, the retreat process was faster than the intrusion process.

Table 4.7. Comparison of the time needed to reach the steady state in step 2 and 5

| Water intake from well A; Q_A (ml/s) | 2.7 | 2.5 | 2.2 |
|--|------------|------------|------------|
| Step 2; intrusion time (min) | 110 | 130 | 130 |
| Step 5; retreat time (min) | 90 | 120 | 100 |

Figure 4.12 shows photographs at the very beginning of step 5, then at 5, 10, and 20 minutes after turning off well A. It was clearly observed that the unconing towards well A disappeared within only 5 minutes. Once the unconing disappeared, the shape of the salt-freshwater interface reversed to its curving position. In addition, Figure 4.13 shows the intrusion length of saltwater in this step. Within 10 minutes, the saltwater toe was observed to slightly advance forward to the freshwater zone before the actual measured retreat started. After 10 minutes, saltwater wedge kept retreating until it reached steady-state position.

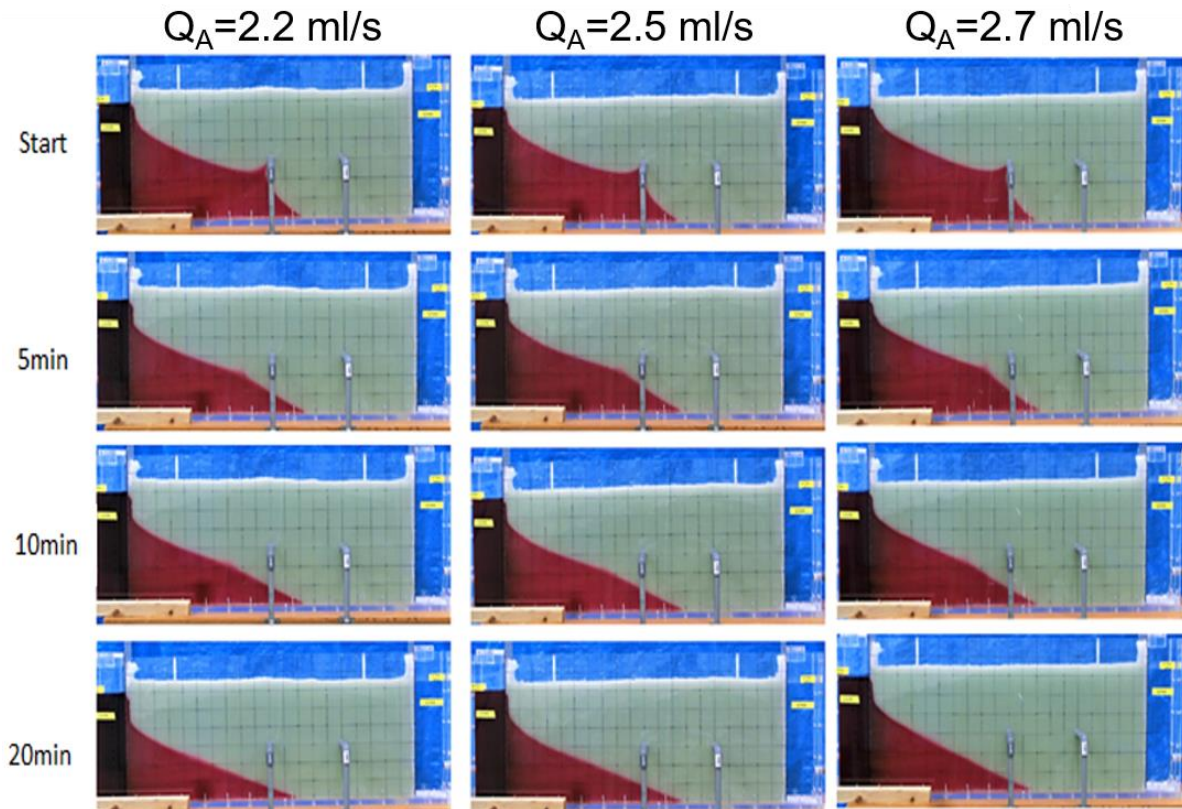


Figure 4.12. Behavior of saltwater in step 5 at the beginning 20 minutes

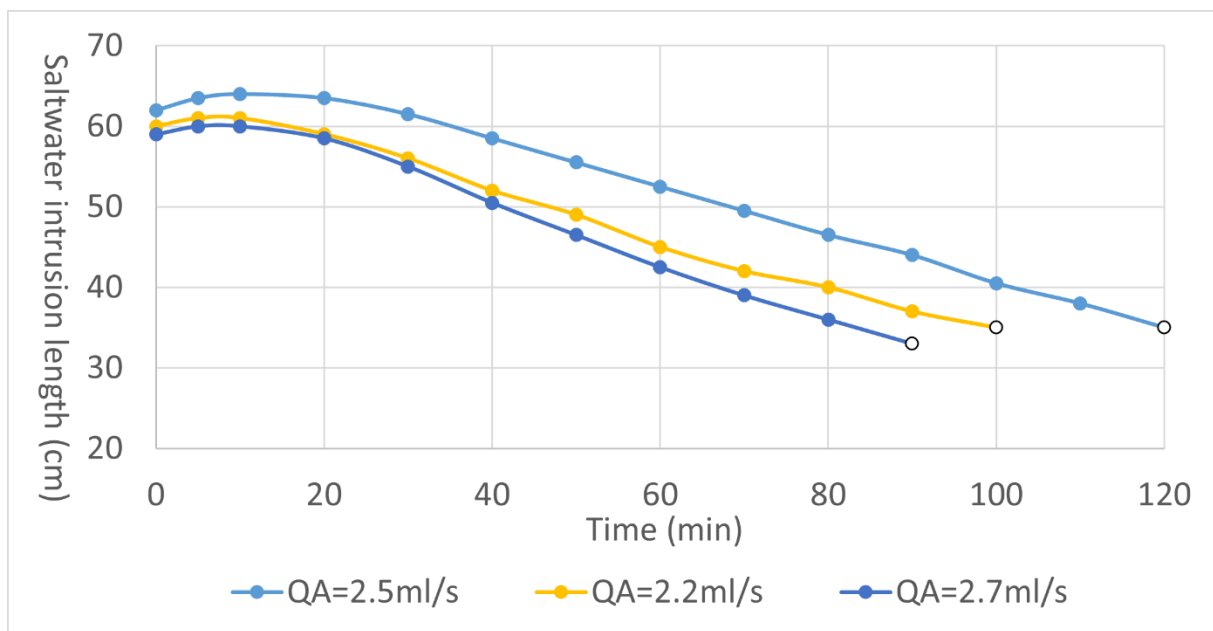


Figure 4.13. Changes in saltwater intrusion length over time in step 5

Furthermore, since the shape of saltwater at the steady state in step 5 was similar to that in step 1, the two were compared in Figure 4.14. The comparison shows that the steady state after retreating is mostly restored. However, the area invaded by the saltwater in step 5 was larger than that during initial invasion.

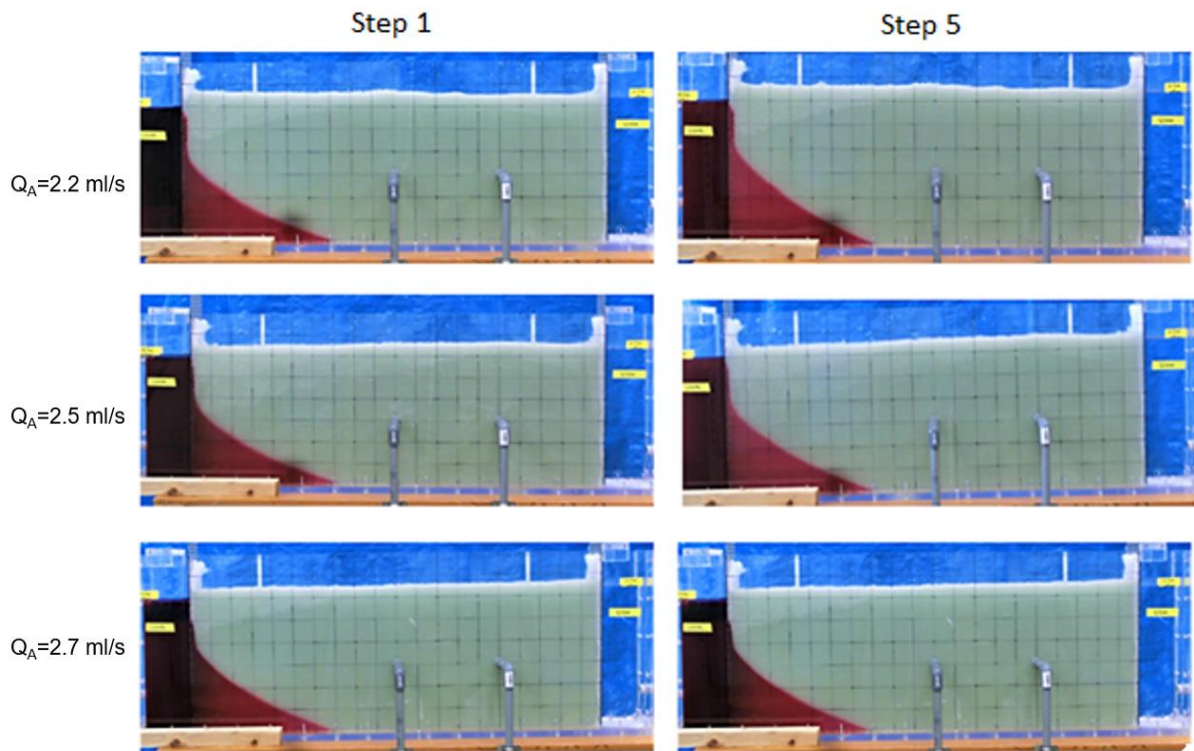


Figure 4.14. Comparison of saltwater intrusion in step 1 and step 5

5. Methodology

In this chapter the methodology of numerical analysis using two-dimensional solute transport model is described. This chapter is mainly divided into three sections: conceptual model, mathematical model, and numerical model.

5.1. Analysis conditions

Numerical simulation was conducted under to reproduce the results obtained from lab-scale experiments with different hydraulic conductivity and pumping rates of barrier well and production well. Through this simulation, the validity of this model was confirmed by comparing experimental and simulated results in terms of the saltwater intrusion length and the shape of salt-freshwater interface over time. Moreover, a sensitivity analysis was carried out under the condition of step 1 to examine the influence of model parameters, such as hydraulic conductivity, longitudinal and transverse dispersion lengths, and extrapolation factor used for SOR method as described below.

The following sections explain the conceptual model, mathematical model, and numerical model, respectively.

5.2. Conceptual model

Figure 5.1 shows the conceptual model used to simulate saltwater intrusion. The conceptual model is two-dimensional model and divided into three parts, saltwater zone, permeation zone, and freshwater zone as well as the experimental device. Boundary conditions are assigned to 6 boundaries, 2 vertical boundaries, saltwater boundary, top boundaries for saltwater and freshwater and bottom boundary. No recharge flow is assigned to the bottom boundary. Pumping well A and well B are located in the middle part of the model. Well A and B are positioned 61.0 cm and 86.0 cm away from the left boundary, respectively. The depths of well A and B are both 15.0 cm from the bottom boundary.

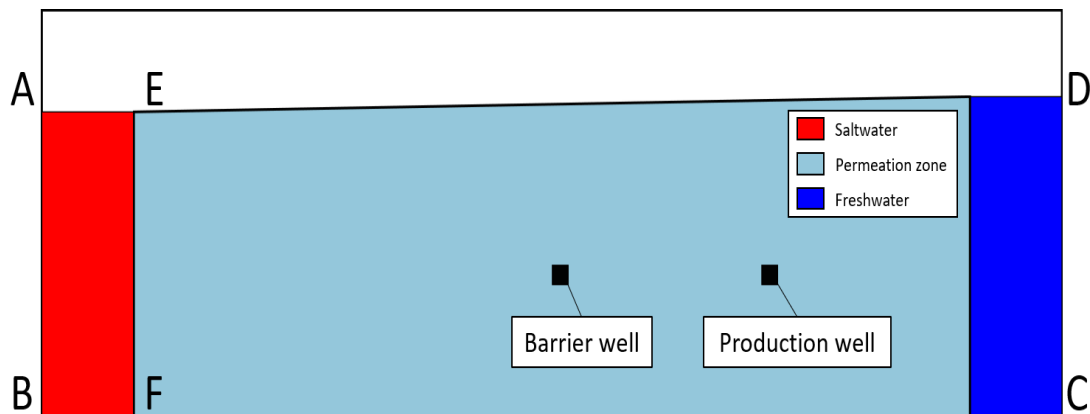


Figure 5.1. Conceptual model for numerical simulation

5.3. Mathematical model

A two-dimensional density dependent solute transport model was used as mathematical model in the present study. The model is composed of groundwater flow equation and solute transport equation for advection and dispersion transport.

5.3.1. Groundwater flow equation

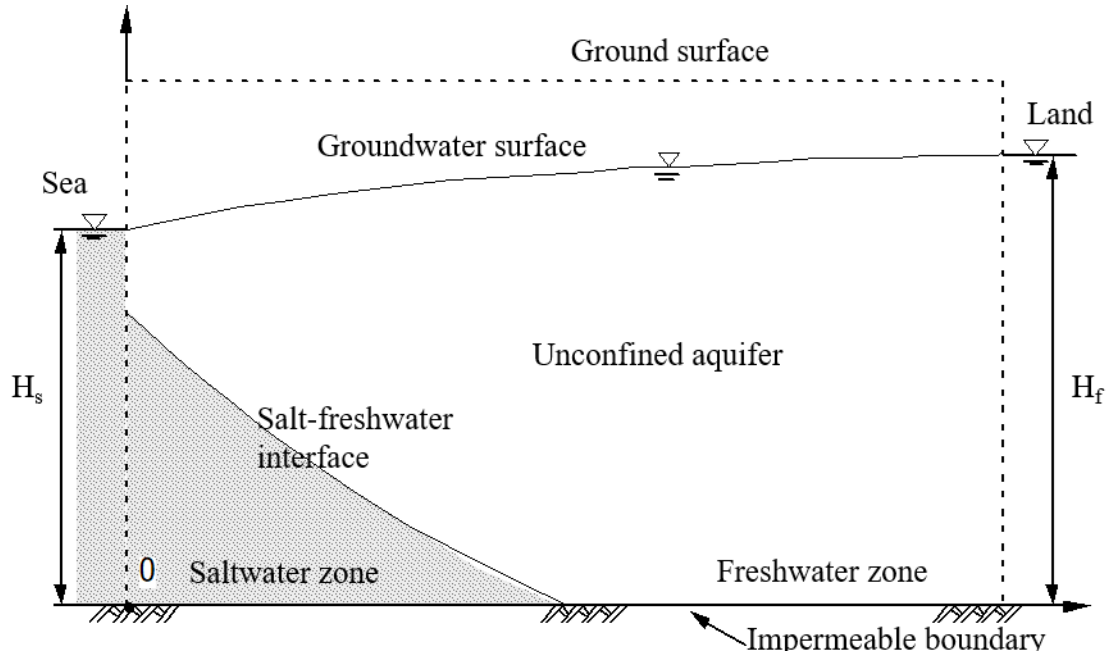


Figure 5.2. Cross section of an unconfined aquifer in coastal region

Figure 5.2 shows a vertical cross section of an unconfined aquifer in a coastal region. Two-dimensional fundamental equations for the potential head in saturated-unsaturated aquifers can be described as follows:

$$(C_w + \alpha_0 S) \frac{\partial h}{\partial t} = -\frac{\partial u}{\partial x} - \frac{\partial v}{\partial y} \quad (5.1)$$

$$u = -k \frac{\partial h}{\partial x} \quad (5.2)$$

$$v = -k \left(\frac{\partial h}{\partial y} + \frac{\rho}{\rho_f} \right) \quad (5.3)$$

where, t is the time period, h is the potential head, k is the hydraulic conductivity, u and v are the Darcy's velocities in x and y directions, respectively, ρ is the fluid density, and ρ_f is the density of freshwater, C_w is the specific moisture capacity, S is the specific storage coefficient, α is the dummy parameter that takes 0 in the unsaturated condition and 1 in the saturated condition. The specific storage coefficient represents the amount of water that is stored in soil per unit volume when the hydraulic head in the unit is raised. It is known that the specific storage coefficient ranges in 10^{-1} to 10^{-2} cm^{-1} in unconfined aquifers and 10^{-6} to 10^{-7} cm^{-1} in confined aquifers (Jinno et al., 2001).

With the volumetric water content, θ , the specific moisture capacity is defined as:

$$C_w = \frac{d\theta}{dh} \quad (5.4)$$

In the saturated zone, the specific moisture capacity is equal to 0.

5.3.1.1 Saturated-unsaturated flow equation in two dimensions

The continuity equation takes into account the mass balance of water inside an infinitesimal control

volume with dimensions x and y in the two-dimensional space (Figure 5.3). Knowing that there is no sink or source inside the control volume, the process of governing Equation (5.1) is explained in the following part under unsaturated and saturated aquifer, respectively.

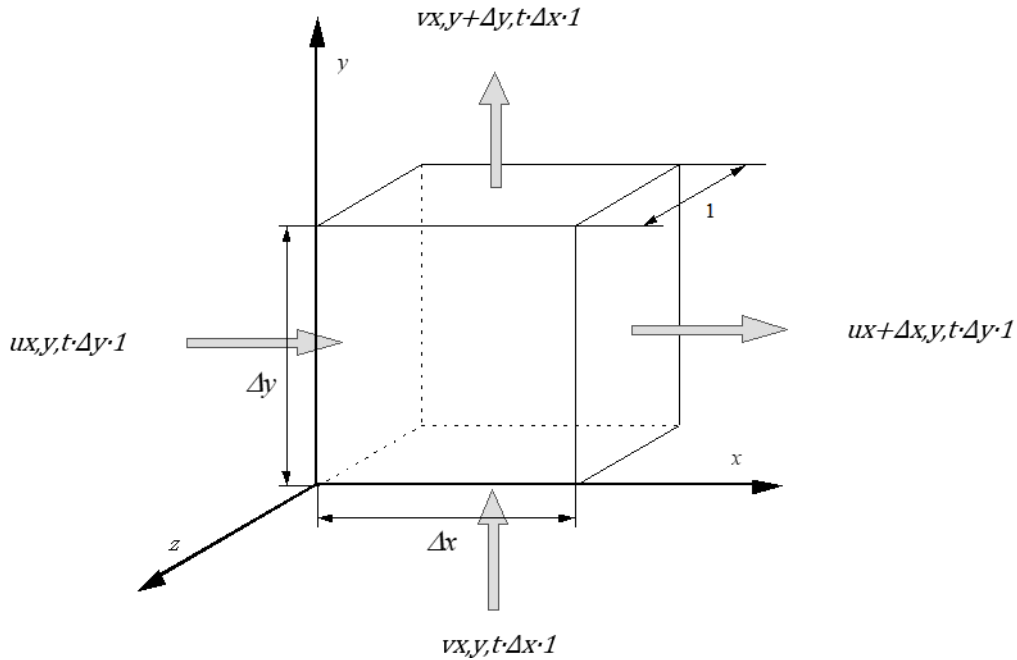


Figure 5.3. Mass balance of water inside the infinitesimal control volume

(1) Unsaturated condition

The mass balance in x direction can be described as:

$$(u(x, y, t) \cdot \Delta y \cdot 1 - u(x + \Delta x, y, t) \cdot \Delta y \cdot 1) \cdot \Delta t = \frac{\partial u}{\partial x} \cdot \Delta x \cdot \Delta y \cdot \Delta t \cdot 1 \quad (5.5)$$

In the same way, the mass balance in y direction can be described as:

$$(v(x, y, t) \cdot \Delta x \cdot 1 - v(x, y + \Delta y, t) \cdot \Delta x \cdot 1) \cdot \Delta t = \frac{\partial v}{\partial y} \cdot \Delta x \cdot \Delta y \cdot \Delta t \cdot 1 \quad (5.6)$$

Combing these equations, the amount of mass stored in the unsaturated zone is written as:

$$-\frac{\partial u}{\partial x} \cdot \Delta x \cdot \Delta y \cdot \Delta t \cdot 1 + \left(-\frac{\partial v}{\partial y} \cdot \Delta x \cdot \Delta y \cdot \Delta t \cdot 1 \right) \quad (5.7)$$

This amount can be equal to the water amount that is stored in the unit volume per unit time, Δt . Thus, it is written as:

$$\Delta\theta \cdot \Delta x \cdot \Delta y = -\frac{\partial u}{\partial x} \cdot \Delta x \cdot \Delta y \cdot \Delta t + \left(-\frac{\partial v}{\partial y} \cdot \Delta x \cdot \Delta y \cdot \Delta t \right) \quad (5.8)$$

Above expression can be reduced to:

$$\frac{\Delta\theta}{\Delta t} = -\frac{\partial u}{\partial x} - \frac{\partial v}{\partial y} \quad (5.9)$$

This can be written as:

$$\frac{\partial\theta}{\partial h} \frac{\partial h}{\partial t} = -\frac{\partial u}{\partial x} - \frac{\partial v}{\partial y} \quad (5.10)$$

Thus, using the specific moisture content, C_w , the continuity equation in the unsaturated zone can be written as:

$$C_w(h) \frac{\partial h}{\partial t} = -\frac{\partial u}{\partial x} - \frac{\partial v}{\partial y} \quad (5.11)$$

(2) Saturated condition

Assuming the saturated unconfined aquifer, the mass balance in x and y direction can be described respectively as follows:

$$(u(x, y, t) \cdot \Delta y \cdot 1 - u(x + \Delta x, y, t) \cdot \Delta y \cdot 1) \cdot \Delta t = \frac{\partial u}{\partial x} \cdot \Delta x \cdot \Delta y \cdot \Delta t \cdot 1 \quad (5.12)$$

$$(v(x, y, t) \cdot \Delta x \cdot 1 - v(x, y + \Delta y, t) \cdot \Delta x \cdot 1) \cdot \Delta t = \frac{\partial v}{\partial y} \cdot \Delta x \cdot \Delta y \cdot \Delta t \cdot 1 \quad (5.13)$$

Thus, the mass amount that is stored in saturated zone is written as:

$$-\frac{\partial u}{\partial x} \cdot \Delta x \cdot \Delta y \cdot \Delta t \cdot 1 + \left(-\frac{\partial v}{\partial y} \cdot \Delta x \cdot \Delta y \cdot \Delta t \cdot 1 \right) \quad (5.14)$$

This equation represents the water amount that is stored in the infinitesimal volume ($\Delta x \times \Delta y \times 1$) per infinitesimal time, Δt . Applying this unit amount to whole width in the aquifer, it is equal to the increment of groundwater level per unit area with Δt :

$$n_e \cdot \Delta h \cdot \Delta x = -\frac{\partial u}{\partial x} \cdot \Delta x \cdot m \cdot \Delta t + \left(-\frac{\partial v}{\partial y} \cdot \Delta x \cdot m \cdot \Delta t \right) \quad (5.15)$$

where, n_e is the possible porosity. Above can be reduced to:

$$\frac{n_e \Delta h}{m \Delta t} = -\frac{\partial u}{\partial x} - \frac{\partial v}{\partial y} \quad (5.16)$$

Assuming that Δt approaches 0, the following equation can be obtained:

$$\frac{n_e \partial h}{m \partial t} = -\frac{\partial u}{\partial x} - \frac{\partial v}{\partial y} \quad (5.17)$$

According to the definition of specific storage coefficient, it can be written as

$$S = \frac{n_e}{m} \quad (5.18)$$

Substituting this to Equation (5.17), the continuity equation in saturated zone can be described as:

$$S \frac{\partial h}{\partial t} = -\frac{\partial u}{\partial x} - \frac{\partial v}{\partial y} \quad (5.19)$$

Therefore, combining both equations for unsaturated and saturated zone, the following equation is obtained:

$$\{C_w(h) + \alpha_0 S\} \frac{\partial h}{\partial t} = -\frac{\partial u}{\partial x} - \frac{\partial v}{\partial y} \quad (5.20)$$

5.3.1.2. van Genuchten formula for unsaturated zone

The model can solve the pressure head in both saturated and unsaturated zones. To calculate the unsaturated zone flow, the unsaturated flow parameters such as the volumetric water content, θ , the ratio

of saturated hydraulic conductivity, k_s , and the unsaturated hydraulic conductivity, k , and the specific moisture capacity, C_w . are needed. However, in the lab-scale experiments, these parameters were not examined. Therefore, the following formulas for unsaturated flow parameters suggested by van Genuchten (1980) were used. With these formulas, the relationship between the negative pressure head and the unsaturated flow parameters mentioned above was obtained.

$$Se = \frac{\theta - \theta_r}{\theta_s - \theta_r}, Se = \left[\frac{1}{1 + (\alpha|h|)^n} \right]^m \quad (5.21)$$

$$k_r = Se^{\frac{1}{2}} \left\{ 1 - \left(1 - Se^{\frac{1}{m}} \right)^m \right\}^2 \quad (5.22)$$

$$C_w = \frac{\alpha \cdot m(\theta_s - \theta) Se^{\frac{1}{m}} \left(1 - Se^{\frac{1}{m}} \right)^m}{1 - m} \quad (5.23)$$

where, θ_r is the residual water content, θ_s is the saturated water content and α , m , and n are the coefficient of the van Genuchten formula. Referring to Jinno et al., these parameters are determined and presented in Table 5.1 (Jinno et al., 2001).

Table 5.1. Parameters for van Genuchten formula

| | | |
|--------------------------------|----------------------------|---------------|
| Saturated water content | | 0.342 |
| Residual water content | | 0.075 |
| Coefficient | <i>α</i> | 0.0491 (cm/s) |
| | <i>m</i> | 0.8599 |
| | <i>n</i> | 7.138 |

5.3.2. Two-dimensional solute transport equation for advection and dispersion

In two-dimensional transient groundwater systems, the fundamental equation for the solute concentration, C , can be written as:

$$\begin{aligned} & \frac{\partial(\theta C)}{\partial t} + \frac{\partial(u'\theta C)}{\partial x} + \frac{\partial(v'\theta C)}{\partial y} \\ &= \frac{\partial}{\partial x} \left(\theta D_{xx} \frac{\partial C}{\partial x} + \theta D_{xy} \frac{\partial C}{\partial y} \right) + \frac{\partial}{\partial y} \left(\theta D_{yy} \frac{\partial C}{\partial y} + \theta D_{yx} \frac{\partial C}{\partial x} \right) \end{aligned} \quad (5.24)$$

where, C is the solute concentration, θ is the volumetric water content, u' and v' are real pore velocities in x and y direction, respectively. Using Darcy's velocity, u and v are described as:

$$u' = \frac{u}{\theta}, v' = \frac{v}{\theta} \quad (5.25)$$

The product of volumetric water content and dispersion coefficient, θD_{xx} , θD_{xy} , θD_{yx} , and θD_{yy} , are expressed as:

$$\theta D_{xx} = \frac{\alpha_L u^2}{V} + \frac{\alpha_T v^2}{V} + \theta D \quad (5.26)$$

$$\theta D_{yy} = \frac{\alpha_T u^2}{V} + \frac{\alpha_L v^2}{V} + \theta D_M \quad (5.27)$$

$$\theta D_{xy} = \theta D_{yx} = \frac{(\alpha_L - \alpha_T) uv}{V} \quad (5.28)$$

V is the magnitude of the velocity vector which is written as:

$$V = (u^2 + v^2)^{\frac{1}{2}} \quad (5.29)$$

where D_{xx} and D_{yy} are the principal components of the dispersion tensor, D_{xy} and D_{yx} are the cross terms of the dispersion tensor, α_L and α_T are the longitudinal dispersion length and the transverse dispersion length, respectively, and D_M is the molecular diffusion coefficient. When the velocity vector is aligned with one of the coordinate axes, all cross terms become zero.

The relationship between the salt concentration of water and fluid densities (Dierch & Koldditz, 2002):

$$C = \frac{\rho - \rho_f}{\rho_s - \rho_f} \times 100(\%) \quad (5.30)$$

where C is the salt concentration of water in the flow domain, ρ_f and ρ_s are the density of freshwater and saltwater, respectively.

The governing process for Equation (5.24) is explained in the following chapter.

5.3.2.1 Governing equation process

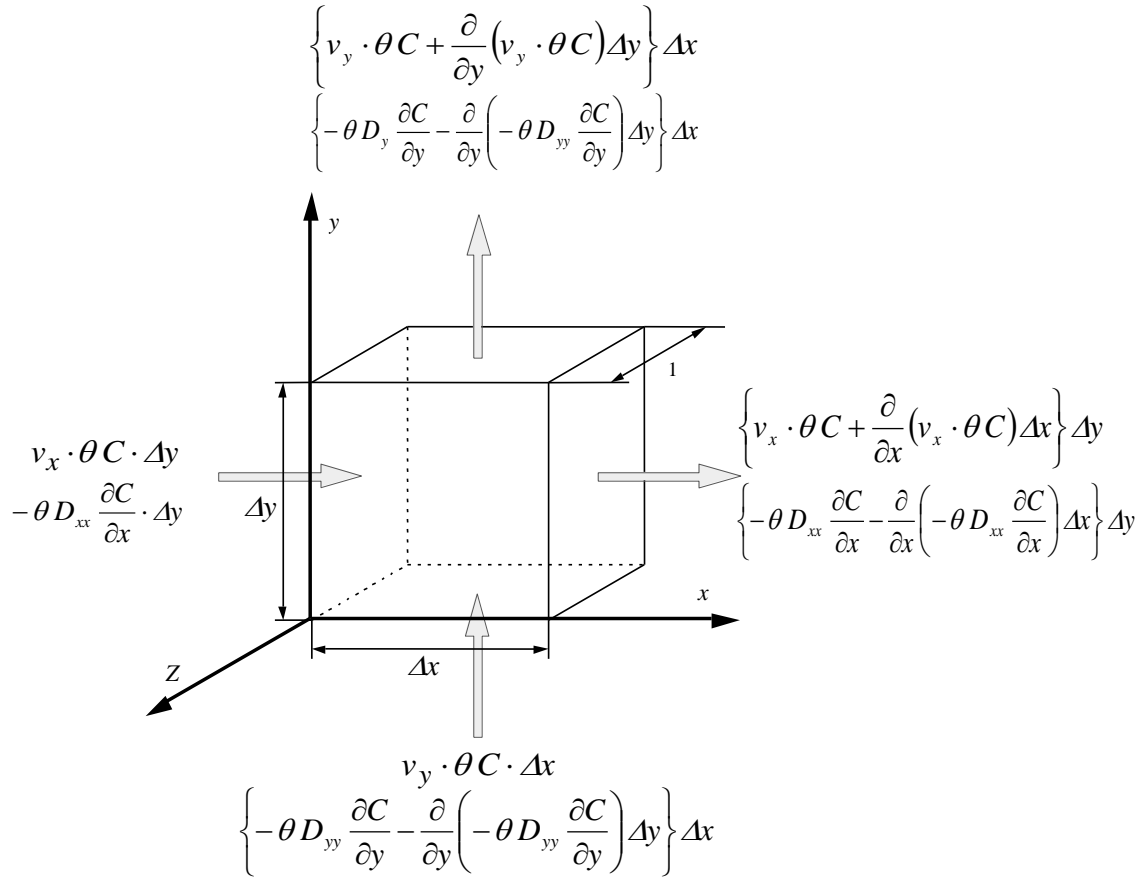


Figure 5.4. Mass balance of the solute concentration inside an infinitesimal control volume

Figure 5.4 illustrates the mass balance of the solute concentration inside an infinitesimal control volume with dimensions x and y in the two-dimensional space. The mass balance can be divided into advection and dispersion components. At first, the mass balance in x direction by advection can be written as:

$$u \cdot \theta C \cdot \Delta y - \left\{ u \cdot \theta C + \frac{\partial}{\partial x} (u \cdot \theta C) \cdot \Delta x \right\} \cdot \Delta y \quad (5.31)$$

Regarding the dispersion component, the mass balance can be written as:

$$-\theta D_{xx} \frac{\partial C}{\partial x} \cdot \Delta y - \left\{ -\theta D_{xx} \frac{\partial C}{\partial x} - \frac{\partial}{\partial x} \left(-\theta D_{xx} \frac{\partial C}{\partial x} \right) \cdot \Delta x \right\} \cdot \Delta y \quad (5.32)$$

As well as in x direction, the mass balance in y direction considering advection component is described as:

$$v \cdot \theta C \cdot \Delta x - \left\{ v \cdot \theta C + \frac{\partial}{\partial y} (v \cdot \theta C) \cdot \Delta y \right\} \cdot \Delta x \quad (5.33)$$

The mass balance of dispersion component is:

$$-\theta D_{yy} \frac{\partial C}{\partial y} \cdot \Delta x - \left\{ -\theta D_{yy} \frac{\partial C}{\partial y} - \frac{\partial}{\partial y} \left(-\theta D_{yy} \frac{\partial C}{\partial y} \right) \cdot \Delta y \right\} \cdot \Delta x \quad (5.34)$$

Thus, solute concentrations stored in the control volume in advection and dispersion terms are written,

respectively:

$$-\frac{\partial}{\partial x}(u \cdot \theta C) \cdot \Delta x \cdot \Delta y - \frac{\partial}{\partial y}(v \cdot \theta C) \cdot \Delta x \cdot \Delta y \quad (5.35)$$

$$\frac{\partial}{\partial x}\left(\theta D_{xx} \frac{\partial C}{\partial x}\right) \cdot \Delta x \cdot \Delta y + \frac{\partial}{\partial y}\left(\theta D_{yy} \frac{\partial C}{\partial y}\right) \cdot \Delta x \cdot \Delta y \quad (5.36)$$

The sum of these equation is equal to the change of solute concentration in the control box.

$$\begin{aligned} \Delta x \cdot \Delta y \cdot \frac{\partial(\theta C)}{\partial t} &= -\frac{\partial}{\partial x}(u \cdot \theta C) \cdot \Delta x \cdot \Delta y - \frac{\partial}{\partial y}(v \cdot \theta C) \cdot \Delta x \cdot \Delta y \\ &+ \frac{\partial}{\partial x}\left(\theta D_{xx} \frac{\partial C}{\partial x}\right) \cdot \Delta x \cdot \Delta y + \frac{\partial}{\partial y}\left(\theta D_{yy} \frac{\partial C}{\partial y}\right) \cdot \Delta x \cdot \Delta y \end{aligned} \quad (5.37)$$

The above can be reduced to:

$$\frac{\partial(\theta C)}{\partial t} = -\frac{\partial}{\partial x}(u \cdot \theta C) - \frac{\partial}{\partial y}(v \cdot \theta C) + \frac{\partial}{\partial x}\left(\theta D_{xx} \frac{\partial C}{\partial x}\right) + \frac{\partial}{\partial y}\left(\theta D_{yy} \frac{\partial C}{\partial y}\right) \quad (5.38)$$

Converting the above equation cartesian coordinate to polar coordinate, the following equation is obtained:

$$\frac{\partial(\theta C)}{\partial t} + \frac{\partial(u' \theta C)}{\partial x} + \frac{\partial(v' \theta C)}{\partial y} = \frac{\partial}{\partial x}\left(\theta D_{XX} \frac{\partial C}{\partial x} + \theta D_{XY} \frac{\partial C}{\partial y}\right) + \frac{\partial}{\partial y}\left(\theta D_{YX} \frac{\partial C}{\partial x} + \theta D_{YY} \frac{\partial C}{\partial y}\right) \quad (5.39)$$

The products of volumetric water content and dispersion coefficient are rewritten to in XY-direction as:

$$\theta D_{XX} = \theta D_{xx} \cos^2 \theta + \theta D_{yy} \sin^2 \theta \quad (5.40)$$

$$\theta D_{XY} = \theta D_{YX} = (\theta D_{xx} - \theta D_{yy}) \cos \theta \sin \theta \quad (5.41)$$

$$\theta D_{YY} = \theta D_{xx} \sin^2 \theta + \theta D_{yy} \cos^2 \theta \quad (5.42)$$

5.3.3 Mathematical solution

The finite difference method is used to solve the groundwater flow equation, and the method of characteristics is used to solve the solute transport equation. Numerical implementation of the finite difference method and method of characteristics are described below.

(1) Groundwater flow equation

The pressure head, h , is calculated by implicit finite difference method. The partial differential equation can be written as below, following the coordinates of differential grid shown in Figure 5.5:

$$(Cw_{i,j}^{n+1/2} + \alpha_0 S) \frac{h_{i,j}^{n+1} - h_{i,j}^n}{\Delta t} = -\frac{u_{i+1/2,j}^{n+1} - u_{i-1/2,j}^{n+1}}{\frac{\Delta x_i + \Delta x_{i+1}}{2}} - \frac{v_{i,j+1/2}^{n+1} - v_{i,j-1/2}^{n+1}}{\Delta y} \quad (5.43)$$

where, Δt is the time increment, Δx and Δy are the grid interval in x and y direction, respectively, n is the time level in calculation, i and j are differential node in x and y direction, respectively.

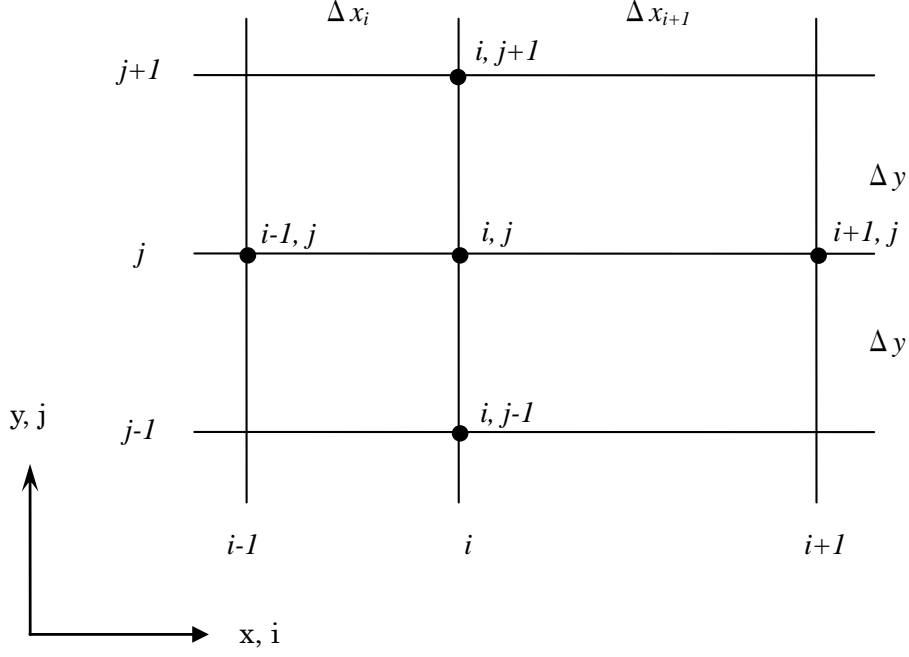


Figure 5.5. Coordinate of differential grids

Substituting Equation (5.2) and (5.3) into Equation (5.4) and rearranging for the pressure head, the following equations are obtained:

$$h_{i,j}^{n+1} = \frac{(b^{n+1} + c^{n+1} + d^{n+1})\Delta t + e^{n+\frac{1}{2}}h_{i,j}^n}{a^{n+1}\Delta t + e^{n+\frac{1}{2}}} \quad (5.43)$$

$$a^{n+1} = \frac{k_{i-1/2,j}^{n+1}/\Delta x_{i+1} + k_{i+1/2,j}^{n+1}/\Delta x_{i+1}}{\frac{\Delta x_i + \Delta x_{i+1}}{2}} + \frac{k_{i,j-1/2}^{n+1} + k_{i,j+1/2}^{n+1}}{\Delta y^2} \quad (5.44)$$

$$b^{n+1} = \frac{k_{i-1/2,j}^{n+1}h_{i-1,j}^{n+1}/\Delta x_{i+1} + k_{i+1/2,j}^{n+1}h_{i+1,j}^{n+1}/\Delta x_{i+1}}{\frac{\Delta x_i + \Delta x_{i+1}}{2}} \quad (5.45)$$

$$c^{n+1} = \frac{k_{i,j-1/2}^{n+1}h_{i,j-1}^{n+1} + k_{i,j+1/2}^{n+1}h_{i,j+1}^{n+1}}{\Delta y^2} \quad (5.46)$$

$$d^{n+1} = \frac{\frac{k_{i,j+1/2}^{n+1}\rho_{i,j+1/2}}{\rho_f} - \frac{k_{i,j-1/2}^{n+1}\rho_{i,j-1/2}}{\rho_f}}{\Delta y} \quad (5.47)$$

$$e^{n+1} = \frac{Cw_{i,j}^{n+1} + Cw_{i,j}^n}{2} + \alpha_0 S \quad (5.48)$$

The physical quantity at the grid point of $i+1/2$ or $j+1/2$ is calculated by the average of physical quantities between the grid points i and $i+1$ or j and $j+1$. The hydraulic conductivity is a function of suction, negative pressure head, which will change over time under unsaturated and saturated condition. Thus, the hydraulic conductivity, k in Eqn. (5.44-48), has an index n , meaning the time level.

Iterative computation is required for an implicit differential equation. In this study, this is why successive

over-relaxation method (SOR) is applied to this model for iterative computation. SOR is one of the iterative methods based on the Gauss-Seidel method. The extrapolation is applied to this method using a weighted average between the previous iterate and the computed Gauss-Seidel iterate successively for each component. Thus, applying this method to the Equation (5.12), the following iteration equation is obtained and used in this simulation:

$${}^{m+1}h_{i,j}^{n+1} = {}^m h_{i,j}^{n+1} + \omega(h_{i,j}^{n+1} - {}^m h_{i,j}^{n+1}) \quad (5.49)$$

where, x denotes a Gauss-Seidel iterate, and ω is the extrapolation factor, m is the number of iterations. The convergence of the iteration computation is judged when the difference of the pressure heads between iterative numbers m and $m+1$ becomes smaller than the judgement criteria ε_0 .

$$|{}^{m+1}h_{i,j}^{n+1} - {}^m h_{i,j}^{n+1}| < \varepsilon_0 \quad (5.50)$$

where, ε_0 is the judgement criteria.

(2) Solute transport equation

Under the groundwater flow condition of this study, the partial change of velocity distribution in the mixing zone of saltwater and freshwater is expected, needing an accurate numerical solution to calculate the concentration flux caused by advection. To solve this problem, the method of characteristics is applied.

The method of characteristics is developed from a conventional partial tracking technique. Particles are distributed in the model field randomly or regularly. Each particle is associated with concentration and coordinates. These particles are exposed to the flow and transported from the initial positions by the flow in each time increment. Tracking the positions of particles within every time increment, the concentrations of particles located in a target cell are recorded and the mean concentration among the recorded concentrations are evaluated as the concentration at the cell. The method has an advantage that the accuracy and stability of the solution are high when the advection domains in the flow rather than the dispersion. The below explained is the procedure and numerical implementation of the method of characteristics. At first, the fundamental theory of the method of characteristics in one direction is explained below.

Advection-dispersion equation in one direction is written as:

$$\frac{\partial C}{\partial t} + u \frac{\partial C}{\partial x} = D \frac{\partial^2 C}{\partial x^2} \quad (5.51)$$

where C is the solute concentration, u is the velocity in x direction, and D is the dispersion coefficient that is described as:

$$D = \alpha_L u' \quad (5.52)$$

where α_L is the longitudinal dispersion length.

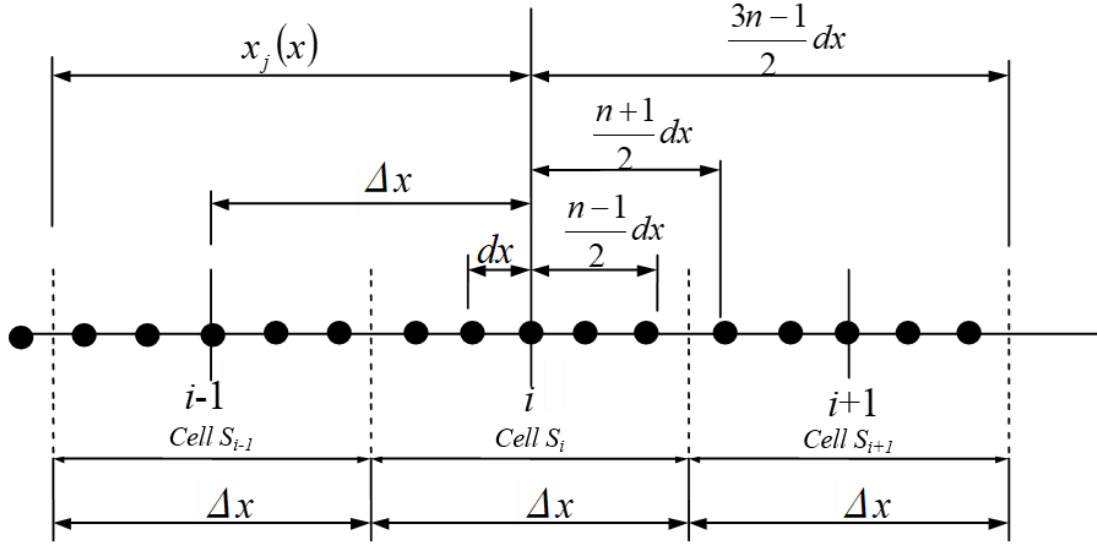


Figure 5.6. Illustration of method of characteristic in one direction

As shown in Figure 5.6, numerous particles are distributed within the whole areas. Each particle has a certain concentration, and the number of each particle is counted as K . Knowing that there are M particles within the cell of S_i at the node of i , the average concentration within the cell is represented as:

$$\bar{C}_i^n = \frac{1}{M} \sum_{K_i=1}^M C^n(K_i) \quad (5.53)$$

where, \bar{C}_i^n is the average concentration at node i , M is the number of particles, n is the time level,

$C^n(K)$ is the concentration of the particle K at time level n , K_i is the particle number in cell S_i .

Differentiating the right term of Equation (5.51) using Equation (5.53), the concentration increment at node i is calculated by:

$$\delta C_i^{n+1} = \frac{kD_i}{\Delta x^2} (\bar{C}_{i+1}^n - 2\bar{C}_i^n + \bar{C}_{i-1}^n) \quad (5.54)$$

At new time level $n+1$, the concentration at the node of i can be described as:

$$C_i^{n+1} = \bar{C}_i^n + \delta C_i^{n+1} \quad (5.55)$$

In Equation (5.54), the concentration increment at the node is regarded as the increase of particle concentration within the cell. Therefore, the gap of the concentration increment between adjacent nodes directly decides the gap of concentration increment of whole particles located within the adjacent cells. This deviation leads to discontinuity of particle concentrations, causing an error on the numerical solution. To reduce discontinuity as much as possible, it is assumed that the change of concentration increment between adjacent cells is a linear relationship. Then, this straight line is calculated using δC_{i-1}^{n+1} with δC_i^{n+1} , and δC_i^{n+1} with δC_{i+1}^{n+1} . Thus, the concentration increment of particle K within cell S_i can be described as:

$$\delta C_i^{n+1}(K) = \delta C_i^{n+1} + \xi \frac{\partial}{\partial x} (\delta C)_i^{n+1} \quad (5.56)$$

where, ξ is the deviation between the particle and node i shown in Figure 5.7 ($\xi = x^{n+1}(K) - ih$).

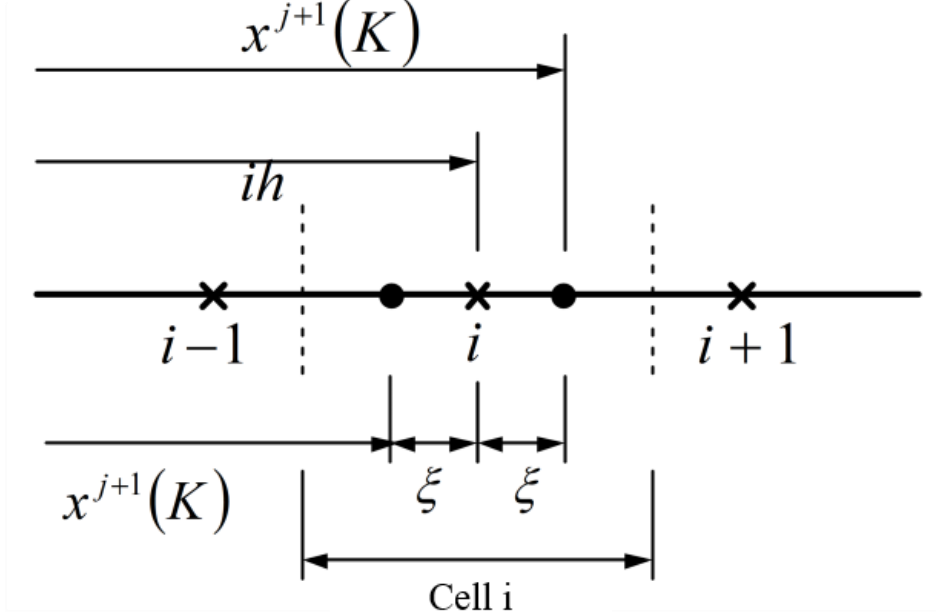


Figure 5.7. Deviation between the particle and node i

The calculation of this deviation is divided into two cases as below.

(i) $\xi \geq 0$

$$\frac{\partial}{\partial x} (\delta C)_i^n = \frac{(\delta C_{i+1}^{n+1} - \delta C_i^{n+1})}{h} \quad (5.57)$$

(ii) $\xi < 0$

$$\frac{\partial}{\partial x} (\delta C)_i^n = \frac{(\delta C_i^{n+1} - \delta C_{i-1}^{n+1})}{h} \quad (5.58)$$

The procedure of the method of characteristic in two-dimensional advection-dispersion equation is explained below.

The two-dimensional advection-dispersion equation is written as:

$$\frac{\partial(\theta C)}{\partial t} = \frac{\partial}{\partial x} \left(\theta D_{xx} \frac{\partial C}{\partial x} + \theta D_{xy} \frac{\partial C}{\partial y} \right) + \frac{\partial}{\partial y} \left(\theta D_{yy} \frac{\partial C}{\partial y} + \theta D_{yx} \frac{\partial C}{\partial x} \right) \quad (5.59)$$

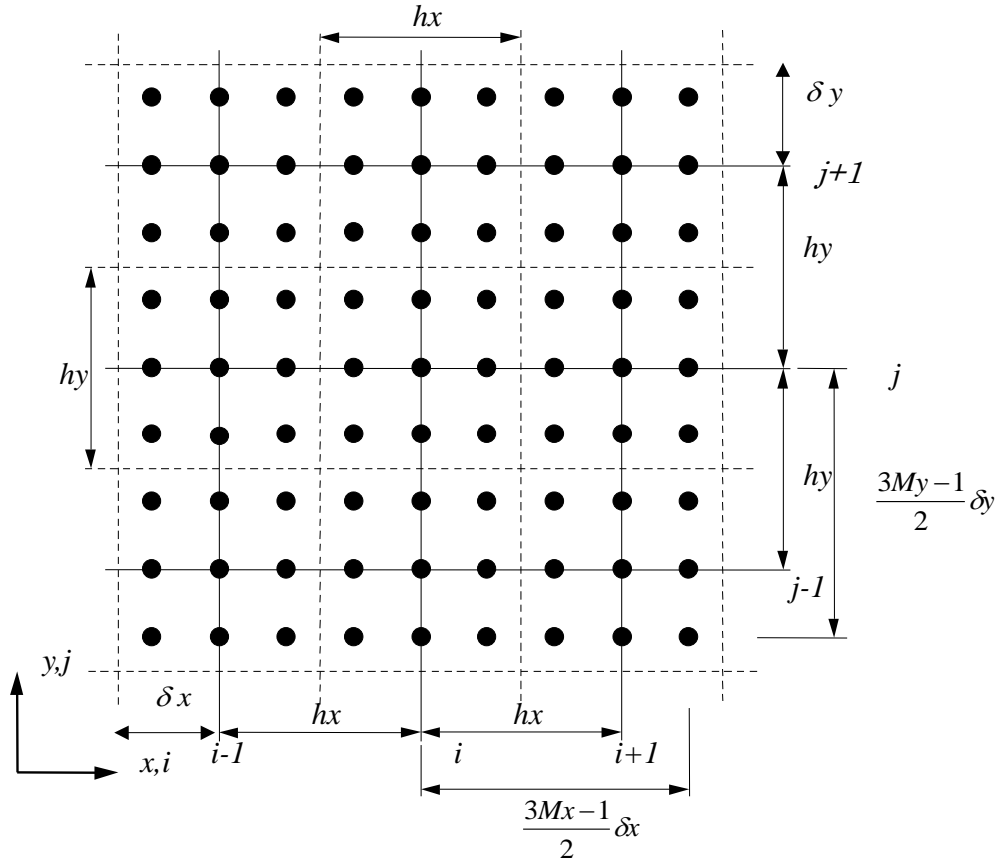


Figure 5.8. Two-dimensional distribution of particles

As shown in Figure 5.8, M_x particles and M_y particles are distributed in x and y direction, respectively, within each cell. The arithmetic mean of the particle concentration within the cell can be calculated using the following equation:

$$\overline{C_{i,j}^n} = \frac{1}{M_x M_y} \sum_{K_i}^{M_x M_y} C^n(K_i) \quad (5.60)$$

where, $\overline{C_{i,j}^n}$ is the arithmetic mean concentration, $C^n(K)$ is the concentration of particle K at node (i, j) at time level n .

Differentiating Equation (5.59) with Equation (5.60), the concentration increment at each node is described as:

$$\delta C_{i,j}^{n+1} = \frac{1}{\theta} \Delta t \left[\begin{aligned} & \frac{1}{hx^2} \left\{ D_{i+\frac{1}{2},j}^{xx} (\overline{C_{i+1,j}^{n+1}} - \overline{C_{i,j}^{n+1}}) - D_{i-\frac{1}{2},j}^{xx} (\overline{C_{i,j}^{n+1}} - \overline{C_{i-1,j}^{n+1}}) \right\} \\ & + \frac{1}{4hxhy} \left\{ D_{i+1,j}^{xy} (\overline{C_{i+1,j+1}^{n+1}} - \overline{C_{i+1,j-1}^{n+1}}) - D_{i-1,j+1}^{xy} (\overline{C_{i-1,j+1}^{n+1}} - \overline{C_{i-1,j-1}^{n+1}}) \right\} \\ & + \frac{1}{4hxhy} \left\{ D_{i,j+1}^{yx} (\overline{C_{i+1,j+1}^{n+1}} - \overline{C_{i-1,j+1}^{n+1}}) - D_{i,j-1}^{yx} (\overline{C_{i+1,j-1}^{n+1}} - \overline{C_{i-1,j-1}^{n+1}}) \right\} \\ & + \frac{1}{hy^2} \left\{ D_{i,j+\frac{1}{2}}^{yy} (\overline{C_{i,j+1}^{n+1}} - \overline{C_{i,j}^{n+1}}) - D_{i,j-\frac{1}{2}}^{yy} (\overline{C_{i,j}^{n+1}} - \overline{C_{i,j-1}^{n+1}}) \right\} \end{aligned} \right] \quad (5.61)$$

where, h_x and h_y are cell lengths in x and y direction, respectively.

It is necessary to interpolate the deviation of particle from the node as well as in one direction (Figure 5.9). In this study, the change of concentration increment between adjacent nodes is assumed as a linear relationship. Equations for interpolation are:

$$\delta C(x^{n+1}(K), y^{n+1}(K)) = \delta C_{i,j}^{n+1} + \xi \frac{\partial}{\partial x} (\delta C)_{i,j}^{n+1} + \eta \frac{\partial}{\partial y} (\delta C)_{i,j}^{n+1} \quad (5.62)$$

(i) $\xi \geq 0, \eta \geq 0$

$$\frac{\partial}{\partial x} (\delta C) = \frac{\delta C_{i+1,j}^{n+1} - \delta C_{i,j}^{n+1}}{\Delta x}, \quad \frac{\partial}{\partial y} (\delta C) = \frac{\delta C_{i,j+1}^{n+1} - \delta C_{i,j}^{n+1}}{\Delta y} \quad (5.63)$$

(ii) $\xi \geq 0, \eta \leq 0$

$$\frac{\partial}{\partial x} (\delta C) = \frac{\delta C_{i+1,j}^{n+1} - \delta C_{i,j}^{n+1}}{\Delta x}, \quad \frac{\partial}{\partial y} (\delta C) = \frac{\delta C_{i,j}^{n+1} - \delta C_{i,j-1}^{n+1}}{\Delta y} \quad (5.64)$$

(iii) $\xi \leq 0, \eta \geq 0$

$$\frac{\partial}{\partial x} (\delta C) = \frac{\delta C_{i,j}^{n+1} - \delta C_{i-1,j}^{n+1}}{\Delta x}, \quad \frac{\partial}{\partial y} (\delta C) = \frac{\delta C_{i,j+1}^{n+1} - \delta C_{i,j}^{n+1}}{\Delta y} \quad (5.65)$$

(iv) $\xi \leq 0, \eta \leq 0$

$$\frac{\partial}{\partial x} (\delta C) = \frac{\delta C_{i,j}^{n+1} - \delta C_{i-1,j}^{n+1}}{\Delta x}, \quad \frac{\partial}{\partial y} (\delta C) = \frac{\delta C_{i,j}^{n+1} - \delta C_{i,j-1}^{n+1}}{\Delta y} \quad (5.66)$$

Therefore, the concentration of particle K at a new time step can be calculated using:

$$C^{n+1}(K) = C^n(K) + \delta C^{n+1}\{x^{n+1}(K), y^{n+1}(K)\} \quad (5.67)$$

The concentration at node (i, j) is:

$$C_{i,j}^{n+1} = \bar{C}_{i,j}^n + \delta C_{i,j}^{n+1} \quad (5.68)$$

Positions of the particle in x and y direction after time level n+1 is:

$$x^{n+1}(K) = x^n(K) + u(K)\Delta t \quad (5.69)$$

$$y^{n+1}(K) = y^n(K) + v(K)\Delta t \quad (5.70)$$

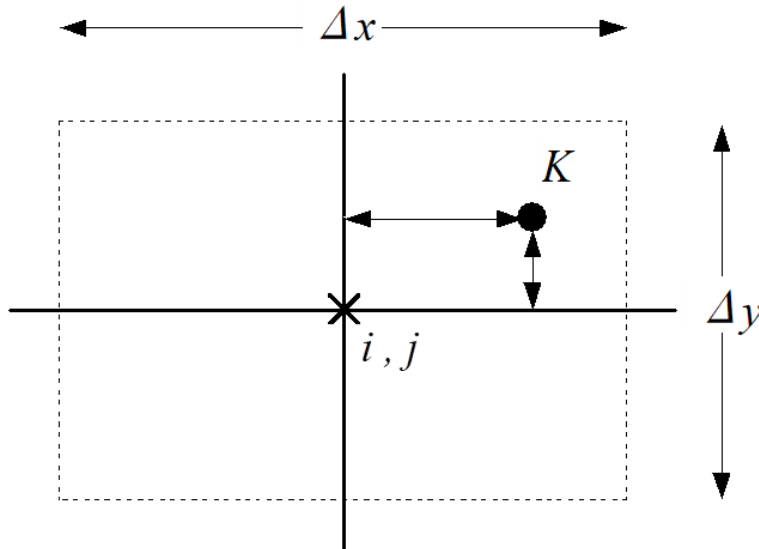


Figure 5.9. Interpolation of particle

5.3.4. Stability of calculation

The stability of the model used in this study was examined to avoid unexpected deviation of numerical solution. In the groundwater flow calculation, the implicit finite difference method was used, which indicates that the model is considered as stable. Regarding the two-dimensional advection-dispersion equation, the following stability conditions are used to examine the stability of the method of characteristics:

$$\frac{\Delta t D_{xx}}{\Delta x^2} < 0.47 \quad (5.71)$$

$$\frac{\Delta t D_{yy}}{\Delta y^2} < 0.47 \quad (5.72)$$

Moreover, the following limitations are given to avoid that particles are transported beyond each cell length during Δt due to advection:

$$\frac{\Delta t u'_{max}}{\Delta x} < 0.50 \quad (5.73)$$

$$\frac{\Delta t v'_{max}}{\Delta y} < 0.50 \quad (5.74)$$

where, D_{xx} and D_{yy} are dispersion coefficients in x and y direction, respectively, and u'_{max} and v'_{max} are the maximum velocity in x and y direction, respectively.

5.4 Numerical model

In this chapter, the numerical model conditions are explained.

The grid sizes and the time increment for the simulation are determined considering the condition of lab-scale experiments. The model domain for the solute transport model is divided with a grid length 0.5 cm in the x direction and 0.5 cm in y direction. The time increment is 0.5 seconds to meet the stability condition as mentioned above. Other parameters for the simulation are needed to be determined from available information. Hydraulic parameters including the hydraulic conductivity, salt and freshwater densities, porosity of glass beads and volumetric water content for the simulation are obtained from the laboratory experiment mentioned in chapter 3 and 4. Moreover, the longitudinal dispersion length and transverse dispersion length are calculated using the following formula reported by Harleman and Rumer (1963):

$$\frac{D_L}{v} = 0.66 \left(\frac{q'^{d_m}}{v} \right)^{1.2} = \frac{\alpha_L q'}{v} \quad (5.75)$$

$$\frac{D_T}{v} = 0.036 \left(\frac{q'^{d_m}}{v} \right)^{0.72} = \frac{\alpha_T q'}{v} \quad (5.76)$$

where, D_L and D_T are longitudinal and transverse dispersion coefficient, respectively.

The above equations are valid when the Reynolds number is within the range of 0.05 to 3.5. In this study, the Reynolds number was calculated to be 0.17, therefore the above equation can be applied for longitudinal and transverse dispersion lengths. The used numerical and hydrological parameters are listed in Table 5.2.

Table 5.2. Numerical and hydrological parameters for the simulation model

| | | |
|--|--------------|---|
| Time interval | Δt | 0.5 (sec) |
| Cell length in x direction | Δx | 0.5 (cm) |
| Cell length in y direction | Δy | 0.5 (cm) |
| Longitudinal dispersion length | α_L | 0.038 (cm) |
| Transverse dispersion length | α_T | 0.0051 (cm) |
| Molecular diffusion | D_M | 1.0×10^{-5} (cm ² /s) |
| Porosity | n_e | 0.35 |
| Freshwater head | H_f | 31.5 (cm) |
| Saltwater head | H_s | 30.0 (cm) |
| Freshwater density | ρ_s | 0.991 (g/cm ³) |
| Saltwater density | ρ_f | 1.025 (g/cm ³) |
| Extrapolation factor for SOR method | ω | 1.6 |
| Criteria for convergence judgement | ϵ_0 | 1.0×10^{-2} |
| Specific storage coefficient | c_w | 0.1 |

In the simulation, hydraulic conductivity and pumping rates from barrier and production wells are changed in each case as well as the lab-scale experiments to run the model under the same condition as the experiments. For the application of the method of characteristics 4 particles are distributed uniformly for each grid as the initial condition of the simulation as shown in Figure 5.10.

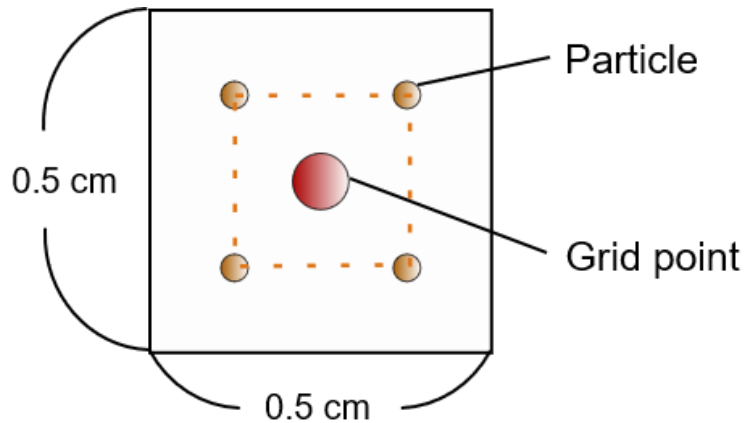


Figure 5.10. Initial arrangement of particles' position

Model boundaries are defined as shown in Figure 5.11. Table 5.4 shows the boundary conditions for each boundary. The model consists of 6 boundaries: top surface of saltwater (AE), top surface of freshwater (ED), bottom surface (BC), saltwater boundary (EF), and two vertical boundaries (AB and CD).

For the bottom surface no discharge flow boundary is assigned. The other boundaries are assigned with timely dependent pressure head boundaries that vary with water table heights of boundaries. The concentrations at the boundaries are defined as: zero concentration at the right vertical boundary and 100% concentration at the left vertical boundary. For the top and bottom boundaries concentration gradient is zero.

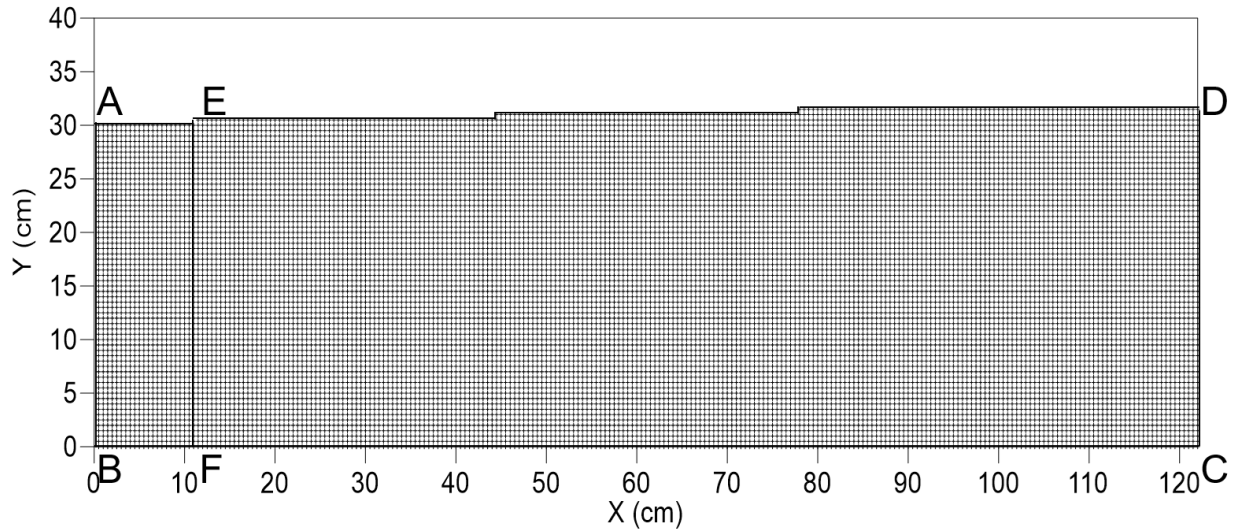


Figure 5.11. Model regions and boundaries

Table 5.4. Boundary conditions for each boundary

| Boundary | Pressure Head | Conc. |
|----------|--|---|
| AB | $h = (H_s - y) \frac{\rho_s}{\rho_f}$ | $C = 100\%$ |
| BC | $-k \left(\frac{\partial h}{\partial y} + \frac{\rho}{\rho_f} \right) = 0$ | $\frac{\partial C}{\partial y} = 0$ |
| CD | $h = (H_s - y)$ | $C = 0\%$ |
| DE | $-k \left(\frac{\partial h}{\partial y} + \frac{\rho}{\rho_f} \right) = -q_w$ | $C = 0\%$ |
| EA | $h = (H_s - y) \frac{\rho_s}{\rho_f}$ | (1) $v \geq 0$ $\frac{\partial C}{\partial y} = 0$ (2) $v < 0$ $C = 100\%$ |
| EF | $h = (H_s - y) \frac{\rho_s}{\rho_f}$ | (1) $u \geq 0$ $\frac{\partial C}{\partial x} = 0$ (2) $u < 0$ $C = 100\%$ |

The numerical model is coded in FORTRAN programming language and run by Microsoft Visual Studio 2008. The chart flow of the simulation is illustrated in Figure 5.11. The program code in FORTRAN programming language is attached in Appendix.

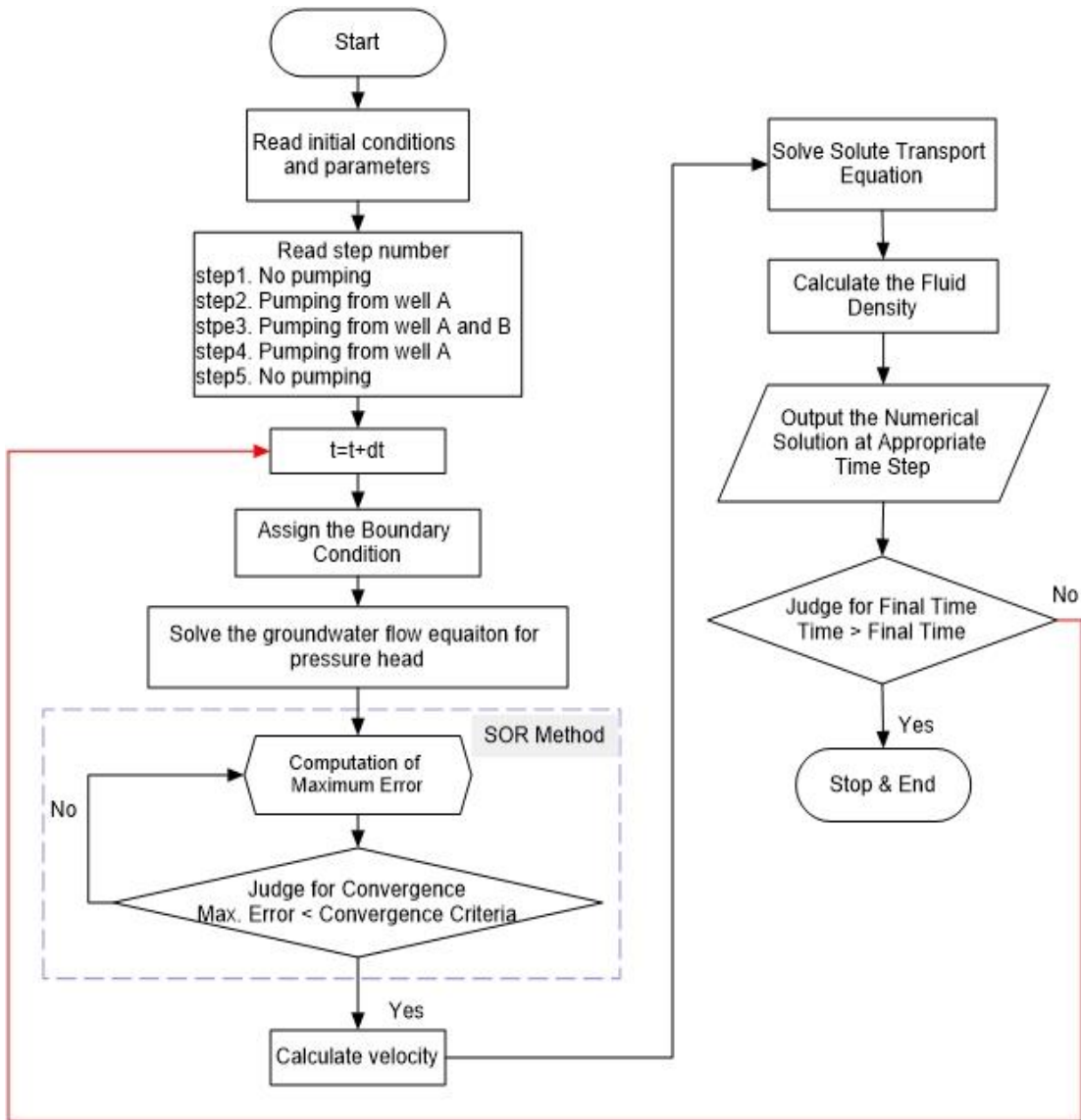


Figure 5.12. Chart flow of the simulation

6. Results and discussion

The simulation conditions and results are described in this chapter. The results are divided into each step as well as the experimental step.

6.1. Model conditions

The numerical model explained in chapter 5 was used to simulate the behavior of saltwater intrusion with the experimental conditions described in chapter 3 and 4. Laboratory experiments were conducted 7 times with different hydraulic conductivity and pumping ratio including the secondary test. The used hydraulic conductivity, pumping rates from barrier and production wells, and the pumping ratio between barrier and production wells are presented at Table 6.1. The simulation number 6 represents the simulation for the secondary test as mentioned above. Therefore, the result of simulation number 6 is only used for step 3. Note that the simulated results of step 1 and 2 of the simulation number 5 were not compared with experimental results since the data of lab-scale experiment related to these steps of this case was not correctly recorded and not reliable due to an error of digital camera.

Table 6.1. Parameters for numerical simulation

| Simulation number | 1 | 2 | 3 | 4 | 5 | 6 | 7 |
|--|----------|----------|----------|----------|----------|----------|----------|
| Hydraulic conductivity (cm/s) | 0.45 | 0.40 | 0.53 | 0.50 | 0.39 | 0.50 | 0.48 |
| Pumping amount from well A (ml/s): Q_A | 1.8 | 2.9 | 2.5 | 2.7 | 2.7 | 2.7 | 2.2 |
| Pumping amount from well B (ml/s): Q_B | 1.7 | 3.5 | 3.8 | 5.2 | 5.3 | 6.1 | 5.7 |
| Pumping ratio between well A and B | 0.9 | 1.2 | 1.5 | 1.9 | 2.0 | 2.3 | 2.6 |

6.2. Sensitivity analysis

Sensitivity analysis was carried out for omega, hydraulic conductivity, and longitudinal and transverse dispersion lengths. As a result, the influence of omega was the largest compared to other parameters. This is because this parameter has a large impact on the calculation of hydraulic head in the simulation, which totally changes the values of pressure head and affects the advancement of saltwater intrusion. To obtain a reliable value for omega, simulated and observed values were compared with changing omega within the range of 0.5 to 1.9 under a hydraulic conductivity of 0.45 cm/s. It was revealed through trial and error that the higher the omega, the longer the length of saltwater intrusion becomes. Furthermore, as a result, it was revealed that omega equal to 1.6 is the most appropriate to reproduce the experimental results. Regarding the effect of hydraulic conductivity, lower hydraulic conductivity showed more accurate results. This may be because the hydraulic conductivity of about 0.5 cm/s, which was used in the experiment and simulation, is relatively high comparing to the range of normal coarse sand. When the higher longitudinal and transverse dispersion lengths are used, the saltwater area is increased. Moreover, it is found that the effect of transverse dispersion length is higher than the longitudinal dispersion length.

6.3. Results of step 1

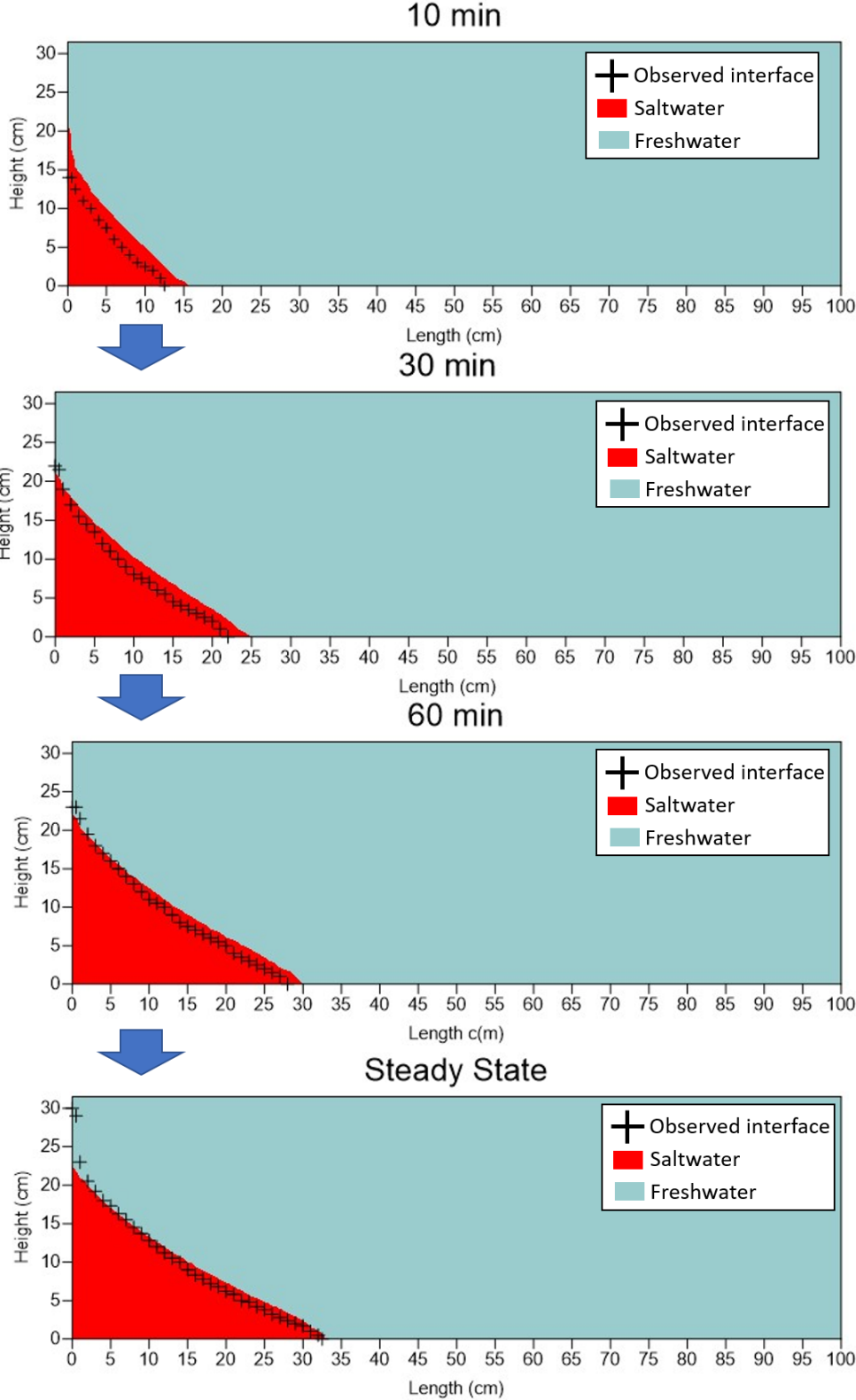


Figure 6.1. Simulated results for step 1 with simulation number 1

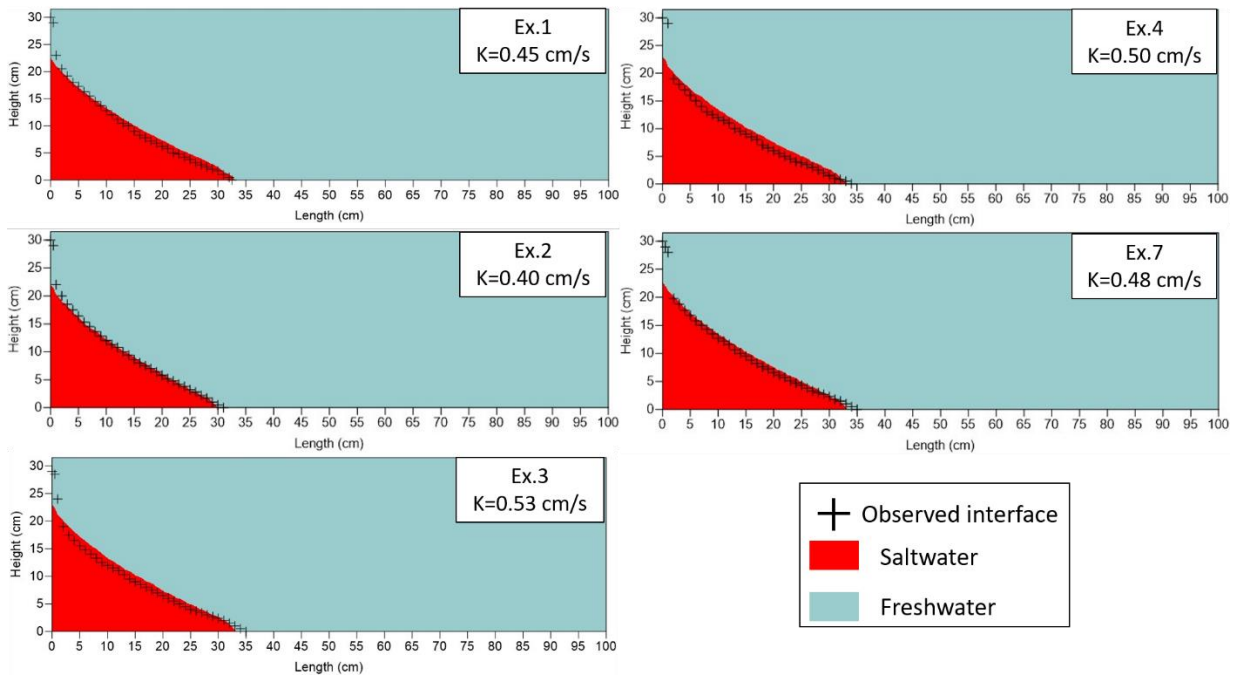


Figure 6.2. Comparison of simulated steady-state conditions with different hydraulic conductivity

Figure 6.1 shows examples of the simulation results with 10, 30, and 60 minutes and steady state conditions of the simulation number 1. Simulated saltwater intrusion regions are illustrated as red and freshwater zone as blue. The positions of observed salt-freshwater interface are plotted as black. Although the simulated salt-freshwater interface slightly advances towards the freshwater zone comparing the observed data for the first 10 minutes, the simulated positions of the interface match the observed positions after 30 minutes. In addition, a comparison of steady states with different hydraulic conductivities is shown in Figure 6.2. All simulated steady state with varying hydraulic conductivity shows the same results as the experimental results. Thus, these results indicate that this numerical model can reproduce the experimental results with high accuracy.

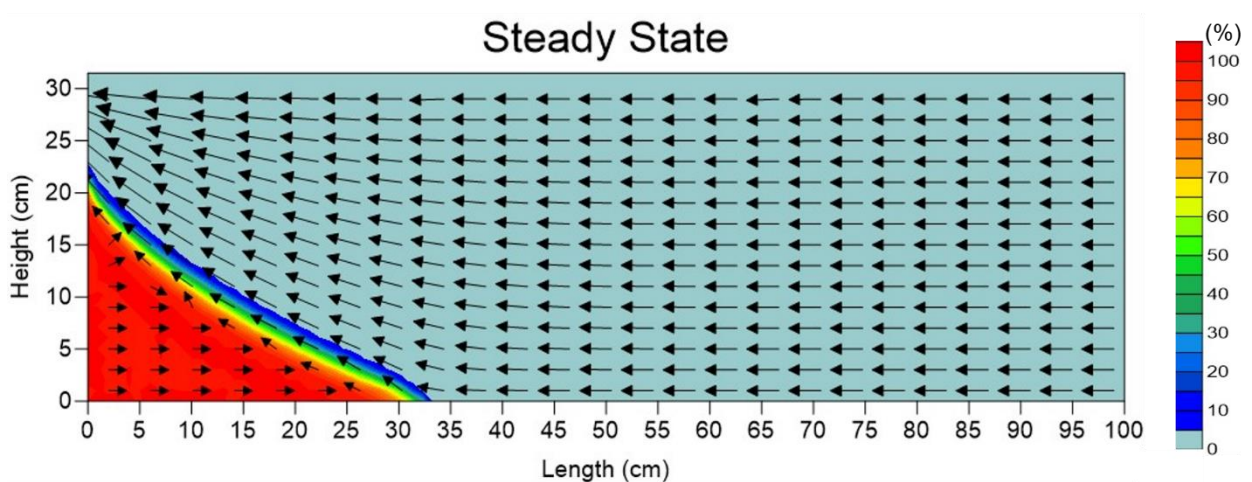


Figure 6.3. Salinity and velocity distribution with simulation number 1 at step 1

Figure 6.3 shows the simulated salinity and velocity distribution of the simulation number 1. As shown in this figure, the saltwater flow is mainly distributed at high salinity zone. Seaward flow from

freshwater zone to the saltwater zone is distributed uniformly. Moreover, saltwater flow along the low salinity zone is observed. It is shown that the equilibrium between saltwater and freshwater flows remains due to this seaward flow, which forms the salt-freshwater interface and prevents further saltwater intrusion.

6.4. Results of step 2

Pumping from the barrier well is considered in this step. The results of this pumping are described in this part.

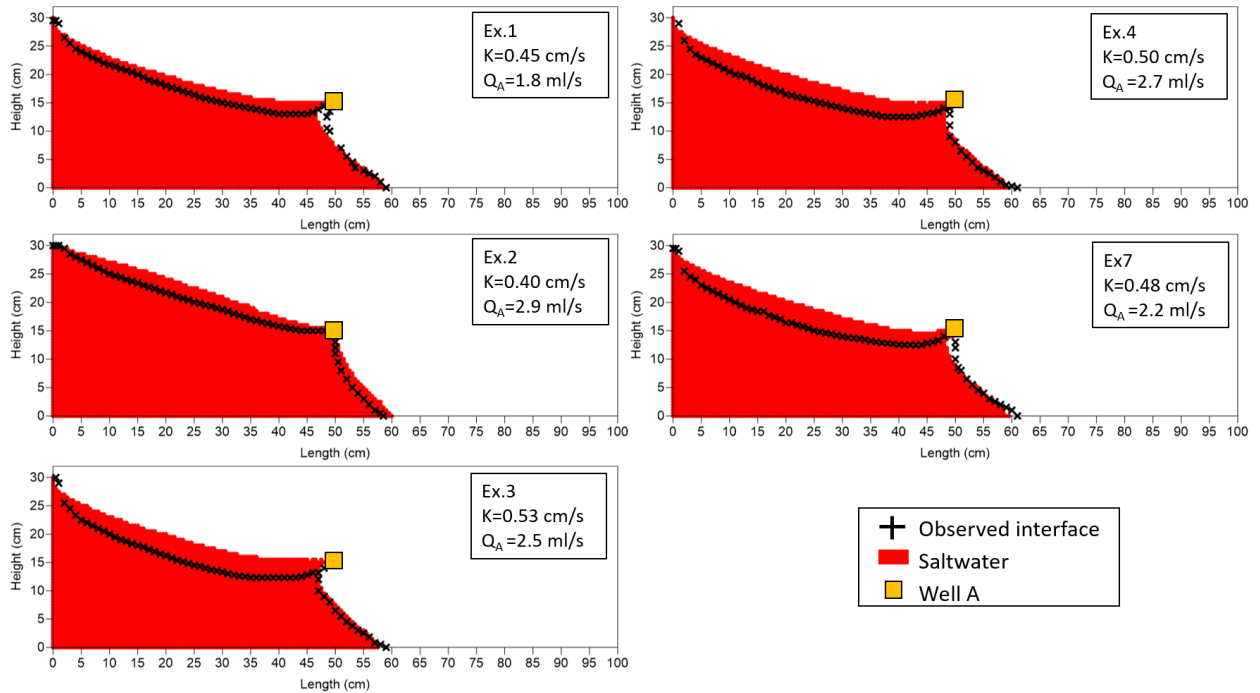


Figure 6.4. Simulation results of steady states with different hydraulic conductivities at step 2

Simulated steady states with different hydraulic conductivities are compared in Figure 6.4. It can be seen that the length of saltwater intrusion toe is well simulated. Moreover, the simulated and observed positions of front interface matches well. With increasing the hydraulic conductivities, however, the simulated upside interface is overestimated comparing to the observed positions.

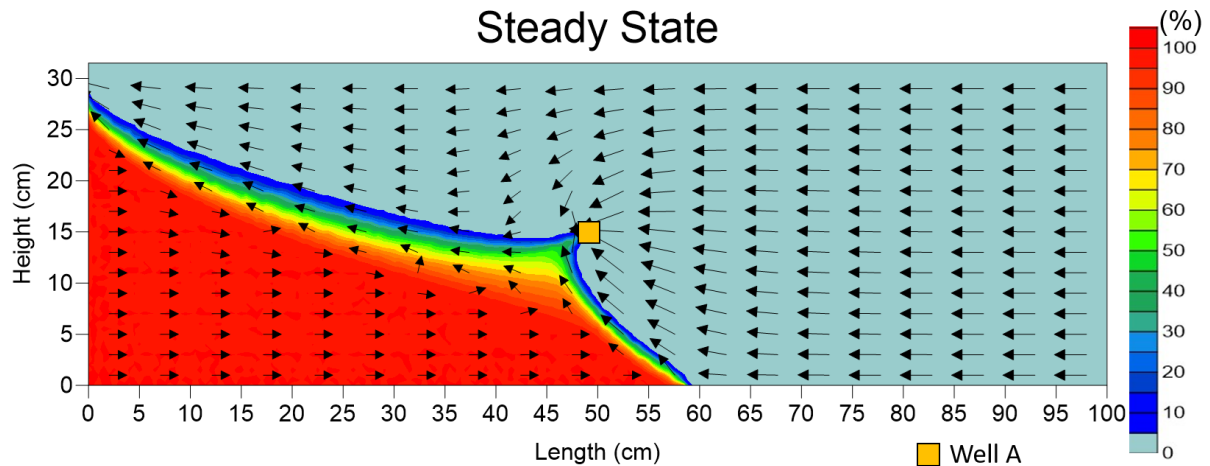


Figure 6.5. Salinity and velocity distribution of the simulation number 1 at step 2

Upconing phenomena is observed in this step with pumping from well A. In addition, with pumping from well A, the flow towards the well A is observed as shown in Figure 6.5. This flow creates the movement of saltwater towards the well A. The flow at the beneath and the left of well A remains the up-coning movement, forming the steady state around the well A.

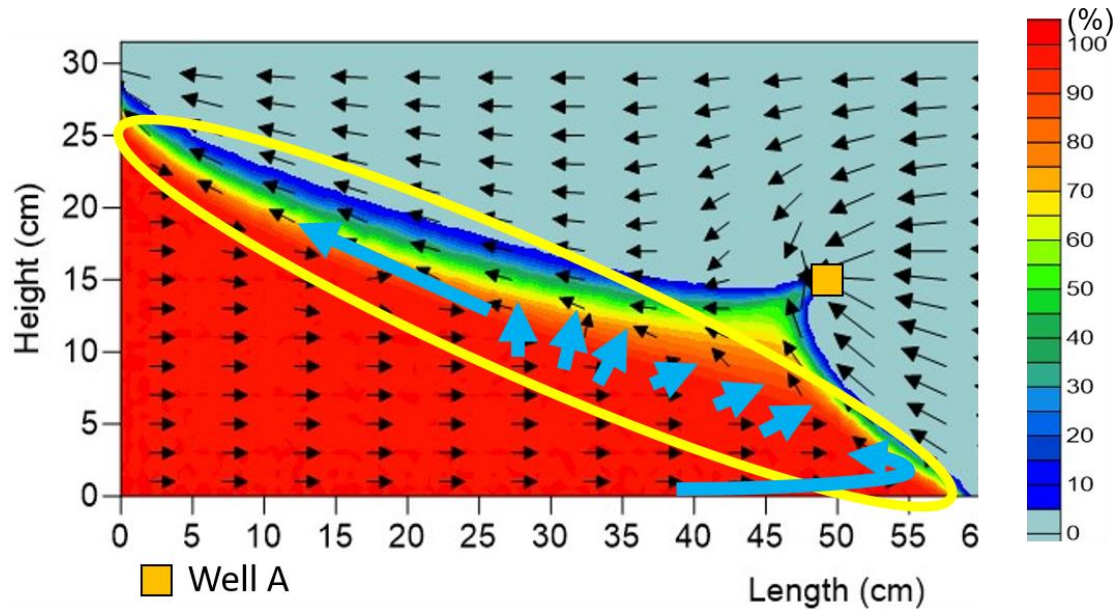


Figure 6.6. Saltwater transportation with saltwater flow

Furthermore, the detailed saltwater flow is shown in Figure 6.6. Sky blue arrows represent the saltwater flow from the high to low concentration zone. The rightwards flow is dominant at the high concentration zone. On the other hand, the saltwater at low concentration zone flows towards the upper left side and forms the salt-freshwater interface. In addition, flow from high to low concentration zone is confirmed. Therefore, it is considered that saltwater and freshwater flow collide, and saltwater is transported along the high concentration zone by the freshwater flow, which forms the mixing zone of saltwater and freshwater.

6.5. Results of step 3

Simultaneous pumping from barrier and production wells are simulated in this step and the results are described in this part.

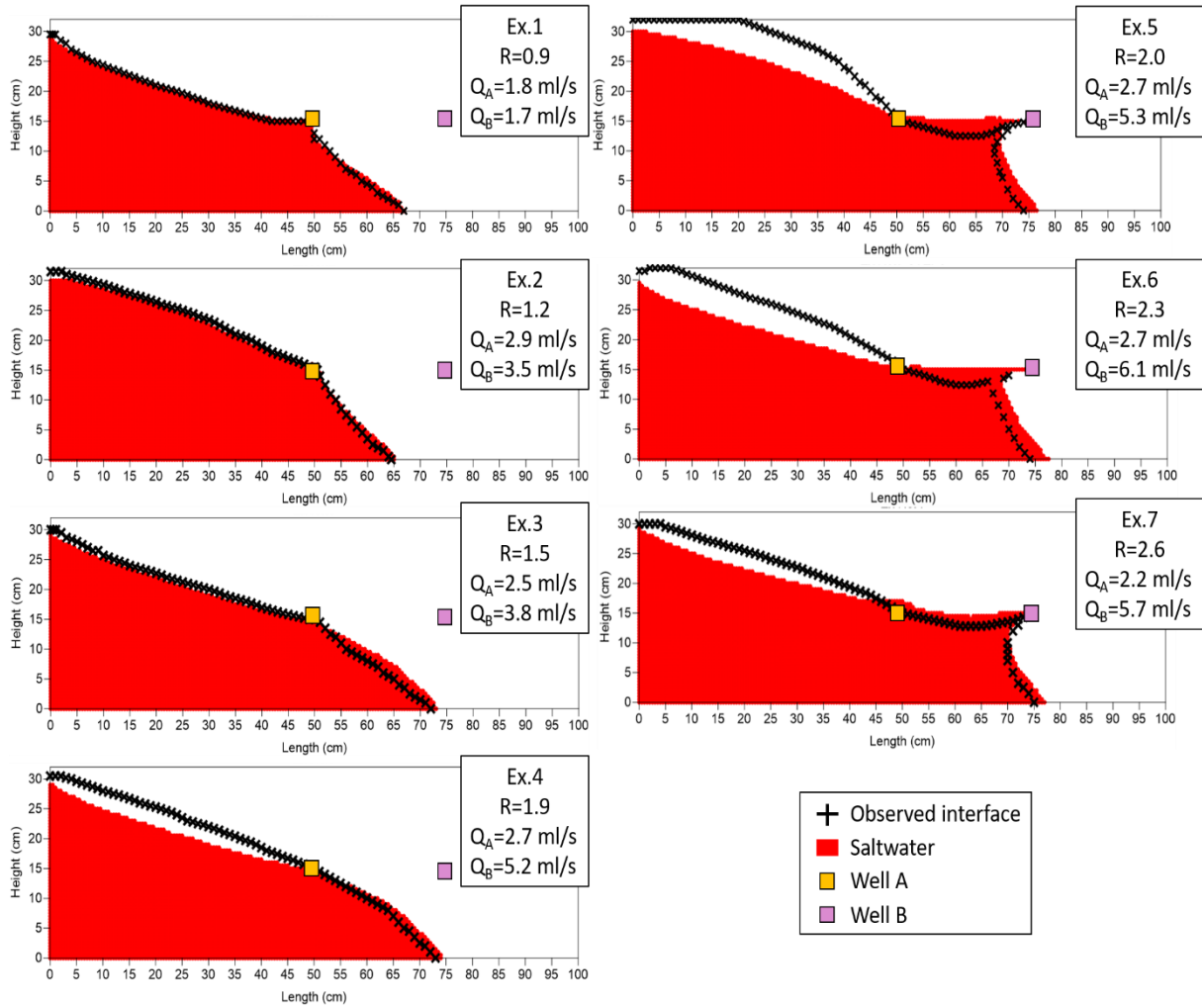


Figure 6.7. Comparison of steady state at the end of step 3

Figure 6.7 shows the comparison of simulated result for step 3 with different pumping ratios from 0.9 to 2.6. Results of all simulation are shown in this figure. At this step, pumping from both barrier and production wells started in the simulation with the same amount of pumping as the laboratory experiment. As a result, under the pumping ratio between barrier and production wells of 1.9, saltwater doesn't reach the production well, which indicates that these simulations show the same results as the experiment with related pumping ratio. On the other hand, as increased hydraulic conductivity, the shape of upper interface shows lower position comparing to the observed interface. The reason of this difference will be discussed in chapter 6.8.

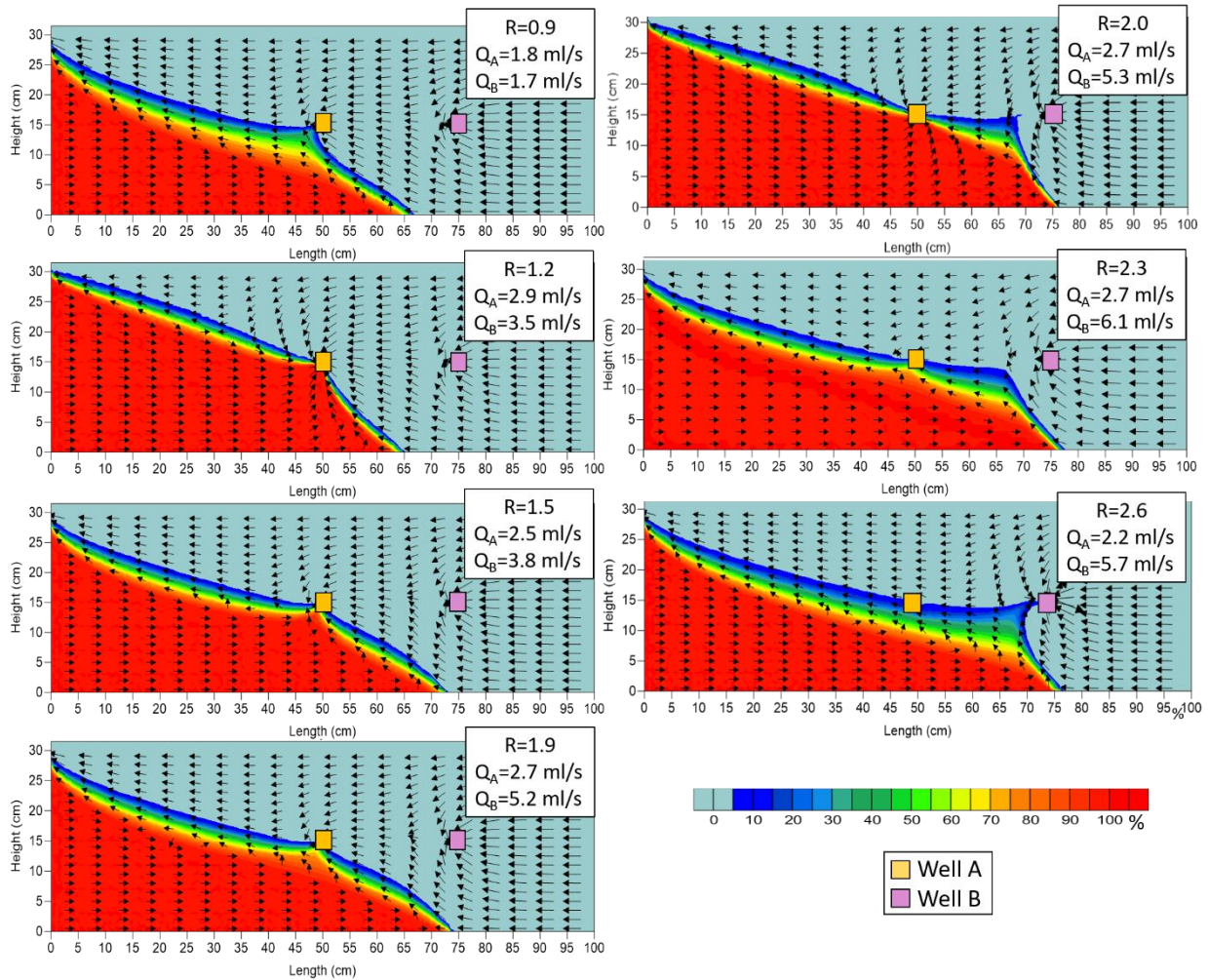


Figure 6.8. Comparison of velocity and salinity distributions with different pumping ratios

The velocity and salinity distributions at step 3 with different pumping ratios are represented in Figure 6.8. It is shown that the high salinity zone further moves towards the well B with increasing pumping ratio. Moreover, upconing of highly concentrated saltwater towards the well A disappears as the pumping ratio exceeds the critical pumping ratio of 1.9. In the case of $R=2.6$, especially, the barrier well does not extract highly concentrated saltwater, leading to further movement of saltwater towards the well B and increase of mixing zone. The detailed result of this step 3 will be discussed in chapter 6.8.

6.6. Results of step 4

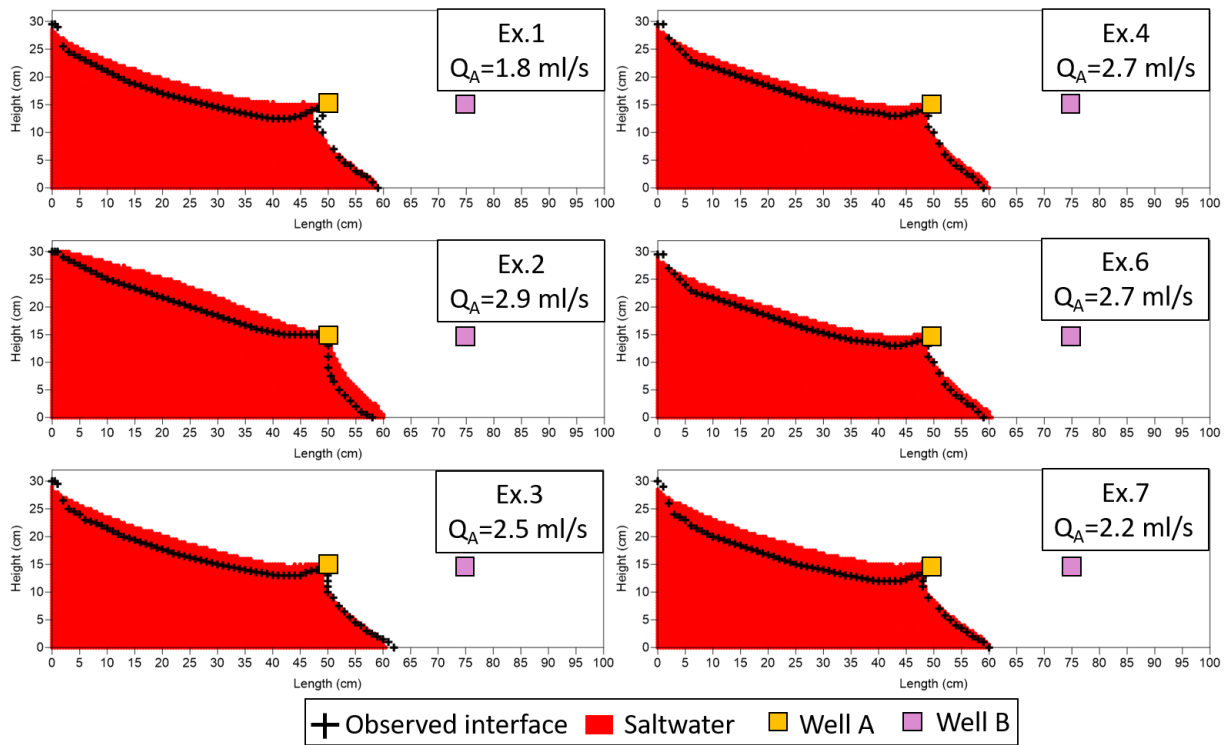


Figure 6.9. Comparison of simulated steady states at step 4

This part represents the results of step 4, the retreating process by barrier well. Figure 6.9 shows a comparison of steady-state conditions at step 4. After turning off the production well, the saltwater retreated towards the saltwater zone and the steady state as shown in this figure was achieved. The simulated shape of saltwater shows the similar shape to the observed interface, although the upper interface is overestimated.

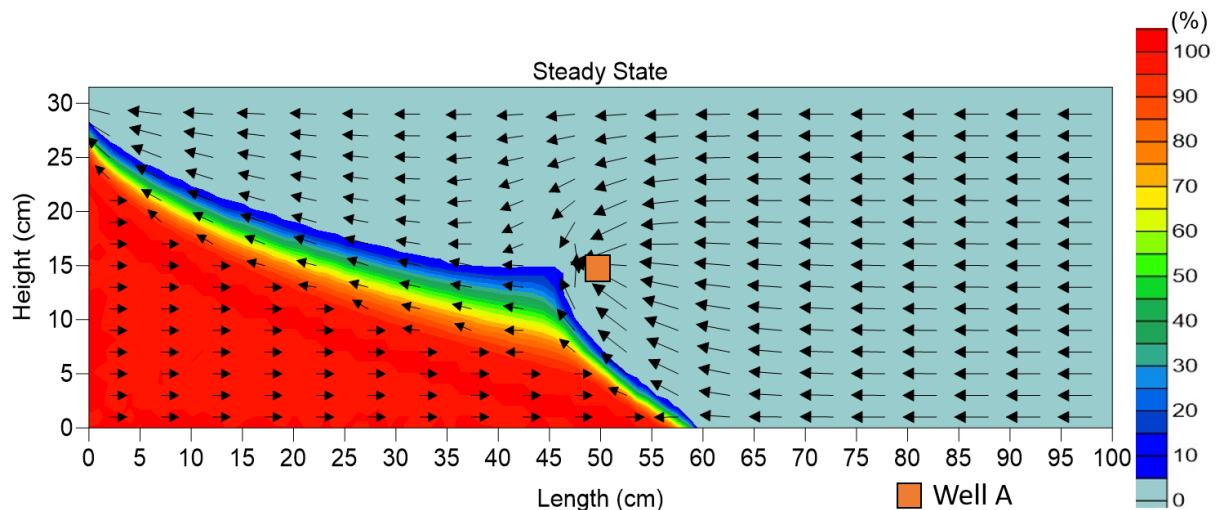


Figure 6.10. Salinity and velocity distribution of step 4

The velocity and salinity distribution at the end of step 4 is shown in Figure 6.10, which shows similar distribution to the result of step 2. Therefore, it is considered that the barrier well can retardant saltwater if the production well is stopped.

6.7. Results of step 5

This step simulated the natural retreat process of saltwater intrusion without any pumping. The simulation of this step was conducted under the conditions of simulation number 3,4,6, and 7 since laboratory experiments for this step were only carried out for these cases. The result is shown in Figure 6.11. The retreat process is confirmed as well as in this simulation. However, the simulated shapes of salt-freshwater interface are different from the observed interface around the upper zone.

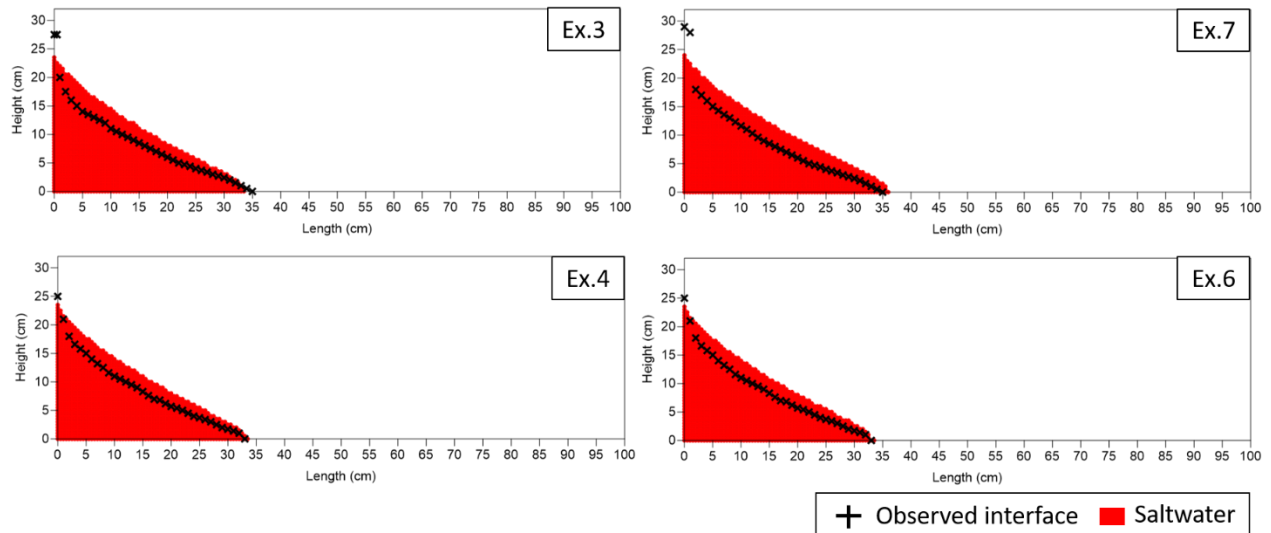


Figure 6.11. Comparison of steady-state conditions at step 5

6.8. Discussion

(1) Validation

Through this simulation, the validity of the model was confirmed, especially in terms of the length of saltwater intrusion toe and the shape of salt-freshwater interface. The length was well simulated and matched the observed values of lab-scale experiments. Moreover, in most cases, the shape of the salt-freshwater interface was well simulated in particular the front interface. However, the shape of the interface around the upper zone was not well simulated in some cases. In step 2, it was observed that the overestimated zone of the upper interface becomes larger with increasing the hydraulic conductivity. Furthermore, in step 3, as the pumping ratio between barrier and production well increased, the deviations of observed and simulated positions of the upper interface became larger. One of the reasons for this error is that the affected zone by pumping from two wells of this simulation model is smaller than that of the real pumping wells. In the simulation model, the function for pumping wells was simulated by changing the pressure head depending on the pumping rates at well points. This method reproduced almost same results obtained from lab-scale experiment to a certain extent. However, with increasing the hydraulic conductivity or the pumping ratio, this method may have a limit to represent pumping wells.

On the other hand, the interface between the barrier and production wells is simulated properly, although large deviation between simulated and observed interface positions occurs with high hydraulic

conductivity and pumping ratio. From this perspective, there may be other reason for this large difference. One reason is the porosity obtained from the lab-scale experiment. The lab-scale experiment was conducted under the condition of unconfined aquifer. Thus, the glass beads were filled in the central tank without any pressure, which may produce a variation in porosity within the experimental device. Moreover, the porosity around the upper side of the experimental device may be higher than that around the bottom of the device. Therefore, the porosity variation may lead to a large inflow of saltwater to the central tank in the upper zone, which formed the observed upward convex interface and caused the deviation between simulated and observed interface positions.

(2) Influence of increasing pumping ratio

In this part, the detailed result of step 3 is discussed. From Figure 6.8 there is a trend that the high concentration zone further moves towards the well B as the pumping ratio increases. In addition, upconing towards the well A shows different behaviors with increasing pumping ratios. When the pumping ratio was 0.9, upconing of highly concentrated saltwater towards the well A was not observed. Within the range from 1.2 to 1.9, upconing of highly concentrated saltwater was observed. However, in the case that the pumping ratio was 2.3, upconing of highly concentrated saltwater became smaller than in the case of 1.9. Moreover, in the case of 2.6, upconing towards the well A completely disappeared. To confirm that the difference of upconing towards the barrier well was caused by pumping ratios, the steady states at step 2 and 3 are compared as shown in Figure 6.12. Comparing the salinity level of upconing towards the well A at step 2 and 3, the salinity level of upconing was increased from step 2 to step 3. Thus, it is considered that the behavior of upconing towards the barrier well will be changed due to the pumping ratio between barrier and production well.

In addition, the cases of $R=1.2$ and 2.0 show a different result that the well A extracts highly concentrated saltwater at step 2. One reason may be the large amount of pumping from the well A. The pumping rates from the well A in these cases were 2.9 ml/s and 2.7 ml/s , which were larger than other cases. Comparing the salinity distributions of $R=1.9$ and 2.0 at step 2, however, the distribution of highly concentrated saltwater was different, although the pumping rates from the well A were the same. The reason of this difference is considered as hydraulic conductivity. Hydraulic conductivities of $R=1.2$ and 2.0 were 0.40 cm/s and 0.39 cm/s , respectively, which were smaller than other cases. To confirm the effect of hydraulic conductivity, the steady states at step 1, 2, and 3 in the cases of $R=1.9$ and 2.0 are compared as shown in Figure 6.13. At step 1, both results show the same salinity distribution. However, at step 2, high concentration zone further moved towards the well A in the case of $R=2.0$. Moreover, the area of highly concentrated saltwater in the case of $R=2.0$ became larger than in the case of $R=1.9$ at both step 2 and 3. Therefore, it is considered that hydraulic conductivity affects the behavior of saltwater pumping. Furthermore, the lower the hydraulic conductivity is, the more saltwater advances towards the inland. From these simulated results, it is considered that the effect of barrier well on saltwater intrusion has 4 stages as follows. At the first stage in which the pumping ratio is significantly lower than the critical ratio, the barrier well prevents saltwater intrusion by extracting low concentrated saltwater. Although the barrier well does not extract highly concentrated saltwater at this stage, pumping from barrier well

forms the freshwater flow towards the barrier well, increasing the seaward flow and preventing the movement of saltwater. At the second stage, in which the pumping ratio is less than or equal to the critical ratio, barrier well extracts highly concentrated saltwater, which prevents the movement of high concentration zone. Extracting of highly concentrated saltwater has a large impact as a prevention of saltwater intrusion since saltwater flow of highly concentrated saltwater dominates the saltwater flow due to the large difference of densities between saltwater and freshwater. At the third stage, in which the pumping ratio exceeds the critical ratio, extraction of highly concentrated saltwater towards the barrier well decreases. Although the barrier well can slightly extract highly concentrated saltwater, the influence of extraction decreases and it cannot prevent the movement of high concentration zone, which increases the mixing zone and a risk of salinization of the inland production well. At the final stage, in which the pumping ratio significantly exceeds the critical ratio, the barrier well only extracts low concentrated saltwater. The saltwater flow in the mixing zone is formed by pumping from the production well and the barrier well cannot have positive effects on saltwater extraction, which indicates that the barrier well cannot work as a prevention of saltwater intrusion at this stage.

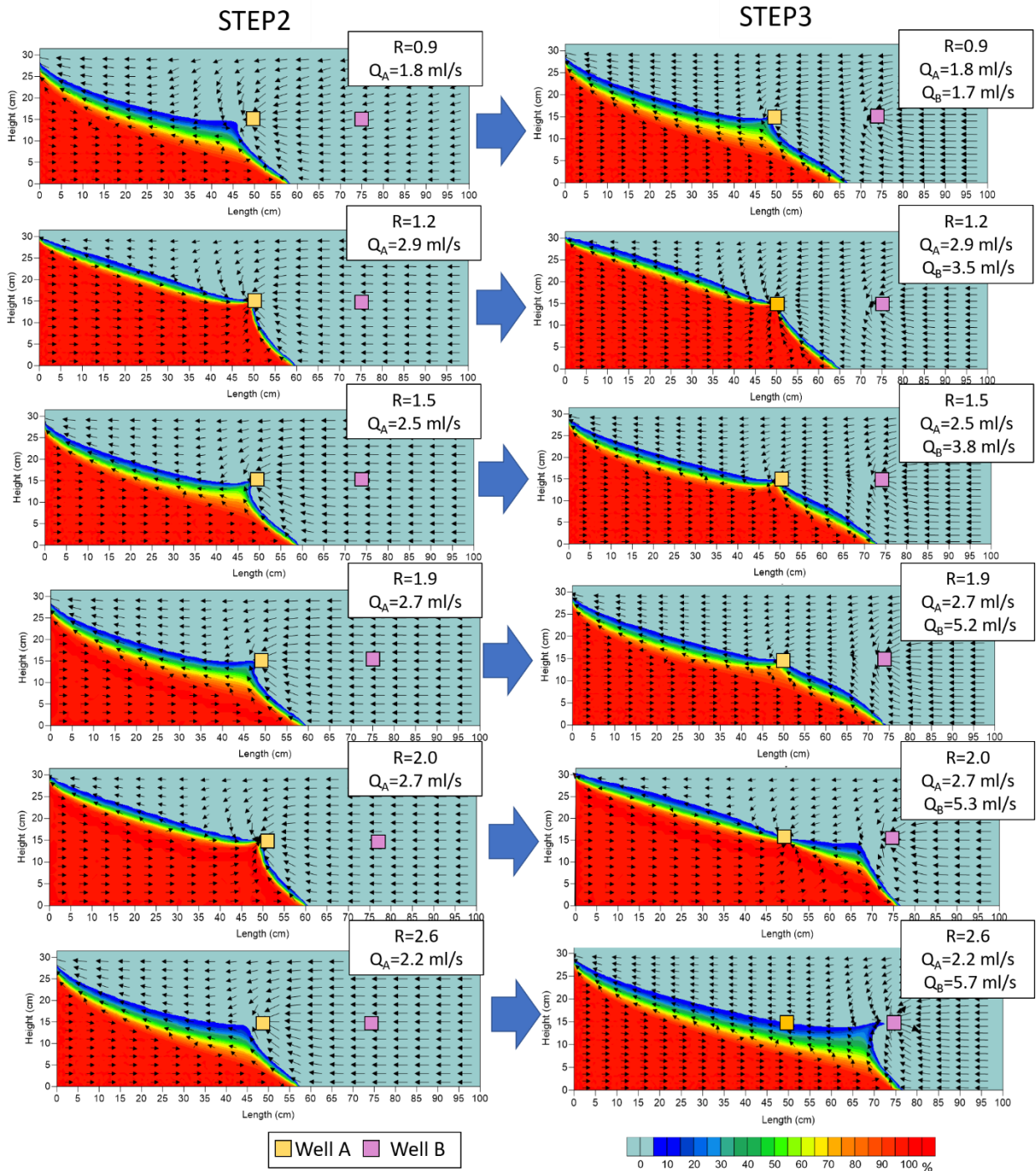


Figure 6.12. Comparison of steady state at step 2 and 3 with different pumping ratios

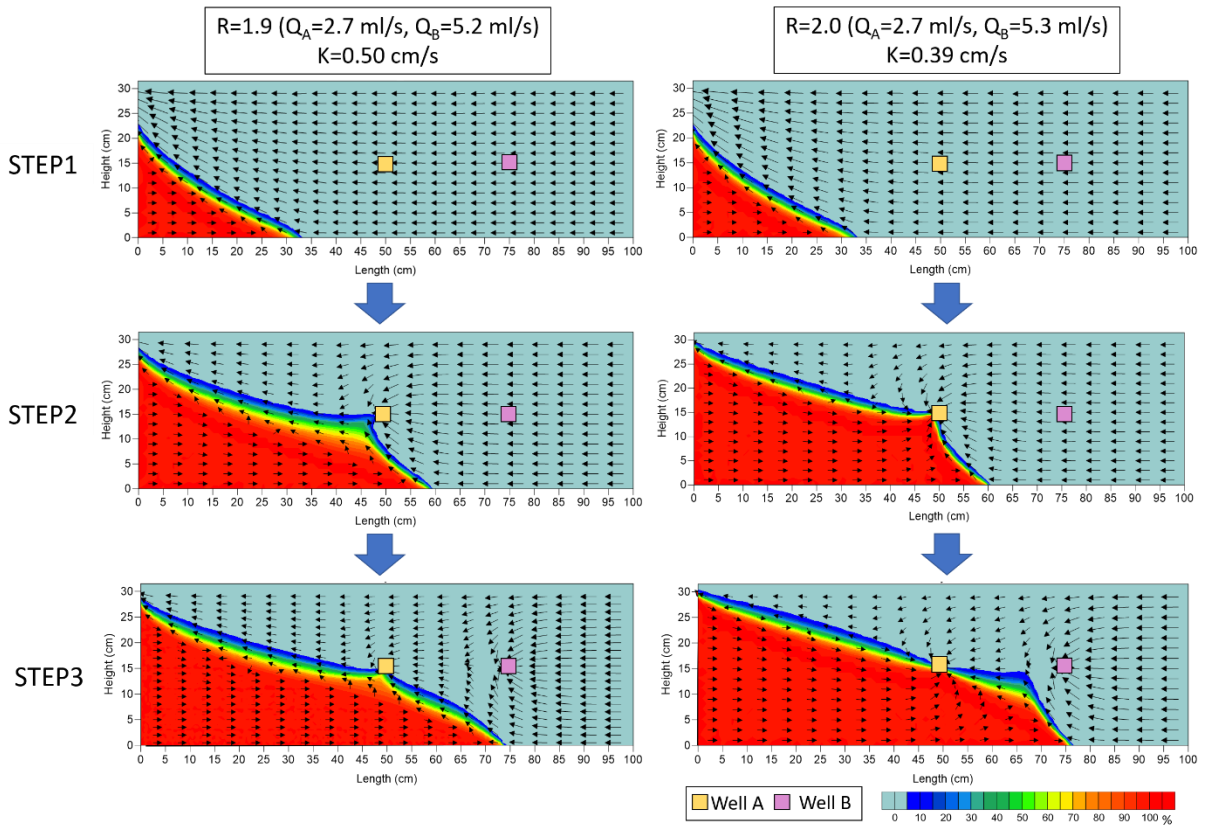


Figure 6.13. Comparison of salinity and velocity distribution of $r=1.9$ and 2.0 with step1~3

7. Conclusions

The effectiveness of the barrier well on the possible pumping amount from the inland production well in a prevention of saltwater intrusion is studied by lab-scale experiments and two-dimensional numerical simulation.

In lab-scale experiments, the behavior of saltwater intrusion with barrier and production well was observed with changing the pumping rates from those two wells. From lab-scale experiments, it was revealed that there was a quantitative relationship in the pumping ratio between barrier and production wells and the critical pumping ratio between them was equal to 1.9 under the experimental conditions. Moreover, the retardant effect of the barrier well on saltwater intrusion was observed.

To reproduce and analyze the experimental results, a numerical model based on groundwater flow equation and solute transport equation was created and simulated under the same conditions as the experiments. The validity of this model was confirmed by comparing simulated and experimental results in each step. This numerical model demonstrated that the barrier well prevented saltwater intrusion by extracting highly concentrated saltwater, when the pumping ratio was less than the critical ratio. In addition, the process of saltwater transport from the high to low salinity zone was revealed. Freshwater flow towards the sea and barrier well transported saltwater along the high concentration zone, which formed the mixing zone of saltwater and freshwater. In a steady state, the equilibrium between saltwater flow and freshwater flow was remained by this transportation of saltwater.

In conclusion, from both lab-scale experiments and numerical simulation, there is a quantitative relationship between barrier and production wells. Moreover, there is a critical pumping ratio between barrier and production well, and the barrier well can prevent saltwater intrusion as long as the pumping ratio is kept less than the critical ratio. Further studies are required to confirm the influence of the positions and numbers of the barrier and production wells. Moreover, a three-dimensional model will be required to simulate the actual condition of coastal aquifers. With these further studies, this result will be developed and can be applied to the actual coastal aquifer. Therefore, it is concluded that pumping ratio control between barrier and production wells has a possibility as an effective method to prevent saltwater intrusion in coastal regions.

References

- Abd-Eelhamid, H. F., Javadi, A. A., & Qahman, K. A. (2015). Impact of over-pumping and sea level rise on seawater intrusion in Gaza aquifer (Palestine). *Journal of Water and Climate*. April. 2015.
- Abdoulhalik, A.; Ahmed, A.A. (2017). The effectiveness of cutoff walls to control saltwater intrusion in multi-layered coastal aquifers: Experimental and numerical study. *J. Environ. Manag.* 2017, 199 (suppl. C),62-73.
- Barlow, P.M. (2003). Ground water in freshwater-saltwater environments of the Atlantic Coast. U.S. *Geological Survey Circular*
- Beth, H.B., Caleb, A.A. & Austin.O. (2016). Water: Availability and use. *Mississippi State University Extension*. 2016. p3011.
- Blair, T.C., & McPherson, John. (1999). Grain-size and textural classification of coarse sedimentary particles. *Journal of Sedimentary Research*, 69, 6-19. 10.2110/jsr.69.6.
- Costall, A., Harris, B., & Pigois, J.P. (2018). Electrical Resistivity Imaging and the Saline Water Interface in High-Quality Coastal Aquifers. *Survey in Geophysics*, 39, 753–816.
- David, M.N. (1991) Practical Handbook of Ground-Water Monitoring. LEWIS PUBLISHERS, INC. pp. 690.
- Dierch, H.j.G. & Koldditz, O. (2002). Variable-density flow and transport in porous media: approaches and challenges. *Advances in Water Resources*, Vol.25, pp.899-944.
- Elizabeth, L.E., Miguel, A., Maria, G. & Eduardo, A. (2008). A model for calculating the density of aqueous multicomponent electrolyte solutions. *Journal of The Chilean Chemical Society - J CHIL CHEM SOC*. Vol. 53.
- FAO (Food and Agriculture Organization). (1997). Seawater intrusion in coastal aquifers: Guidelines for study, monitoring and control. Rome, Italy: *FAO Water Reports*.
- Fetter. (2001). Applied Hydrogeology. 4th Addition. Pearson. Pp15-16
- Glover, R.E. (1959). The pattern of fresh-water flow in a coastal aquifer, *J. Geophy. Res.* 64(4), pp.457-459.
- Harleman, D.R.F. and Rumer, R.R. (1963). Longitudinal and lateral dispersion in an isotropic porous medium, *J. Fluid Mech.*, Vol. 16, pp.385-394, 1963.
- Hussain, M.S., Abd-Elhamid, H.F., Javadi, A.A., & Sherif, M.M. (2019). Management of Seawater

- Intrusion in Coastal Aquifers: A Review. *Water*, 11, 2467.
- Ingham, J., McConchie, A. & Cozens, N. (2006). Measuring and monitoring saltwater intrusion in shallow unconfined coastal aquifers using direct current resistivity traverses. *Journal of Hydrology*. New Zealand. January 2006. 45(2). pp.69-82.
- IPCC. (2013): Summary for Policymakers. In: *Climate Change 2013: The Physical Science Basis. Contribution of Working Group I to the Fifth Assessment Report of the Intergovernmental Panel on Climate Change* [Stocker, T.F., D. Qin, G.-K. Plattner, M. Tignor, S.K. Allen, J. Boschung, A. Nauels, Y. Xia, V. Bex & P.M. Midgley (eds.)]. Cambridge University Press, Cambridge, United Kingdom and New York, NY, USA, pp. 25-26, doi:10.1017/CBO9781107415324.004.
- Jinno, K., Momii, K., Fujino, K., Nakagawa, K., Hosokawa, T., Egusa, N., & Hiroshiro, Y. (2001). Numerical analysis of mass transport in groundwater (In Japanese). *Kyushu University Press*. pp.13-72.
- Jinno, K., Momii, K., Fujino, K., Nakagawa, K., Hosokawa, T., Egusa, N., & Hiroshiro, Y. (2001). Numerical analysis of mass transport in groundwater (In Japanese). *Kyushu University Press*. pp.83-84.
- Kaleris, V.K.; Ziogas, A.I. (2013). The effect of cutoff walls on saltwater intrusion and groundwater extraction in coastal aquifers. *J. Hydrol.* 2013, 476, 370-383.
- Luyun, R.; Momii, K.; Nakagawa, K. (2011). Effects of Recharge Wells and Flow Barriers on Seawater Intrusion. *Ground Water*, 2011, 49, 239-249.
- Mahesha, A. (1996). Steady-State Effect of Freshwater Injection on Seawater Intrusion. *J. Irrig. Drain. Eng.* 1996, 122, 149-154.
- Oscar Castro-Orgaz (2011) Steady free-surface flow in porous media: generalized Dupuit–Fawer equations, *Journal of Hydraulic Research*, 49:1, 55-63, DOI: 10.1080/00221686.2010.526758
- Park, S., Kim, J., Yum, B., & Yeh, G. (2011). Three-Dimensional Numerical Simulation of Saltwater Extraction Schemes to Mitigate Seawater Intrusion due to Groundwater Pumping in a Coastal Aquifer System. *Journal of Hydrologic Engineering*, 17, 10–22.
- Pool, M., & Carrera, J. (2010) Dynamics of negative hydraulic barriers to prevent seawater intrusion. *Hydrogeology Journal*, 18(1), 95–105.
- Sherif, M, M. & Singh, V, P. (2002). Effect of Groundwater Pumping on Seawater Intrusion in Coastal Aquifers. *Agricultural science*. 7(2):61-67, 2002.

- Sherif, M., & Hamza, K. (2001). Mitigation of seawater intrusion by pumping brackish water. *Transport in Porous Media*, 43(1), 29–44.
- Simion, A.I., Cristina, G., Ana-Maria, R., & Lucian, G. (2015). Mathematical modelling of density and viscosity of NaCl aqueous solutions. *Journal of Agroalimentary Processing and Technologies*. 21. 41-52.
- Van Genuchten. (1980). A closed-form equation for predicting the hydraulic conductivity of unsaturated soils. *Soil Science Society of America Journal*, Vol. 44, pp.893-898.
- Werner, A. D., and Simmons, C. T. (2009). Impact of Sea-Level Rise on Sea Water Intrusion in Coastal Aquifers. *Ground Water*. March-April 2009, No.2, Vol.47. pp197-204.
- Yu, C., Cheng, J.J., Jones, L.G., Wang, Y.Y., Faillace, E., Loureiro, C., & Chia, Y P. (1993). Data collection handbook to support modeling the impacts of radioactive material in soil. United States. doi:10.2172/10162250.

Appendix

! TWO-DIMENSIONAL NUMERICAL SIMULATION
OF SALTWATER INTRUSION AND DISPERSION
FOR LABORATORY EXPERIMENTS

Shinichi Ozaki

Urban and Environmental Engineering

Graduate School of Engineering

Kyushu University

!-----!

PROGRAM SALTWATER

IMPLICIT REAL*8(A-H,O-Z)

PARAMETER(IEMPTY=2000, ILIMIT=500,
JLIMIT=500, KDIM=200000, IJMAX=22000)

INTEGER IEMPTY(IEMPTY),
JEMPTY(IEMPTY), NS1(ILIMIT,JLIMIT),
KPKOSU(ILIMIT,JLIMIT), NO(KDIM)

INTEGER ANS

REAL JGL(ILIMIT),JGL22(ILIMIT),JGLN(ILIMIT)

DIMENSION XX(ILIMIT),
YY(JLIMIT),XX2(ILIMIT),H(ILIMIT,JLIMIT,25),
H0(ILIMIT,JLIMIT,25),HJGL(ILIMIT),
HDUMMY(ILIMIT,JLIMIT),U(ILIMIT,JLIMIT),
V(ILIMIT,JLIMIT), UD(ILIMIT,JLIMIT),
VD(ILIMIT,JLIMIT),HWOLD(ILIMIT,JLIMIT)

DIMENSION CMIX(ILIMIT,JLIMIT),
CAVE(ILIMIT,JLIMIT),DELC(ILIMIT,JLIMIT),
ROU(ILIMIT,JLIMIT)

DIMENSION SITA(ILIMIT,JLIMIT),
SITAS(ILIMIT,JLIMIT), TKSAT(ILIMIT,JLIMIT),
T(ILIMIT,JLIMIT),TCH(ILIMIT,JLIMIT),
CW(ILIMIT,JLIMIT),CTOEI(ILIMIT,50)

DIMENSION XP(KDIM), YP(KDIM), CP(KDIM),
KGRID(KDIM,2), KPRYUSI(ILIMIT,JLIMIT,25)

DIMENSION
GRID0(IJMAX),XGRID(IJMAX),YGRID(IJMAX),XP1
(KDIM),YP1(KDIM)

WRITE(*,*)EX No. ='

READ(*,*)EXNUM

WRITE(*,*)EXNUM

!---OPEN READ FILE-----

-----!

OPEN(UNIT=10,FILE='C:\2014_ozaki\DATA\DATATR
Y\STEP3\INPUT3_EX1\DELC.DAT')

OPEN(UNIT=11,FILE='C:\2014_ozaki\DATA\DATATR
Y\STEP3\INPUT3_EX1\ROU.DAT')

OPEN(UNIT=12,FILE='C:\2014_ozaki\DATA\DATATR
Y\STEP3\INPUT3_EX1\HEAD.DAT')

OPEN(UNIT=13,FILE='C:\2014_ozaki\DATA\DATATR
Y\STEP3\INPUT3_EX1\KPKOSU.DAT')

OPEN(UNIT=14,FILE='C:\2014_ozaki\DATA\DATATR
Y\STEP3\INPUT3_EX1\NS1.DAT')

OPEN(UNIT=15,FILE='C:\2014_ozaki\DATA\DATATR
Y\STEP3\INPUT3_EX1\IEMPTY.DAT')

OPEN(UNIT=16,FILE='C:\2014_ozaki\DATA\DATATR
Y\STEP3\INPUT3_EX1\PARTICLE.DAT')

OPEN(UNIT=17,FILE='C:\2014_ozaki\DATA\DATATR
Y\STEP3\INPUT3_EX1\WATERLEVEL.DAT')

!---OPEN WRITE FILE-----

-----!

OPEN(UNIT=31,FILE='C:\2014_ozaki\DATA\DATATR
Y\STEP3\OUTPUT3_EX1\TKSAT_OUT.DAT')

OPEN(UNIT=32,FILE='C:\2014_ozaki\DATA\DATATR
Y\STEP3\OUTPUT3_EX1\SITA_OUT.DAT')

OPEN(UNIT=33,FILE='C:\2014_ozaki\DATA\DATATR
Y\STEP3\OUTPUT3_EX1\XPYPTRY_OUT.DAT')

OPEN(UNIT=34,FILE='C:\2014_ozaki\DATA\DATATR
Y\STEP3\OUTPUT3_EX1\H2_OUT.DAT')

!RESULT FILE FOR TIME

OPEN(UNIT=50,FILE='C:\2014_ozaki\DATA\DATATR
Y\STEP3\OUTPUT3_EX1\TIME_C_RESULT_OUT.DA
T')

```

OPEN(UNIT=51,FILE='C:\2014_ozaki\DATA\DATATR
Y\STEP3\OUTPUT3_EX1\TIME_H_RESULT_OUT.DA
T')
OPEN(UNIT=52,FILE='C:\2014_ozaki\DATA\DATATR
Y\STEP3\OUTPUT3_EX1\TIME_U_RESULT_OUT.DA
T')
OPEN(UNIT=53,FILE='C:\2014_ozaki\DATA\DATATR
Y\STEP3\OUTPUT3_EX1\TIME_V_RESULT_OUT.DA
T')
OPEN(UNIT=54,FILE='C:\2014_ozaki\DATA\DATATR
Y\STEP3\OUTPUT3_EX1\TIME_ROU_RESULT_OUT.
DAT')
OPEN(UNIT=55,FILE='C:\2014_ozaki\DATA\DATATR
Y\STEP3\OUTPUT3_EX1\TIME_KPKOSU_RESULT_
OUT.DAT')
    !FINAL RESULT FOR INPUT OF NEXT STEP
OPEN(UNIT=60,FILE='C:\2014_ozaki\DATA\DATATR
Y\STEP3\OUTPUT3_EX1\FINAL_C_OUT.DAT')
OPEN(UNIT=61,FILE='C:\2014_ozaki\DATA\DATATR
Y\STEP3\OUTPUT3_EX1\FINAL_H_OUT.DAT')
OPEN(UNIT=62,FILE='C:\2014_ozaki\DATA\DATATR
Y\STEP3\OUTPUT3_EX1\FINAL_U_OUT.DAT')
OPEN(UNIT=63,FILE='C:\2014_ozaki\DATA\DATATR
Y\STEP3\OUTPUT3_EX1\FINAL_V_OUT.DAT')
OPEN(UNIT=64,FILE='C:\2014_ozaki\DATA\DATATR
Y\STEP3\OUTPUT3_EX1\FINAL_ROU_OUT.DAT')
OPEN(UNIT=65,FILE='C:\2014_ozaki\DATA\DATATR
Y\STEP3\OUTPUT3_EX1\FINAL_KPKOSU_OUT.DA
T')
OPEN(UNIT=66,FILE='C:\2014_ozaki\DATA\DATATR
Y\STEP3\OUTPUT3_EX1\FINAL_PARTICLE_OUT.D
AT')
    !FINAL STEP
OPEN(UNIT=70,FILE='C:\2014_ozaki\DATA\DATATR
Y\STEP3\OUTPUT3_EX1\KOSUFINAL_OUT.DAT')
OPEN(UNIT=71,FILE='C:\2014_ozaki\DATA\DATATR
Y\STEP3\OUTPUT3_EX1\KPRYUSI1_OUT.DAT')
    !OTHERS

```

```

OPEN(UNIT=80,FILE='C:\2014_ozaki\DATA\DATATR
Y\STEP3\OUTPUT3_EX1\GOSA_OUT.DAT')
OPEN(UNIT=81,FILE='C:\2014_ozaki\DATA\DATATR
Y\STEP3\OUTPUT3_EX1\EMPTY_OUT.DAT')
OPEN(UNIT=82,FILE='C:\2014_ozaki\DATA\DATATR
Y\STEP3\OUTPUT3_EX1\NEMPTY_OUT.DAT')
OPEN(UNIT=83,FILE='C:\2014_ozaki\DATA\DATATR
Y\STEP3\OUTPUT3_EX1\H0_OUT.DAT')
    !CTOE
OPEN(UNIT=93,FILE='C:\2014_ozaki\DATA\DATATR
Y\STEP3\OUTPUT3_EX1\CTOEI2_OUT.DAT')
OPEN(UNIT=94,FILE='C:\2014_ozaki\DATA\DATATR
Y\STEP3\OUTPUT3_EX1\CTOEJ_OUT.DAT')
OPEN(UNIT=95,FILE='C:\2014_ozaki\DATA\DATATR
Y\STEP3\OUTPUT3_EX1\CTOE_OUT.DAT')
OPEN(UNIT=96,FILE='C:\2014_ozaki\DATA\DATATR
Y\STEP3\OUTPUT3_EX1\CTOE100_OUT.DAT')
    !PARAMETER INCLUDING PUMP
OPEN(UNIT=99,FILE='C:\2014_ozaki\DATA\DATATR
Y\STEP3\OUTPUT3_EX1\PARAMETER_OUT.DAT')
!-----
-----!
!---INITIAL PARAMETER-----!
    ROUS=1.0250D0
    ROUF=0.9910D0
    HS=30.0D0
    HF=31.5D0
    DH=(HF-HS)/100.0D0
    DH5=DH/2.0D0
    qw=0.0D0
    SITA0=0.348D0
    SR=0.075D0
    ALPH=4.91D-02
    EM=0.8599D0
    EN=7.138D0
    CA0=0.10D0
!---DISPERSION COEFFICIENT-----!
    DM=1.0D-05

```

```

AL=0.038030D0
AT=0.005018D0
!---JUDGEMENT FOR ERROR---!
EPSI=1.0D-2
OMEGA=1.60D0
!---GRID PARAMETER-----!
DX=0.50D0
DY=0.50D0
DT=0.50D0
IMIN=1
JMIN=1
ISMIN=23
ISMAX=223
IMAX=245
JMAX=81
JSMAX=65
!---STEP-----!
-----!
!KAI=1 !STEP 1
!KAI=2 !STEP 2
KAI=3 !STEP 3
!KAI=4 !STEP 4
!KAI=5 !STEP 5
!---PUMPING WELLS PARAMETER-----!
-----!
!!!!BARRIER WELL (WELL1)
XE1=61.0
XE1L=60.5
XE1R=61.5
YE1=15.0
YE1B=14.5 !WELL BOUNDARY
BOTTOM
YE1T=15.5 !WELL BOUNDARY TOP
IE1=123
IE1L=122
IE1R=124
JE1=31
JE1B=30
JE1T=32
PE1=-0.3
!!!!PRODUCTION WELL (WELL2)
XE2=86.0
XE2L=85.5
XE2R=86.5
YE2=15.0
YE2B=14.5
YE2T=15.5
IE2=173
IE2L=172
IE2R=174
JE2=31
JE2B=30
JE2T=32
!!!!PUMPING RATE
!!!!WELL A (BARRIER WELL)
IF(EXNUM.EQ.1)THEN
TKSAT0=0.452D0
RAB=0.90D0
QP1=1.84D0 !EXPERIMENT NUMBER 1
QP2=1.73D0 !EXPERIMENT NUMBER 1
ELSE IF(EXNUM.EQ.2)THEN
TKSAT0=0.395D0
RAB=1.20D0
QP1=2.93D0 !EXPERIMENT NUMBER
2(3.33=>2.93)
QP2=3.47D0 !EXPERIMENT NUMBER
2(3.33=>2.93)
ELSE IF(EXNUM.EQ.3)THEN
TKSAT0=0.386D0
RAB=2.00D0
QP1=2.67D0 !EXPERIMENT NUMBER 3
QP2=5.33D0 !EXPERIMENT NUMBER 3
ELSE IF(EXNUM.EQ.4)THEN
TKSAT0=0.482D0
RAB=2.60D0
QP1=2.20D0 !EXPERIMENT NUMBER 4

```

```

QP2=5.70D0 !EXPERIMENT NUMBER 4
ELSE IF(EXNUM.EQ.5)THEN
TKSAT0=0.527D0
RAB=1.50D0
QP1=2.47D0 !EXPERIMENT NUMBER 5
QP2=3.80D0 !EXPERIMENT NUMBER 5
ELSE IF(EXNUM.EQ.6)THEN
TKSAT0=0.500D0
RAB=1.90D0
!RAB=2.30D0
QP1=2.69D0 !EXPERIMENT NUMBER
6 !Q_PUMPED(cm3/s) (BARRIER WELL)
QP2=5.23D0 !EXPERIMENT NUMBER 6(5.23
FOR QA/AB=1.9, 6.13 FOR QA/AB=2.3)
!QP2=6.13D0
END IF
WRITE(*,1162) QP1,QP2,RAB

1162FORMAT('QP1=',F6.3,'QP2=',F6.3,'R(QA/QB)=' ,F
6.3)
WIDTH=10.6D0 !WIDTH OF
EXPERIMENTAL DEVICE(cm)
!-----
----!
DO I=IMIN,IMAX
IF(I.EQ.IMIN) THEN
XX(I)=0.0D0
ELSE
XX(I)=XX(I-1)+DX
END IF
END DO
XL=XX(IMAX)
DO J=JMIN,JMAX
IF(J.EQ.JMIN)THEN
YY(J)=0.0D0
ELSE
YY(J)=YY(J-1)+DY
END IF

```

```

END DO
!---SPM AREA(cm) ----!
XLEFT=XX(IMIN)-DX/2.0D0 !LEFT(cm)=0
XRIGHT=XX(IMAX)+DX/2.0D0 !RIGHT(cm)=150.
0
YLOW=0.0D0 !BOTTOM(cm)=0.0
YLOW1=YLOW+DY/4.0D0 !
YLOW2=YLOW+DY/4.0D0 !
!---READ-----
-!
DO J=JMAX,JMIN,-1
READ(10,*)
(DELC(I,J),I=IMIN,IMAX) !DELC(I,J) !%
READ(11,*)
(ROU(I,J),I=IMIN,IMAX) !DENSITY(I,J) !g/
cm3
READ(12,*)
(H(I,J,1),I=IMIN,IMAX) !HEAD(I,J) !cm
READ(13,*)
(KPKOSU(I,J),I=IMIN,IMAX) !KPKOSU(I,J)
!(No.)
READ(14,*)
(NS1(I,J),I=IMIN,IMAX) !NS1(I,J) !(-)
END DO
DO K=1,120000
READ(16,*)
NO(K),XP(K),YP(K),KGRID(K,1),KGRID(K,2)
1016 FORMAT(I6,1X,F8.3,1X,F8.3,1X,I6,1X,I6)
END DO
DO K=120001,KDIM
NO(K)=K
XP(K)=999
YP(K)=999
KGRID(K,1)=999
KGRID(K,1)=999
END DO
READ(17,*) (JGL(I),I=IMIN,IMAX)

```

```

IF(KALEQ.2)THEN
  GO TO 6310
END IF
1030 FORMAT(245F10.2)
1084 FORMAT(245I5)
1085 FORMAT(I6,1X,F8.3,1X,F8.3,1X,I6,1X,I6)
!---KAI 2-----!
6310CONTINUE
DO I=IMIN,IMAX
  DO J=JMIN,JMAX
    HWOLD(I,J)=0.0
  END DO
END DO
!---HEAD
DO I=IMIN,IMAX
  DO J=JMIN,JMAX
    H0(I,J,2)=H(I,J,1)
  END DO
END DO
!---WRITE FOR HEAD-----
-----!
DO I=IMIN,IMAX
  DO J=JMIN,JMAX
    H(I,J,2)=H0(I,J,2)
    H(I,J,1)=H(I,J,2)
    H0(I,J,1)=H(I,J,1)
  END DO
END DO
WRITE(34,*) 'INITIAL HEAD 2'
WRITE(34,1040)
((H(I,J,2),I=IMIN,IMAX),J=JMAX,JMIN,-1)
WRITE(34,*) 'INITIAL HEAD 1'
WRITE(34,1040)
((H(I,J,1),I=IMIN,IMAX),J=JMAX,JMIN,-1)
WRITE(83,1040)
((H(I,J,2),I=IMIN,IMAX),J=JMAX,JMIN,-1)
WRITE(83,1040)
((H(I,J,1),I=IMIN,IMAX),J=JMAX,JMIN,-1)

```

```

!---WELL HEAD WRITE-----
-----!
BW=9.0D0
HWELL1=H(IE1,JE1,2)
HWELL2=H(IE2,JE2,2)
QP1M=QP1/BW
QP2M=QP2/BW
HEADQ1=HWELL1-QP1M
HEADQ2=HWELL2-QP2M
DO I=IE1L,IE1R
  DO J=JE1B,JE1T
    HWOLD(I,J)=H(I,J,2)-QP1M
  END DO
END DO
DO I=IE2L,IE2R
  DO J=JE2B,JE2T
    HWOLD(I,J)=H(I,J,2)-QP2M
  END DO
END DO
748FORMAT('HWELL1=',F8.4,'HEADQ1=',F8.4)
749FORMAT('HWELL2=',F8.4,'HEADQ2=',F8.4)
750FORMAT('H(IE1,JE1,2)=',F8.4,'HWOLD(IE1,JE1)=',F8.4)
!---SITAS AND TKSAT-----
---!
DO I=IMIN,IMAX
  DO J=JMIN,JMAX
    IF(J.GT.JSMAX)THEN
      SITAS(I,J)=0.0D0
      TKSAT(I,J)=0.0D0
    ELSE
      SITAS(I,J)=SITA0
      TKSAT(I,J)=TKSAT0      !(-)
    END IF
  END DO
END DO
CALL WATER(H,SITA,SITAS,IMIN,IMAX,JGL)

```

```

!---WRITE FOR TKSAT,SITA,SITAS-----
-----!
DO J=JMAX,JMIN,-1
WRITE(31,1031)
(TKSAT(I,J),I=IMIN,IMAX)  !(cm/s)
1031 FORMAT(245F10.4)
END DO
DO J=JMAX,JMIN,-1
WRITE(32,1032) ((SITA(I,J)),I=IMIN,IMAX)
1032 FORMAT(245F10.6)
END DO
!---TIME STEP-----!
WRITE(*,*) 'FINAL TIME = ' !FINAL TIME
=12000s
READ(*,*) FT
WRITE(*,*) FT
WRITE(50,1443) FT
1443 FORMAT(F8.2)
IFTS=FT/DT+0.00005
=====
=====!
!====CALCULATION
START=====
=====!
=====
=====!
TIME=0.0D0
IPMAX=IMAX
IPMIN=IMIN
ISTEP=TIME/DT+0.00005
!<<<<<<<REPEAT>>>>>>>!
5555 CONTINUE
!<<<<<<<<<<<<<<>>>>>>>>>>!

ISTEP=ISTEP+1  !STEP
TIME=TIME+DT  !TIME(sec)
TIMEM=TIME/60.0D0  !TIME(min)

```

```

TIMEH=TIME/3600.0D0  !TIME(hour)
DAY=TIMEH/24.0D0  !TIME(day)
IT=0  !ITERATION LEVEL(-)

!-----
-----!
! Successive Over Relaxation Method for head
distribution calculation  !
!-----
-----!
=====
=====!
555 CONTINUE
=====
=====!
IT=IT+1  ! ITERATION(-)
ERROR=0  ! NUMBER OF GRID THAT EXCEED
THE CRITERIA(-)
GMAX=0.0D0  ! MAXIMUM ERROR(m)
IGOSA=0
JGOSA=0

! *==== GRID FORMATION OF H-DUMMY AND
PERMEABILITY =====*
! * <4> *
! * I *
! * T4 *
! * I *
! * <3>--T3--<1>--T2--<2> *
! * I *
! * T5 *
! * I *
! * <5> *
!
*=====
=====*

```

!---CALCULATION FOR PRESSURE HEAD IN
SATURATE/UNSATURATED AREA-----

-----!

DO I=IMIN,IMAX
DO J=JMIN,JGL(I)

!!!WELL POSITION

IF(KAL.EQ.2.OR.KAL.EQ.4)**THEN**
IF(I.GE.IE1L.AND.I.LE.IE1R)**THEN**
IF(J.GE.JE1B.AND.J.LE.JE1T)**THEN**
H(I,J,2)=HWOLD(I,J)
GO TO 101
END IF
END IF

ELSE IF(KAL.EQ.3)**THEN**
IF(I.GE.IE1L.AND.I.LE.IE1R)**THEN**
IF(J.GE.JE1B.AND.J.LE.JE1T)**THEN**
GO TO 101
END IF
END IF

IF(I.GE.IE2L.AND.I.LE.IE2R)**THEN**
IF(J.GE.JE2B.AND.J.LE.JE2T)**THEN**
H(I,J,2)=HWOLD(I,J)
GO TO 101
END IF
END IF
END IF

!---NORMAL CALCULATION

HOLD=H(I,J,2)
IF(I.EQ.IMAX)**THEN**
H(I,J,2)=HOLD
GO TO 101
END IF

!---BOUNDARY CONDITION-----

-----!

!---<1>BOTTOM

IF(J.EQ.JMIN)**THEN**
HJ5=H(I,J+1,2)+(ROU(I,J)/ROUF)*DY*2.0D0
ROUJ5=ROU(I,J+1)

TK5=TKSAT(I,J+1)

ELSE

HJ5=H(I,J-1,2)
ROUJ5=ROU(I,J-1)
TK5=TKSAT(I,J-1)

END IF

!---<2>TOP

IF(J.EQ.JGL(I))**THEN**
IF(I.GT.ISMIN.AND.I.LE.IMAX)**THEN**
CALL TOSUI(HOLD,TX)
TEND=TX*TKSAT(I,J)
IF(TEND.LE.1.0D-05)**THEN**
TEND=1.0D-05
END IF

H(I,J+1,2)=H(I,J-1,2)+(qw/TEND-
ROU(I,J)/ROUF)*(2.0*DY)

ROU(I,J+1)=ROU(I,J-1)
TKSAT(I,J+1)=TKSAT(I,J-1)

ELSE IF(I.LE.ISMIN)**THEN**

H(I,J+1,2)=H(I,J-1,2)+(qw/TEND-
ROU(I,J)/ROUF)*(2.0*DY)

ROU(I,J+1)=ROU(I,J-1)
TKSAT(I,J+1)=TKSAT(I,J-1)

END IF

END IF

!---<3>LEFT

IF(I.EQ.IMIN)**THEN**

IH2=I+1

IH3=I+1

!---<4>RIGHT

ELSE IF(I.EQ.IMAX)**THEN**

IH2=I-1

IH3=I-1

ELSE IF(I.EQ.ISMIN)**THEN**

IH2=I-1

IH3=I-1

ELSE

IF(NS1(I,J).EQ.3)**THEN**


```

      IH2=I+1
      IH3=I+1
      ELSE IF(NS1(I,J).EQ.1)THEN
      IH2=I+1
      IH3=I-1
      END IF
      END IF
!---HYDRAULIC CONDUCTIVITY-----
-----!
      T(1,1)=TKSAT(I,J)
      T(2,1)=TKSAT(IH2,J)
      T(3,1)=TKSAT(IH3,J)
      T(4,1)=TKSAT(I,J+1)
      T(5,1)=TK5
      HDUMMY(1,2)=H(I,J,2)
      HDUMMY(2,2)=H(IH2,J,2)
      HDUMMY(3,2)=H(IH3,J,2)
      HDUMMY(4,2)=H(I,J+1,2)
      HDUMMY(5,2)=HJ5
      DO K=1,5
      CALL TOSUI(HDUMMY(K,2),TX)
      T(K,2)=TX*T(K,1)
      IF(T(K,2).LE.1.0D-05)THEN
      T(K,2)=1.0D-05
      END IF
      END DO
!---SPECIFIC WATER CAPACITY-----
-----!
      HMEAN=H(I,J,2)
      S=SITA(I,J)
      SS=SITAS(I,J)
      CALL CAPA(HMEAN,CA,S,SS,CA0)
      CW(I,J)=CA
!---HARMONIC MEAN-----
-----!
      TT2=2.0*(T(1,2)*T(2,2))/(T(1,2)+T(2,2)) ! !=TK(I+1/2,J)
      TT3=2.0*(T(1,2)*T(3,2))/(T(1,2)+T(3,2)) ! !=TK(I-1/2,J)
      TT4=2.0*(T(1,2)*T(4,2))/(T(1,2)+T(4,2)) ! !=TK(I,J+1/2)
      TT5=2.0*(T(1,2)*T(5,2))/(T(1,2)+T(5,2)) ! !=TK(I,J-1/2)
      RR4=(ROU(I,J)+ROU(I,J+1))*0.5D0 !=ROU(I,J+1/2)
      RR5=(ROU(I,J)+ROU(I,J-1))*0.5D0 !=ROU(I,J-1/2)
      A1=(TT2/DX+TT3/DX)*2.0D0/(DX+DX)
      A2=(TT4+TT5)/(DY*DY)
      AA=A1+A2
      B1=TT2*H(IH2,J,2)/DX
      B2=TT3*H(IH3,J,2)/DX
      BB=(B1+B2)/DX
      C1=TT4*H(I,J+1,2)
      C2=TT5*H(I,J-1,2)
      CC=(C1+C2)/(DY*DY)
      D1=TT4*RR4/ROUF
      D2=TT5*RR5/ROUF
      DD=(D1-D2)/DY
      EE=CA
      BUNBO=AA*DT+EE
      BUNSI=(BB+CC+DD)*DT+EE*H(I,J,1)
      HNEW=BUNSI/BUNBO
!---SOR METHOD-----
-----!
      H(I,J,2)=HOLD+OMEGA*(HNEW-HOLD) !REPEAT STEP (m+1)times
!-----
----!
      GOSA=DABS(H(I,J,2)-HOLD)
      IF(GOSA.GT.EPSI)THEN

```

```

IERROR=IERROR+1
IGOSA=I
IGOSA=J
ELSE
END IF
IF(GOSA.GT.GMAX)THEN
  GMAX=GOSA
END IF
101 CONTINUE
END DO
END DO

IF(IERROR.EQ.0)THEN
ELSE
  GO TO 555
END IF

IF(ISTEP.EQ.1)THEN
  WRITE(34,1444) ISTEP,TIME
  WRITE(34,*) 'AFTER SOR METHOD'
  WRITE(34,1040)
((H(I,J,2),I=IMIN,IMAX),J=JMAX,JMIN,-1)
END IF

!---VOLUME WATER CONTENT-----
-----!
  CALL WATER(H,SITA,SITAS,IMIN,IMAX,JGL)
!---DARCY'S VELOCITY-----
-----!

DO I=IMIN,IMAX
DO J=JMIN,JGL(I)
  CALL TOSUI(H(I,J,2),TX)
  TX=TX*TKSAT(I,J)
  IF(TX.LE.1.0D-05)THEN
    TX=1.0D-05
  END IF
  TCH(I,J)=TX

!---BOUNDARY CONDITION-----
-----!

I---<1>LEFT
  IF(I.EQ.IMIN)THEN
    I2=I+1
    I3=I
    XCON=DX
  I---<2>RIGHT
  ELSE IF(I.EQ.IMAX)THEN
    I2=I
    I3=I-1
    XCON=DX
  I---<3>NORMAL GRID
  ELSE
    IF(NS1(I,J).EQ.3)THEN
      U(I,J)=0.0D0
      I2=I+1
      I3=I
      XCON=DX
    ELSE IF(NS1(I,J).EQ.1)THEN
      I2=I+1
      I3=I-1
      XCON=DX*2.0D0
    END IF
  END IF

I---<4>BOTTOM + U,V
  IF(J.EQ.JMIN)THEN
    V(I,J)=0.0D0
    U(I,J)=-TX*(H(I2,J,2)-H(I3,J,2))/XCON
  I---<5>TOP + U,V
  ELSE IF(J.EQ.JGL(I))THEN
    U(I,JGL(I))=0.0D0
    IF(I.GE.IMIN.AND.I.LE.ISMIN)THEN
      J2=J
      J3=J-1
      YCON=DY
      V(I,J)=-TX*((H(I,J2,2)-
H(I,J3,2))/YCON+ROU(I,J)/ROUF)
    ELSE IF(I.GT.ISMIN.AND.I.LE.IMAX)THEN
      IF(H(I,J,2).GE.0.0D0)THEN

```

```

      J2=J
      J3=J-1
      H(I,J,2)=0.0D0
      YCON=DY
      V(I,J)=-TX*((H(I,J,2)-
H(I,J3,2))/YCON+ROU(I,J)/ROUF)
      ELSE IF(H(I,J,2).LT.0.0D0)THEN
      V(I,J)=-qw
      END IF
      END IF
!---<6>NORMAL GRID
      ELSE
      458CONTINUE
      J2=J+1
      J3=J-1
      YCON=DY*2.0D0
      V(I,J)=-TX*((H(I,J,2)-
H(I,J3,2))/YCON+ROU(I,J)/ROUF)
      U(I,J)=-TX*(H(I2,J,2)-H(I3,J,2))/XCON
      END IF
      END DO
      END DO
!---VELOCITY WITHIN WELL POSITION-----
-----!
      IF(KA1.EQ.2.OR.KA1.EQ.4)THEN
      DO I=IE1L,IE1R
      DO J=JE1B,JMAX
      U(I,J)=0.0D0
      V(I,J)=0.0D0
      END DO
      END DO
      ELSE IF(KA1.EQ.3)THEN
      DO I=IE1L,IE1R
      DO J=JE1B,JE1T
      U(I,J)=0.0D0
      V(I,J)=0.0D0
      END DO
      END DO

```

```

      DO I=IE2L,IE2R
      DO J=JE2B,JE2T
      U(I,J)=0.0D0
      V(I,J)=0.0D0
      END DO
      END DO
      END IF
!---IF J>JGL -----!
      DO I=IMIN,IMAX
      DO J=JGL(I)+1,JMAX
      U(I,J)=0.0D0
      V(I,J)=0.0D0
      END DO
      END DO
      DO I=IMIN,IMAX
      DO J=JMIN,JMAX
      IF(J.GT.JGL(I)) THEN
      H(I,J,2)=0.0D0
      ELSE IF(I.GT.ISMIN.AND.J.EQ.JGL(I)) THEN
      IF (H(I,J,2).GT.0.000D0) THEN
      H(I,J,2)=0.0D0
      END IF
      END IF
      H(I,J,1)=H(I,J,2)
      END DO
      END DO
!---CALCULATION FOR STABILITY-----
-----!
      DO I=IMIN,IMAX
      DO J=JMIN,JGL(I)
      VV=SQRT(U(I,J)**2+V(I,J)**2) !(cm/sec)
      DXX=(AL*(U(I,J)**2)+AT*(V(I,J)**2))/VV+DM !(cm2
/sec)
      DYY=(AT*(U(I,J)**2)+AL*(V(I,J)**2))/VV+DM !(cm2
/sec)
      DT1=DT*DXX/(DX*DX) !(-)

```

```

DT2=DT*DYY/(DY*DY)
DT3=DT*DABS(U(I,J))/DX !(-)
DT4=DT*DABS(V(I,J))/DY !(-) !(-)

IF((DT1.GE.0.47D0).OR.(DT2.GE.0.47D0).OR.(DT3.GE.0.5D0).OR.(DT4.GE.0.5D0)) THEN
    WRITE(*,7777)
    ISTEP,I,J,U(I,J),V(I,J),DM,DXX,DYY,DT1,DT2,DT3,DT4
    7777
FORMAT(1H,'ISTEP:',I10,2X,'I:',I8,2X,'J:',J8,2X,'U:',F10.4,2X,'V:',F10.4,2X,'DM:',F12.9,2X,'DXX:',F10.6,2X,'DYY:',F10.4,2X,'DT1:',F10.6,2X,'DT2:',F10.6,2X,'DT3:',F10.6,2X,'DT4:',F10.6)
    WRITE(*,*) 'NEW DT='
    READ(*,*) DT
    WRITE(*,9999) DT
    9999 FORMAT(1X,'#### TIME INCREMENT
#### DT=',F10.2,' sec')
END IF
END DO
END DO
!---WRITE H,U,V-----
-----!
IF(ISTEP.EQ.1)THEN
    WRITE(34,1444) ISTEP,TIME
END IF
!---DENSITY->CONCENTRATION----!
DO I=IMIN,IMAX
DO J=JMIN,JMAX
IF(J.GT.JGL(I)) THEN
    CMIX(I,J)=0.0D0
ELSE
    CMIX(I,J)=(ROU(I,J)-ROUF)*100.0D0/(ROUS-ROUF)
END IF
END DO
END DO

```

```

XLR=XX(IMIN)
XRL=XX(IMAX)
!
! | | ~ | |
! | | ~ | |
! | | ~ | |
! | | ~ | |
! XLEFT XLR ~ XRL XRIGHT
!
IF(KOSU.GE.(KDIM-500))THEN
    GOTO 222
END IF
IF(ISTEP.NE.1)THEN
    GOTO 333
END IF
IF(KAL.EQ.2)THEN
    GO TO 333
END IF
!---<STEP1> Initial arrangement of particles
222 CONTINUE
WRITE(*,*) 'INITIAL ARRANGEMENT STEP1 IN SPM'
CALL
INI(DX,XX,DY,XP,YP,KOSU,KDIM,IMIN,IMAX,JGL)
IF(ISTEP.EQ.1)THEN
DO K=1,KOSU
    WRITE(33,1033) K,XP(K),YP(K)
    1033 FORMAT(I10,1X,F10.5,1X,F10.5)
END DO
END IF
!---<STEP2> Arrange particles and give particle numbers
at each grid point
DO I=IMIN,IMAX
DO J=JMIN,JGL(I)

```

```

      KPKOSU(I,J)=0
    END DO
  END DO

  CALL
GRID(XP,YP,DX,XX,DY,KGRID,CP,KOSU,XLEFT,XR
IGHT,YLOW,YLOW1,YLOW2, &

KDIM,KPKOSU,KPRYUSI,IMIN,IMAX,JGL,NS1)
!---<STEP3> Calculation of particle concentration
  DO K=1,KDIM
    CP(K)=0.0D0
  END DO
  CALL
HOKAN(CMIX,XP,YP,DX,DY,XX,KGRID,CP,KOSU,
&
      KDIM,IMIN,IMAX,JGL,NS1)
!---SETTING OF PARTICLE CONCENTRATION AT
BOUNDARY----!
! (Adjust boundary concentrations of particles)
! LEFT : FRESHWATER BOUNDARY, RIGHT :
SALTWATER BOUNDARY)
  I=IMIN ! LEFT
  DO J=JMIN,JGL(I)
    NUM=KPKOSU(I,J) !KPKOSU(I,J):PARTICLE
NUMBER(I,J)
    IF(NUM.NE.0) THEN
      DO KP=1,NUM
        KNAME=KPRYUSI(I,J,KP) !KPRYUSI(I,J,KP)
        IF(XP(KNAME).LT.XLR) THEN
          CP(KNAME)=100.0D0 !CONCEN(I,J)
        END IF
      END DO
    END IF
  END DO

  I=IMAX ! RIGHT
  DO J=JMIN,JGL(I)

```

```

      NUM=KPKOSU(I,J) !KPKOSU(I,J)
    IF(NUM.NE.0) THEN
      DO KP=1,NUM
        KNAME=KPRYUSI(I,J,KP) !KPRYUSI(I,J,KP)
        IF(XP(KNAME).GE.XRL) THEN
          CP(KNAME)=0.0D0 !CONCEN(I,J)
        END IF
      END DO
    END IF
  END DO
  END DO

  DO I=IMIN,IMAX
    YTOP=DY*(JGL(I)-1)
    NUM=KPKOSU(I,JGL(I)) !KPKOSU(I,J)
    IF(NUM.NE.0) THEN
      DO KP=1,NUM
        KNAME=KPRYUSI(I,JGL(I),KP) !KPRYUSI(I,J,KP)
        IF(YP(KNAME).GE.YTOP) THEN
          IF(I.LE.ISMIN) THEN
            CP(KNAME)=CMIX(I,JGL(I))
          ELSE IF(I.GT.ISMIN) THEN
            CP(KNAME)=0.0D0
          END IF
        END IF
      END DO
    END IF
  END DO
  333 CONTINUE

!---<STEP 4> Movement of particle with actual velocity
U,V
!***AFTER DT *****
  DO K=1,KOSU
    IK=KGRID(K,1)
    JK=KGRID(K,2)
    YTOPU=DY*(JGL(IK)-1)+DY/2.0D0
    YTOP=DY*(JGL(IK)-1)

```

```

      IF(YP(K).LT.YLOW .OR. YP(K).GE.YTOPU .OR.
XP(K).LT.XLEFT.OR.XP(K).GE.XRIGHT) THEN
      ELSE
      IF(IK.LT.0.OR.JK.LT.0) THEN
!====DISPLAY:4=====
      WRITE(*,990) IK,JK,K,XP(K),YP(K)
      990 FORMAT(12X,'ERROR IN
SPM:',3I6,3X,2F12.1)
!=====
=====
      WRITE(*,*) 'CONTINUE???'
      READ(*,*) CODE
      STOP
      END IF

      IF(KAL.EQ.2.OR.KAL.EQ.4)THEN

IF((XP(K).GE.XE1L.AND.XP(K).LE.XE1R).AND.(YP(
K).GE.YE1B.AND.YP(K).LE.YE1T))THEN
      GO TO 400
      END IF

IF((IK.GE.IE1L.AND.IK.LE.IE1R).AND.(JK.GE.JE1B.
AND.JK.LE.JE1T))THEN
      GO TO 400
      END IF
      ELSE IF(KALEQ.3)THEN

IF((XP(K).GE.XE1L.AND.XP(K).LE.XE1R).AND.(YP(
K).GE.YE1B.AND.YP(K).LE.YE1T))THEN
      GO TO 400
      END IF

IF((XP(K).GE.XE2L.AND.XP(K).LE.XE2R).AND.(YP(
K).GE.YE2B.AND.YP(K).LE.YE2T))THEN
      GO TO 400
      END IF

```

```

IF((IK.GE.IE1L.AND.IK.LE.IE1R).AND.(JK.GE.JE1B.
AND.JK.LE.JE1T))THEN
      GO TO 400
      END IF

IF((IK.GE.IE2L.AND.IK.LE.IE2R).AND.(JK.GE.JE2B.
AND.JK.LE.JE2T))THEN
      GO TO 400
      END IF
      END IF
!!!!!!!BOUNDARY OF PUMPING AREA-----
-----
!!!!!!!STEP 2 OR STEP 4-----
-----
      IF(KAL.EQ.2.OR.KAL.EQ.4)THEN
      IF(IK.EQ.(IE1L-
1).AND.(JK.GE.JE1B.AND.JK.LE.JE1T))THEN
      UK=U(IE1L-1,JK)/SITA(IE1L-1,JK)
      VK=V(IE1L-1,JK)/SITA(IE1L-1,JK)
      GO TO 411
      END IF

IF(IK.EQ.(IE1R+1).AND.(JK.GE.JE1B.AND.JK.LE.JE1
T))THEN
      UK=U(IE1R+1,JK)/SITA(IE1R+1,JK)
      VK=V(IE1R+1,JK)/SITA(IE1R+1,JK)
      GO TO 411
      END IF

IF((IK.GE.IE1L.AND.IK.LE.IE1R).AND.JK.EQ.(JE1B-
1))THEN
      UK=U(IK,JE1B-1)/SITA(IK,JE1B-1)
      VK=V(IK,JE1B-1)/SITA(IK,JE1B-1)
      GO TO 411
      END IF

```

IF((IK.GE.IE1L.AND.IK.LE.IE1R).AND.JK.EQ.(JE1T+1))**THEN**

UK=U(IK,JE1T+1)/SITA(IK,JE1T+1)

VK=V(IK,JE1T+1)/SITA(IK,JE1T+1)

GO TO 411

END IF

!!!!!!!STEP 3-----

ELSE IF(KALEQ.3)**THEN**

IF(IK.EQ.(IE1L-1).AND.(JK.GE.JE1B.AND.JK.LE.JE1T))**THEN**

UK=U(IE1L-1,JK)/SITA(IE1L-1,JK)

VK=V(IE1L-1,JK)/SITA(IE1L-1,JK)

GO TO 411

END IF

IF(IK.EQ.(IE1R+1).AND.(JK.GE.JE1B.AND.JK.LE.JE1T))**THEN**

UK=U(IE1R+1,JK)/SITA(IE1R+1,JK)

VK=V(IE1R+1,JK)/SITA(IE1R+1,JK)

GO TO 411

END IF

IF((IK.GE.IE1L.AND.IK.LE.IE1R).AND.JK.EQ.(JE1B-1))**THEN**

UK=U(IK,JE1B-1)/SITA(IK,JE1B-1)

VK=V(IK,JE1B-1)/SITA(IK,JE1B-1)

GO TO 411

END IF

IF((IK.GE.IE1L.AND.IK.LE.IE1R).AND.JK.EQ.(JE1T+1))**THEN**

UK=U(IK,JE1T+1)/SITA(IK,JE1T+1)

VK=V(IK,JE1T+1)/SITA(IK,JE1T+1)

GO TO 411

END IF

IF(IK.EQ.(IE2L-1).AND.(JK.GE.JE2B.AND.JK.LE.JE2T))**THEN**

UK=U(IE2L-1,JK)/SITA(IE2L-1,JK)

VK=V(IE2L-1,JK)/SITA(IE2L-1,JK)

GO TO 411

END IF

IF(IK.EQ.(IE2R+1).AND.(JK.GE.JE2B.AND.JK.LE.JE2T))**THEN**

UK=U(IE2R+1,JK)/SITA(IE2R+1,JK)

VK=V(IE2R+1,JK)/SITA(IE2R+1,JK)

GO TO 411

END IF

IF((IK.GE.IE2L.AND.IK.LE.IE2R).AND.JK.EQ.(JE2B-1))**THEN**

UK=U(IK,JE2B-1)/SITA(IK,JE2B-1)

VK=V(IK,JE2B-1)/SITA(IK,JE2B-1)

GO TO 411

END IF

IF((IK.GE.IE2L.AND.IK.LE.IE2R).AND.JK.EQ.(JE2T+1))**THEN**

UK=U(IK,JE2T+1)/SITA(IK,JE2T+1)

VK=V(IK,JE2T+1)/SITA(IK,JE2T+1)

GO TO 411

END IF

END IF

!!!!!!!BOUNDARY OF PUMPING AREA-----

!!!!!!!INSIDE PUMPING POINTS-----

XXL1=XX(IE1L)-DX/2.0

XXL2=XX(IE1R)+DX/2.0

YYL1=(JE1B-1)*DY-DY/2.0

YYL2=(JE1T-1)*DY+DY/2.0

XXT1=XX(IE2L)-DX/2.0

XXT2=XX(IE2R)+DX/2.0

```

      YYT1=(JE2B-1)*DY-DY/2.0
      YYT2=(JE2T-1)*DY+DY/2.0
!!!!!!!STEP 2 OR 4-----
-----
      IF(KA1.EQ.2.OR.KA1.EQ.4)THEN

IF((XP(K).GE.XXL1).AND.(XP(K).LE.XXL2))THEN

IF((YP(K).GE.YYL1).AND.(YP(K).LE.YYL2))THEN
      GO TO 400
      END IF
      END IF
!!!!!!!STEP 3-----
-----
      ELSE IF(KA1.EQ.3)THEN

IF((XP(K).GE.XXL1).AND.(XP(K).LE.XXL2))THEN

IF((YP(K).GE.YYL1).AND.(YP(K).LE.YYL2))THEN
      GO TO 400
      END IF
      END IF

IF((XP(K).GE.XXT1).AND.(XP(K).LE.XXT2))THEN

IF((YP(K).GE.YYT1).AND.(YP(K).LE.YYT2))THEN
      GO TO 400
      END IF
      END IF
      END IF
!-----
-----
IF(XP(K).LT.XLEFTR.AND.YP(K).LT.YTOPU.OR. &
      XP(K).GE.XRL.AND.YP(K).LT.YTOPU.OR. &
(XP(K).GE.XLEFTR.AND.XP(K).LT.XRL).AND.YP(K)
      .GE.YTOP) THEN

```

```

      UK=U(IK,JK)
      VK=V(IK,JK)
ELSE
      IF(IK.EQ.IMIN) THEN
            IU2=IK+1
            IU0=IK
      ELSE IF(IK.EQ.IMAX) THEN
            IU2=IK
            IU0=IK-1
      ELSE IF(IK.GT.IMIN.AND.IK.LT.IMAX) THEN
            IF(NS1(IK,JK).EQ.3)THEN
                  IU2=IK+1
                  IU0=IK
            ELSE IF(NS1(IK,JK).EQ.1)THEN
                  IU2=IK+1
                  IU0=IK-1
            END IF
            END IF
      !***INTERPOLATION OF VELOCITY *****
      XPOINT=XX(IK)
      YPOINT=FLOAT(JK-1)*DY
      DXP=XP(K)-XPOINT
      DYP=YP(K)-YPOINT
      IF(DXP.LT.0.0) THEN
            IF(DYP.LT.0.0) THEN
                  UK=U(IK,JK)+(U(IK,JK)-
U(IU0,JK))*DXP/DX+(U(IK,JK)-U(IK,JK-
1))*DYP/DY !REGION3
                  VK=V(IK,JK)+(V(IK,JK)-
V(IU0,JK))*DXP/DX+(V(IK,JK)-V(IK,JK-1))*DYP/DY
            ELSE
                  UK=U(IK,JK)+(U(IK,JK)-
U(IU0,JK))*DXP/DX+(U(IK,JK+1)-
U(IK,JK))*DYP/DY !REGION2
                  VK=V(IK,JK)+(V(IK,JK)-
V(IU0,JK))*DXP/DX+(V(IK,JK+1)-
V(IK,JK))*DYP/DY
            END IF

```



```

ELSE
  IF(DYP.LT.0.0) THEN
    UK=U(IK,,JK)+(U(IU2,,JK)-
U(IK,,JK))*DXP/DX+(U(IK,,JK)-U(IK,,JK-
1))*DYP/DY !REGION4
    VK=V(IK,,JK)+(V(IU2,,JK)-
V(IK,,JK))*DXP/DX+(V(IK,,JK)-V(IK,,JK-1))*DYP/DY
  ELSE
    UK=U(IK,,JK)+(U(IU2,,JK)-
U(IK,,JK))*DXP/DX+(U(IK,,JK+1)-
U(IK,,JK))*DYP/DY !REGION1
    VK=V(IK,,JK)+(V(IU2,,JK)-
V(IK,,JK))*DXP/DX+(V(IK,,JK+1)-V(IK,,JK))*DYP/DY
  END IF
END IF
END IF
XP(K)=XP(K)+UK/SITA(IK,,JK)*DT
YP(K)=YP(K)+VK/SITA(IK,,JK)*DT
GO TO 464
411CONTINUE
XP(K)=XP(K)+UK*DT
YP(K)=YP(K)+VK*DT
464CONTINUE
END IF
400 CONTINUE
END DO
!---<STEP 5> Rearrangement particles after the
movement
DO I=IMIN,IMAX
DO J=JMIN,JGL(I)
KPKOSU(I,J)=0
END DO
END DO
!***SUBROUTINE REARRANGEMENT OF
PARTICLES OUT OF
BOUNDARY*****

```

```

CALL
GRID(XP,YP,DX,XX,DY,KGRID,CP,KOSU,XLEFT,XR
IGHT,YLOW,YLOW1,YLOW2, &
KDIM,KPKOSU,KPRYUSI,IMIN,IMAX,JGL,NS1)
!*****
*****
!---<STEP 6> Calculate intermediate grid point
concentration
!***AVERAGE CONCENTRATION AT GRID(I,J)
(ADVECTION) *****
DO I=IMIN,IMAX
DO J=JMIN,JGL(I)
CAVE(I,J)=CMIX(I,J)
END DO
END DO
NEMPTY=0
K2=KOSU
DO I=IMIN,IMAX
DO J=JMIN,JGL(I)
M=KPKOSU(I,J)
MP=M
IF(M.EQ.0)THEN !WHEN THE NUMBER OF
PARITCLES IN THE GRID IS 0
NEMPTY=NEMPTY+1
IF(NEMPTY.GT.IJEMPTY)THEN
WRITE(*,6666) NEMPTY
6666 FORMAT('NEMPTY>IJEMP WHEN
NEMPTY=',I10)
WRITE(81,1081) I,J,NEMPTY
1081 FORMAT(I8,1X,I8,1X,I8)
WRITE(*,*) 'CONTINUE???'
READ(*,*) CODE
STOP
ELSE
END IF
IEMPTY(NEMPTY)=I

```


ELSE
IF((I.GT.IMIN.AND.I.LT.IMAX).AND.J.EQ.JMIN)
THEN

UI0=U(I-1,J)
VI0=V(I-1,J)
UI2=U(I+1,J)
VI2=V(I+1,J)
UJ0=0.0D0
VJ0=0.0D0
UJ2=U(I,J+1)
VJ2=V(I,J+1)
C1I0=CAVE(I-1,J)
C1J0=CAVE(I,J+1)
C1J2=CAVE(I,J+1)
C1I2=CAVE(I+1,J)
C0J0=CAVE(I-1,J+1)
C0J2=CAVE(I-1,J+1)
C2J0=CAVE(I+1,J+1)
C2J2=CAVE(I+1,J+1)

!---(4) RIGHT BOTTOM(I=IMAX AND J=JMIN)

ELSE IF(I.EQ.IMAX.AND.J.EQ.JMIN) **THEN**

UI0=U(I-1,J)
VI0=V(I-1,J)
UI2=0.0D0
VI2=0.0D0
UJ0=0.0D0
VJ0=0.0D0
UJ2=U(I,J+1)
VJ2=V(I,J+1)
C1I0=CAVE(I-1,J)
C1J0=CAVE(I,J+1)
C1J2=CAVE(I,J+1)
C1I2=CAVE(I-1,J)
C0J0=CAVE(I-1,J+1)
C0J2=CAVE(I-1,J+1)
C2J0=(C1J0+C1I2)/2.0D0
C2J2=CAVE(I-1,J+1)

!---(5) RIGHT(I=IMAX AND JMIN~JGL(IMAX))

ELSE
IF(I.EQ.IMAX.AND.(J.GT.JMIN.AND.J.LT.JGL(IMAX
))) **THEN**

UI0=U(I-1,J)
VI0=V(I-1,J)
UI2=0.0D0
VI2=0.0D0
UJ0=U(I,J-1)
VJ0=V(I,J-1)
UJ2=U(I,J+1)
VJ2=V(I,J+1)
C1I0=CAVE(I-1,J)
C1J0=CAVE(I,J-1)
C1J2=CAVE(I,J+1)
C1I2=CAVE(I-1,J)
C0J0=CAVE(I-1,J-1)
C0J2=CAVE(I-1,J+1)
C2J0=CAVE(I-1,J-1)
C2J2=CAVE(I-1,J+1)

!---(6) RIGHT TOP(I=IMAX AND J=JGL(IMAX))

ELSE IF(I.EQ.IMAX.AND.J.EQ.JGL(IMAX))

THEN

UI0=U(I-1,J)
VI0=V(I-1,J)
UI2=0.0D0
VI2=0.0D0
UJ0=U(I,J-1)
VJ0=V(I,J-1)
UJ2=0.0D0
VJ2=0.0D0
C1I0=CAVE(I-1,J)
C1J0=CAVE(I,J-1)
C1J2=CAVE(I,J-1)
C1I2=CAVE(I-1,J)
C0J0=CAVE(I-1,J-1)
C0J2=CAVE(I-1,J-1)
C2J0=CAVE(I-1,J-1)
C2J2=(C1J2+C1I2)/2.0D0

!---(7) TOP(IMIN~IMAX AND J=JGL)

ELSE

IF((I.GT.IMIN.AND.I.LT.IMAX).AND.J.EQ.JGL(I))

THEN

! (A) RIGHT UP

IF(NS1(I,J).EQ.3)**THEN**

UI0=0.0D0

VI0=0.0D0

UI2=U(I+1,J)

VI2=V(I+1,J)

UJ0=U(I,J-1)

VJ0=V(I,J-1)

UJ2=0.0D0

VJ2=0.0D0

C1I0=CAVE(I+1,J)

C1J0=CAVE(I,J-1)

C1J2=CAVE(I,J-1)

C1I2=CAVE(I+1,J)

C0J0=CAVE(I-1,J-1)

COJ2=(C1I0+C1J2)/2.0D0

C2J0=CAVE(I+1,J-1)

C2J2=CAVE(I+1,J-1)

! (B) HORIZON

ELSE IF(NS1(I,J).EQ.1)**THEN**

UI0=U(I-1,J)

VI0=V(I-1,J)

UI2=U(I+1,J)

VI2=V(I+1,J)

UJ0=U(I,J-1)

VJ0=V(I,J-1)

UJ2=0.0D0

VJ2=0.0D0

C1I0=CAVE(I-1,J)

C1J0=CAVE(I,J-1)

C1J2=CAVE(I,J-1)

C1I2=CAVE(I+1,J)

C0J0=CAVE(I-1,J-1)

COJ2=CAVE(I-1,J-1)

C2J0=CAVE(I+1,J-1)

C2J2=CAVE(I+1,J-1)

END IF

!---(8) LEFT TOP(I=IMIN AND J=JGL(IMIN))

ELSE IF(I.EQ.IMIN.AND.J.EQ.JGL(IMIN))

THEN

UI0=0.0D0

VI0=0.0D0

UI2=U(I+1,J)

VI2=V(I+1,J)

UJ0=U(I,J-1)

VJ0=V(I,J-1)

UJ2=0.0D0

VJ2=0.0D0

C1I0=CAVE(I+1,J)

C1J0=CAVE(I,J-1)

C1J2=CAVE(I,J-1)

C1I2=CAVE(I+1,J)

C0J0=CAVE(I+1,J-1)

COJ2=(C1I0+C1J2)/2.0D0

C2J0=CAVE(I+1,J-1)

C2J2=CAVE(I+1,J-1)

!---(9) LEFT(I=IMIN AND JMIN~JGL(IMIN))

ELSE

IF(I.EQ.IMIN.AND.(J.GT.JMIN.AND.J.LT.JGL(IMIN))

) **THEN**

UI0=0.0D0

VI0=0.0D0

UI2=U(I+1,J)

VI2=V(I+1,J)

UJ0=U(I,J-1)

VJ0=V(I,J-1)

UJ2=U(I,J+1)

VJ2=V(I,J+1)

C1I0=CAVE(I+1,J)

C1J0=CAVE(I,J-1)

C1J2=CAVE(I,J+1)

C1I2=CAVE(I+1,J)

```

C0J0=CAVE(I+1,J-1)
C0J2=CAVE(I+1,J+1)
C2J0=CAVE(I+1,J-1)
C2J2=CAVE(I+1,J+1)
!---(10) WITHIN AREA
ELSE
IF(NS1(I,J).EQ.3)THEN
UI0=0.0D0
VI0=0.0D0
UI2=U(I+1,J)
VI2=V(I+1,J)
UJ0=U(I,J-1)
VJ0=V(I,J-1)
UJ2=U(I,J+1)
VJ2=V(I,J+1)
C1I0=CAVE(I+1,J)
C1J0=CAVE(I,J-1)
C1J2=CAVE(I,J+1)
C1I2=CAVE(I+1,J)
C0J0=CAVE(I-1,J-1)
COJ2=CAVE(I,J+1)
C2J0=CAVE(I+1,J-1)
C2J2=CAVE(I,J+1)
ELSE IF(NS1(I,J).EQ.1)THEN
UI0=U(I-1,J)
VI0=V(I-1,J)
UI2=U(I+1,J)
VI2=V(I+1,J)
UJ0=U(I,J-1)
VJ0=V(I,J-1)
UJ2=U(I,J+1)
VJ2=V(I,J+1)
C1I0=CAVE(I-1,J)
C1J0=CAVE(I,J-1)
C1J2=CAVE(I,J+1)
C1I2=CAVE(I+1,J)
C0J0=CAVE(I-1,J-1)
COJ2=CAVE(I-1,J+1)
C2J0=CAVE(I+1,J-1)
C2J2=CAVE(I-1,J+1)
C0J0=CAVE(I+1,J-1)
C2J0=CAVE(I+1,J-1)
END IF
END IF
!---POROSITY----!
!---<1> LEFT
IF(I.EQ.IMIN) THEN
SI0=SITA(I+1,J)
SI2=SITA(I+1,J)
!---<2> RIGHT
ELSE IF(I.EQ.IMAX) THEN
SI0=SITA(I-1,J)
SI2=SITA(I-1,J)
!---<3> NOMAL GRID
ELSE !HORIZON
IF(NS1(I,J).EQ.3)THEN
SI0=SITA(I+1,J)
SI2=SITA(I+1,J)
ELSE IF(NS1(I,J).EQ.1)THEN
SI0=SITA(I-1,J)
SI2=SITA(I+1,J)
END IF
END IF
!---<4> BOTTOM
IF(J.EQ.JMIN) THEN
SJ0=SITA(I,J+1)
SJ2=SITA(I,J+1)
!---<5> 上端
ELSE IF(J.EQ.JGL(I)) THEN
SJ0=SITA(I,J-1)
SJ2=SITA(I,J-1)
ELSE IF(J.GT.JMIN.AND.J.LT.JGL(I)) THEN
SJ0=SITA(I,J-1)
SJ2=SITA(I,J+1)
END IF
!---V(I,J)=SQRT(U**2+V**2)(m/sec) +++++
V01=SQRT(UI0**2+VI0**2)   !=(I-1,J)
V10=SQRT(UJ0**2+VJ0**2)   !=(I,J-1)

```

```

V11=SQRT(U(I,J)**2+V(I,J)**2) !=(I,J)
V12=SQRT(UJ2**2+VJ2**2) !=(I,J+1)
V21=SQRT(UI2**2+VI2**2) !=(I+1,J)
!---DISPERSION COEFFICIENT(m2/sec) +++++
IF(V01.LE.0.0D0) THEN !DXX01 AND
DXY01 (V01=<0.0 OR V01>0.0)
DXX01=DM
DXY01=0.0D0
ELSE
DXX01=(AL*UI0**2+AT*VI0**2)/V01+DM
DXY01=(AL-AT)*UI0*VI0/V01
END IF
IF(V10.LE.0.0D0) THEN !DYY10 AND
DYX10 (V10=<0.0 OR V10>0.0)
DYY10=DM
DYX10=0.0D0
ELSE
DYY10=(AT*UJ0**2+AL*VJ0**2)/V10+DM
DYX10=(AL-AT)*UJ0*VJ0/V10
END IF
IF(V11.LE.0.0D0) THEN !DXX11 AND
DYY11 AND DXY11 AND DYX11 (V11=<0.0 OR
V11>0.0)
DXX11=DM
DYY11=DM
DXY11=0.0D0
DYX11=0.0D0
ELSE
DXX11=(AL*U(I,J)**2+AT*V(I,J)**2)/V11+DM
DYY11=(AT*U(I,J)**2+AL*V(I,J)**2)/V11+DM
DXY11=(AL-AT)*U(I,J)*V(I,J)/V11
DYX11=DXY11
END IF
IF(V12.LE.0.0D0) THEN !DYY12 AND
DYX12 (V12<0.0 OR V12>=0.0)
DYY12=DM
DYX12=0.0D0
ELSE
DYY12=(AT*UJ2**2+AL*VJ2**2)/V12+DM
DYX12=(AL-AT)*UJ2*VJ2/V12
END IF
IF(V21.LE.0.0D0) THEN !DXX21 AND
DXY21 (V21<0.0 OR V21>=0.0)
DXX21=DM
DXY21=0.0D0
ELSE
DXX21=(AL*UI2**2+AT*VI2**2)/V21+DM
DXY21=(AL-AT)*UI2*VI2/V21
END IF
D1=(SI2*DXX21+SITA(I,J)*DXX11)/2.0D0
D2=(SI0*DXX01+SITA(I,J)*DXX11)/2.0D0
D3=(SJ2*DYY12+SITA(I,J)*DYY11)/2.0D0
D4=(SJ0*DYY10+SITA(I,J)*DYY11)/2.0D0
D5=(SI2*DXY21+SITA(I,J)*DXY11)/2.0D0
D6=(SI0*DXY01+SITA(I,J)*DXY11)/2.0D0
D7=(SJ2*DYX12+SITA(I,J)*DYX11)/2.0D0
D8=(SJ0*DYX10+SITA(I,J)*DYX11)/2.0D0
A1=D1*(C1I2-CAVE(I,J))/DX
A2=D2*(CAVE(I,J)-C1I0)/DX
A3=D3*(C1J2-CAVE(I,J))/DY
A4=D4*(CAVE(I,J)-C1J0)/DY
A5=D5*((C1J2+C2J2)/2.0D0-
(C1J0+C2J0)/2.0D0)/(2.0D0*DY) !(C(AVERAGE)-
C(AVERAGE))/2DY
A6=D6*((C1J2+C0J2)/2.0D0-
(C1J0+C0J0)/2.0D0)/(2.0D0*DY)
A7=D7*((C1I2+C2J2)/2.0D0-
(C1I0+C0J2)/2.0D0)/(2.0D0*DX)
A8=D8*((C1I2+C2J0)/2.0D0-
(C1I0+C0J0)/2.0D0)/(2.0D0*DX)
RIGHT=(A1-A2)/DX+(A3-A4)/DY+(A5-
A6)/DX+(A7-A8)/DY
IF(I.EQ.ISMIN)THEN
IF(U(I,J).LT.0.0D0)THEN

```

```

    RIGHT=(A3-A4)/DY
END IF
END IF
!---INCREMENT OF CONCENTRATION
(DISPERSION COMPONENT) -----
--
    DELC(I,J)=DT*RIGHT/SITA(I,J)
!-----
    737CONTINUE
END DO
END DO
!---<STEP 8> Processing empty grid points
!***REARRANGEMENT OF PARTICLE *****
    K2=KOSU
    MM=1
IF(NEMPTY.EQ.0) GO TO 119
    103 CONTINUE
    NN=1
    NNN=4
    IK=IEMPTY(MM)
    JK=JEMPTY(MM)
IF(JK.EQ.1) NN=3
IF(JK.EQ.JGL(IK)) NNN=2
DO LL=NN,NNN
    K2=K2+1
    KMOVE=K2
IF(K2.GE.KDIM) GO TO 999
    KGRID(KMOVE,1)=IK
    KGRID(KMOVE,2)=JK
IF(LL.EQ.1)THEN
    XP(KMOVE)=XX(IK)-DX/4.0D0
    YP(KMOVE)=FLOAT(JK-1)*DY-DY/4.0D0
    CP(KMOVE)=CAVE(IK,JK)
ELSE IF(LL.EQ.2)THEN
    XP(KMOVE)=XX(IK)+DX/4.0D0
    YP(KMOVE)=FLOAT(JK-1)*DY-DY/4.0D0
    CP(KMOVE)=CAVE(IK,JK)
ELSE IF(LL.EQ.3)THEN

```

```

    XP(KMOVE)=XX(IK)-DX/4.0D0
    YP(KMOVE)=FLOAT(JK-1)*DY+DY/4.0D0
    CP(KMOVE)=CAVE(IK,JK)
ELSE IF(LL.EQ.4)THEN
    XP(KMOVE)=XX(IK)+DX/4.0D0
    YP(KMOVE)=FLOAT(JK-1)*DY+DY/4.0D0
    CP(KMOVE)=CAVE(IK,JK)
END IF
END DO
    MM=MM+1
IF(MM.LE.NEMPTY) GO TO 103
    119 CONTINUE
    KOSU=K2
!***CALCULATION OF GRID CONCENTRATION
*****
    DO I=IMIN,IMAX
    DO J=JMIN,JGL(I)
IF(I.EQ.IMAX.AND.U(IMAX,J).LT.0.0D0)THEN !RIG
HT
    CMIX(I,J)=0.0D0
ELSE IF(I.LT.ISMIN.AND.J.EQ.JGL(I))THEN
    IF (V(I,J).LT.0.0D0) THEN
    CMIX(I,J)=100.0D0
END IF
ELSE
IF(I.EQ.ISMIN.AND.J.LT.JGL(ISMIN))THEN
    IF(U(ISMIN,J).LT.0.0D0)THEN
    CMIX(I,J)=CAVE(I,J)+DELC(I,J)
ELSE IF(U(ISMIN,J).GE.0.0D0)THEN
    CMIX(I,J)=100.0D0
END IF
ELSE
    CMIX(I,J)=CAVE(I,J)+DELC(I,J)
END IF
END DO
END DO

```



```

!***SUBROUTINE TO INTERPOLATE PARTICLE
CONCENTRATION*****
CALL
HOKAN(DEL,XP,YP,DX,DY,XX,KGRID,CP,KOSU,K
DIM, &
IMIN,IMAX,JGL,NS1)
!*****
*****
!---<STEP 9> UPDATE OF BOUNDARY
CONCENTRATION
! (Adjust boundary conditions for new concentration)
!***RIGHT*****
I=IMAX
DO J=JMIN,JGL(I)
NUM=KPKOSU(I,J)
IF(NUM.EQ.0)THEN
ELSE
DO KP=1,NUM
KNAME=KPRYUSI(I,J,KP)
IF(XP(KNAME).GE.XRL) THEN
CP(KNAME)=0.0D0
ELSE
END IF
END DO
END IF
END DO
!***LEFT*****
I=IMIN
DO J=JMIN,JGL(I)
NUM=KPKOSU(I,J)
IF(NUM.EQ.0)THEN
ELSE
DO KP=1,NUM
KNAME=KPRYUSI(I,J,KP)
IF(XP(KNAME).LT.XLEFTR) THEN
CP(KNAME)=100.0D0
ELSE
END IF

```

```

END DO
END IF
END DO
DO I=IMIN,IMAX
YTOP=DY*(JGL(I)-1)
NUM=KPKOSU(I,JGL(I)) !KPKOSU(I,J)
IF(NUM.EQ.0)THEN
ELSE
DO KP=1,NUM
KNAME=KPRYUSI(I,JGL(I),KP) !KPRYUSI(I,J,KP)
IF(YP(KNAME).GE.YTOP) THEN
IF(I.LE.ISMIN) THEN
CP(KNAME)=CMIX(I,JGL(I))
ELSE IF(I.GT.ISMIN) THEN
CP(KNAME)=0.0D0
END IF
ELSE
END IF
END DO
END IF
END DO
!---REMOVE PARTICLES AT WELL POSITIONS-----
-----!
IF(ISTEP.NE.1)THEN
CALL
WELLREMOVE(CP,XP,YP,DX,DY,KOSU,XLEFT,XRI
GHT,ISMIN,ISMAX,KDIM,XX,YLOW,KAI,XE1,XE1L
,XE1R,YE1,YE1B,YE1T,IE1,IE1L,IE1R,JE1,JE1B,JE1T
,XE2,XE2L,XE2R,YE2,YE2B,YE2T,IE2,IE2L,IE2R,JE2
,JE2B,JE2T)
END IF
GO TO 888
!===DISPLAY:15=====
=====
999 CONTINUE
IF(KOSU.GE.KDIM-500) THEN
WRITE(* ,998) KOSU,KDIM

```

```

998 FORMAT(12X,' NO. OF PARTICLES :',I6,'
<I,I6,' OK ?')
WRITE(*,*) 'CONTINUE???'
READ(*,*) CODE
END IF
=====
=====
WRITE(*,*) 'CONTINUE???'
READ(*,*) CODE
STOP
888 CONTINUE
!---CONCENTRATION TO DENSITY----!
DO I=IMIN,IMAX
DO J=JMIN,JMAX
IF(J.GT.JGL(I)) THEN
ROU(I,J)=0.0D0
CMIX(I,J)=0.0D0
ELSE
IF(CMIX(I,J).LE.0.10D0)
THEN !CMIX=<0.10 ==> CMIX=0
CMIX(I,J)=0.0D0
ELSE IF(CMIX(I,J).GE.99.9D0)
THEN !CMIX>=99.9 ==> CMIX=100
CMIX(I,J)=100.0D0
END IF
ROU(I,J)=CMIX(I,J)*(ROUS-
ROUF)/100.0D0+ROUF
END IF
END DO
END DO
!---WRITE FOR EVERY STEP-----!
WRITE(*,1000) ISTEP,TIME
1000 FORMAT('ISTEP=',I12,2X,'TIME=',F12.4)
WRITE(80,1080) ISTEP,GOSA,GMAX,IERROR
1080 FORMAT(I8,1X,F10.6,1X,F10.6,1X,I8)
WRITE(70,1070) ISTEP, KOSU
1070 FORMAT(I8,1X,I20)

```

```

!---FORMAT-----!
1444 FORMAT(I8,1X,F10.2)
1040 FORMAT(245F10.4)
1046 FORMAT(245I6,1X)
1047
FORMAT(I8,1X,F12.3,1X,F12.3,1X,F12.3,1X,I12)
1045 FORMAT(245I5)
!---FOR THE RESULT-----!
IF((TIME.GE.60.0D0.AND.TIME.LT.(60.0D0+DT)).OR
.(TIME.GE.120.0D0.AND.TIME.LT.(120.0D0+DT)).OR
.(TIME.GE.180.0D0.AND.TIME.LT.(180.0D0+DT)).OR
.(TIME.GE.240.0D0.AND.TIME.LT.(240.0D0+DT)) &
.OR.(TIME.GE.300.0D0.AND.TIME.LT.(300.0D0+
DT)).OR.(TIME.GE.600.0D0.AND.TIME.LT.(600.0D0+
DT)).OR.(TIME.GE.1200.0D0.AND.TIME.LT.(1200.0D
0+DT)).OR.(TIME.GE.1800.0D0.AND.TIME.LT.(1800.
0D0+DT)) &
.OR.(TIME.GE.2400.0D0.AND.TIME.LT.(2400.0D
0+DT)).OR.(TIME.GE.3000.0D0.AND.TIME.LT.(3000.
0D0+DT)).OR.(TIME.GE.3600.0D0.AND.TIME.LT.(36
00.0D0+DT)).OR.(TIME.GE.4200.0D0.AND.TIME.LT.(
4200.0D0+DT)).OR.(TIME.GE.4800.0D0.AND.TIME.L
T.(4800.0D0+DT)) &
.OR.(TIME.GE.5400.0D0.AND.TIME.LT.(5400.0D
0+DT)).OR.(TIME.GE.6000.0D0.AND.TIME.LT.(6000.
0D0+DT)).OR.(TIME.GE.6600.0D0.AND.TIME.LT.(66
00.0D0+DT)).OR.(TIME.GE.7200.0D0.AND.TIME.LT.(
7200.0D0+DT)).OR.(TIME.GE.7800.0D0.AND.TIME.L
T.(7800.0D0+DT)) &
.OR.(TIME.GE.8400.0D0.AND.TIME.LT.(8400.0D
0+DT)).OR.(TIME.GE.9000.0D0.AND.TIME.LT.(9000.
0D0+DT)).OR.(TIME.GE.9600.0D0.AND.TIME.LT.(96
00.0D0+DT)).OR.(TIME.GE.10200.0D0.AND.TIME.LT.
(10200.0D0+DT)).OR.(TIME.GE.10800.0D0.AND.TIM
E.LT.(10800.0D0+DT)) &

```

```

        .OR.(TIME.GE.11400.0D0.AND.TIME.LT.(11400.0
D0+DT)).OR.(TIME.GE.12000.0D0.AND.TIME.LT.(12
000.0D0+DT)).OR.(TIME.GE.12600.0D0.AND.TIME.L
T.(12600.0D0+DT)).OR.(TIME.GE.13200.0D0.AND.TI
ME.LT.(13200.0D0+DT)).OR.(TIME.GE.13800.0D0.AN
D.TIME.LT.(13800.0D0+DT)) &
        .OR.(TIME.GE.14400.0D0.AND.TIME.LT.(14400.
0D0+DT)).OR.(TIME.GE.15000.0D0.AND.TIME.LT.(1
5000.0D0+DT)))THEN

```

```

        WRITE(50,1444) ISTEP,TIME
        WRITE(51,1444) ISTEP,TIME
        WRITE(52,1444) ISTEP,TIME
        WRITE(53,1444) ISTEP,TIME
        WRITE(54,1444) ISTEP,TIME
        WRITE(55,1444) ISTEP,TIME
        WRITE(50,1040)
        (((CMIX(I,J)),I=IMIN,IMAX),J=JMAX,JMIN,-1)
        WRITE(51,1040)
        (((H(I,J,1)),I=IMIN,IMAX),J=JMAX,JMIN,-1)
        WRITE(52,1040)
        (((U(I,J)),I=IMIN,IMAX),J=JMAX,JMIN,-1)
        WRITE(53,1040)
        (((V(I,J)),I=IMIN,IMAX),J=JMAX,JMIN,-1)
        WRITE(54,1040)
        (((ROU(I,J)),I=IMIN,IMAX),J=JMAX,JMIN,-1)
        WRITE(55,1045)
        (((KPKOSU(I,J)),I=IMIN,IMAX),J=JMAX,JMIN,-1)
        END IF
        !---JUDGE FOR FINAL STEP-----
        -----!
        IF(TIME.LE.FT)THEN
            GO TO 5555 !GO TO START
        ELSE
            END IF
        !---WRITE FOR FINAL STEP-----
        -----!
        WRITE(70,1444) ISTEP,TIME

```

```

        WRITE(71,1444) ISTEP,TIME
        DO K=1,KDIM
            WRITE(66,1072)
            K,XP(K),YP(K),KGRID(K,1),KGRID(K,2)
            1072 FORMAT(I7,1X,F8.3,1X,F8.3,1X,I7,1X,I7)
        END DO
        WRITE(70,1073) KOSU
        1073 FORMAT(I20)
        DO K=1,25
            WRITE(71,1071) K
            1071FORMAT(I5)
            WRITE(71,1074)
            (((KPRYUSI(I,J,K)),I=IMIN,IMAX),J=JMAX,JMIN,-1)
            1074 FORMAT(245I8)
        END DO
        WRITE(60,1040)
        (((CMIX(I,J)),I=IMIN,IMAX),J=JMAX,JMIN,-1)
        WRITE(61,1040)
        (((H(I,J,1)),I=IMIN,IMAX),J=JMAX,JMIN,-1)
        WRITE(62,1040)
        (((U(I,J)),I=IMIN,IMAX),J=JMAX,JMIN,-1)
        WRITE(63,1040)
        (((V(I,J)),I=IMIN,IMAX),J=JMAX,JMIN,-1)
        WRITE(64,1040)
        (((ROU(I,J)),I=IMIN,IMAX),J=JMAX,JMIN,-1)
        WRITE(65,1045)
        (((KPKOSU(I,J)),I=IMIN,IMAX),J=JMAX,JMIN,-1)
        !---WRITE PARAMETER-----
        -----!
        WRITE(99,992) DT
        WRITE(99,993) HF
        WRITE(99,994) SITA0
        WRITE(99,994) TKSAT0
        WRITE(99,994) CA0
        WRITE(99,995) AL
        WRITE(99,995) AT
        WRITE(99,996) EPSI
        WRITE(99,994) OMEGA

```

| | |
|----------------------------------|-------------------------|
| WRITE(99,991) EXNUM | 1998FORMAT(F7.4) |
| WRITE(99,1997) QP1 | 545CONTINUE |
| WRITE(99,1997) QP2 | !===CLOSE ALL |
| WRITE(99,1997) RAB | FILES===== |
| WRITE(99,997) XE1L | =====! |
| WRITE(99,997) XE1R | CLOSE(10) |
| WRITE(99,997) YE1B | CLOSE(11) |
| WRITE(99,997) YE1T | CLOSE(12) |
| WRITE(99,997) XE2L | CLOSE(13) |
| WRITE(99,997) XE2R | CLOSE(14) |
| WRITE(99,997) YE2B | CLOSE(15) |
| WRITE(99,997) YE2T | CLOSE(16) |
| WRITE(99,1998) HWELL1 | CLOSE(17) |
| WRITE(99,1998) HEADQ1 | CLOSE(31) |
| WRITE(99,1998) HWELL2 | CLOSE(32) |
| WRITE(99,1998) HEADQ2 | CLOSE(33) |
| WRITE(99,1997) QP1M | CLOSE(34) |
| WRITE(99,1997) QP2M | CLOSE(50) |
| WRITE(99,996) BW | CLOSE(51) |
| DO I=IE1L,IE1R | CLOSE(52) |
| DO J=JE1B,JE1T | CLOSE(53) |
| WRITE(99,1998) HWOLD(I,J) | CLOSE(54) |
| END DO | CLOSE(55) |
| END DO | CLOSE(60) |
| DO I=IE2L,IE2R | CLOSE(61) |
| DO J=JE2B,JE2T | CLOSE(62) |
| WRITE(99,1998) HWOLD(I,J) | CLOSE(63) |
| END DO | CLOSE(64) |
| END DO | CLOSE(65) |
| 991FORMAT(F6.1) | CLOSE(66) |
| 992FORMAT(F4.2) | CLOSE(70) |
| 993FORMAT(F5.2) | CLOSE(71) |
| 994FORMAT(F5.3) | CLOSE(80) |
| 995FORMAT(F8.6) | CLOSE(81) |
| 996FORMAT(F6.4) | CLOSE(82) |
| 997FORMAT(F5.2) | CLOSE(83) |
| 1098FORMAT(F8.4) | CLOSE(99) |
| 1997FORMAT(F6.4) | |

!---TO WRITE CTOE AND CTOE100-----
-----!

OPEN(UNIT=50,FILE='C:\2014_ozaki\DATA\DATATR
Y\STEP3\OUTPUT3_EX1\TIME_C_RESULT_OUT.DA
T')

!---WRITE CTOE-----
-----!

CALL
RESULTS(DX,DY,XX,YY,IMIN,ISMIN,ISMAX,IMAX,
JMIN,JMAX)

!-----
-----!

CLOSE(50)

CLOSE(93)

CLOSE(94)

CLOSE(95)

CLOSE(96)

!-----
-----!

STOP

END PROGRAM SALTWATER

!===SUBROUTINE=====

!*****

!* SUBROUTINE WATER (CALCULATION OF
SITA) *

!*****

SUBROUTINE

WATER(H,SITA,SITAS,IMIN,IMAX,JGL)

PARAMETER

(ILIMIT=500,JLIMIT=500,KDIM=120000)

IMPLICIT REAL*8(A-H,O-Z)

DIMENSION

H(ILIMIT,JLIMIT,2),SITA(ILIMIT,JLIMIT),SITAS(IL
MIT,JLIMIT)

REAL JGL(ILIMIT)

SR=0.075D0 ! RESIDUAL WATER CONTENT

ALPH=4.91D-02 ! (1/cm)

EM=0.8599D0 ! (-)

EN=7.138D0 ! (-)

JMIN=1

DO I=IMIN,IMAX

DO J=JMIN,JGL(I)

H0=H(I,J,2)

IF(H0.GE.0.0) **THEN**

SITA(I,J)=SITAS(I,J)

ELSE

AH1=1+(ALPH*DABS(H0))**EN

SITA(I,J)=SR+(SITAS(I,J)-SR)/(AH1**EM)

END IF

END DO

END DO

RETURN

END

!*****

!* SUBROUTINE TOSUI (CALCULATION OF
HYDRAULIC CONDUCTIVITY) *

!*****

SUBROUTINE TOSUI(H,T)

IMPLICIT REAL*8(A-H,O-Z)

HT=H !*100.0D0

IF(HT.GE.0.0D0) **THEN**

T=1.0D0 !(-)定数

ELSE

ALPH=4.91D-02 ! 定数(1/cm)

```

EM=0.8599D0 ! 定数(-)
EN=7.138D0 ! 定数(-)
AH=ALPH*DABS(HT)
AH1=1+AH**EN
SE=(1.0/AH1)**EM
T=SE**0.5*(1.0-(1.0-SE**(1.0/EM))**EM)**2.0
END IF
CONTINUE
RETURN
END
!*****
*****
!* SUBROUTINE CAPA (CALCULATION OF
SPECIFIC CAPACITY) *
!*****
*****
SUBROUTINE CAPA(H,CA,S,SS,CA0)
IMPLICIT REAL*8(A-H,O-Z)

SR=0.075D0 !
ALPH=4.91D-02 ! (1/cm)
EM=0.8599D0 ! (-)
EN=7.138D0 ! (-)
IF(H.GE.0.0D0)THEN
CA=CA0 !1.0D-03 ! (1/cm)
ELSE
HC=H
AH=(ALPH*DABS(HC))**EN
AH1=1+AH
C1=ALPH*EM*(SS-SR)/(1-
EM)/AH1*((AH/AH1)**EM)
IF(C1.LT.0.0D0) THEN
C1=0.0D0
END IF
CA=C1
END IF
RETURN
END

```

```

!*****
*****
!* SUBROUTINE INI (INITIAL ARRENGEMENT
OF PARTICLES)
!*****
*****
SUBROUTINE
INI(DX,XX,DY,XP,YP,KOSU,KDIM,IMIN,IMAX,JGL)
PARAMETER (ILIMIT=500,JLIMIT=500)
IMPLICIT REAL*8(A-H,O-Z)
REAL JGL(ILIMIT)
INTEGER KOSUY(KDIM)
DIMENSION XP(KDIM),YP(KDIM)
DIMENSION XX(ILIMIT)

DYP=DY/2.0D0
DYP0=DY/4.0D0
!****INITIAL POSITIONS OF PARTICLES*****
K1=1
DO I=IMIN,IMAX
KOSUY(I)=(JGL(I)-1)*2+1
XP(K1)=XX(I)-DX/4.0D0
YP(K1)=DYP0
K2=K1+KOSUY(I)-1
K1=K1+1
DO K=K1,K2
XP(K)=XP(K-1)
YP(K)=YP(K-1)+DYP
END DO
K1=K2+1
XP(K1)=XX(I)+DX/4.0D0
YP(K1)=YP(K1-KOSUY(I))
K2=K1+KOSUY(I)-1
K1=K1+1
DO K=K1,K2
XP(K)=XP(K-1)
YP(K)=YP(K-1)+DYP
END DO

```

```

      K1=K2+1
END DO
      KOSU=K2
RETURN
END
!*****
*****
!* SUBROUTINE GRID (ARRANGEMENT OF
PARTICLES)
!*****
*****
      SUBROUTINE
      GRID(XP,YP,DX,XX,DY,KGRID,CP,KOSU,XLEFT,XR
      IGH,YLOW,YLOW1,YLOW2, &
      KDIM,KPKOSU,KPRYUSI,IMIN,IMAX,JGL,NS1)
      PARAMETER (ILIMIT=500,JLIMIT=500)
      IMPLICIT REAL*8(A-H,O-Z)
      DIMENSION
      CP(KDIM),XP(KDIM),YP(KDIM),XX(ILIMIT)
      REAL JGL(ILIMIT)
      INTEGER KGRID(KDIM,2)
      INTEGER
      KPKOSU(ILIMIT,JLIMIT),KPRYUSI(ILIMIT,JLIMIT,2
      5),NS1(ILIMIT,JLIMIT)
      INTEGER PK,PMAX,PKMAX

      PMAX=25 ! MAXIMUM PARTICLE NUMBER AT
      ONE GRID
      PKMAX=1 ! PARTICLE NUMBER IN ONE GRID
      DO K=1,KOSU
!****BOUNDARY CONDITION ****
!----STEP1 X-AXIS OF GRID
      IF(XP(K).LT.XX(IMIN)) THEN
          IK=IMIN
          KGRID(K,1)=IK
      ELSE IF(XP(K).GE.XX(IMAX)) THEN
          IK=IMAX

```

```

      KGRID(K,1)=IK
ELSE
      DO I=IMIN,IMAX-1 !DO 1038
          X1=XP(K)-XX(I)
          X2=XP(K)-XX(I+1)
          X3=X1*X2
          X4=DX/2.0D0
IF(X1.GE.0.0D0.AND.X2.LT.0.0D0.AND.X3.LE.0.0D0)
THEN
      IF(X1.GE.X4) THEN
          IK=I+1
      ELSE
          IK=I
      END IF
      END IF
      END DO !1038 CONTINUE
      KGRID(K,1)=IK !
END IF
!----STEP2 REARRANGEMENT OF PARTICLES OUT
OF BOUNDARY
      YTOPU=DY/2.0D0+DY*(JGL(IK)-1) ! TOP
      YTOPU1=DY/2.0D0+DY*(JGL(IMIN)-1)
      YTOPU2=DY/2.0D0+DY*(JGL(IMAX)-1)
!----(1) PARTICLE EXCEEDS THE RIGHT
BOUNDARY==>>MOVE TO LEFT BOUNDARY
      IF(XP(K).GE.XRIGHT) THEN
          YLOW1=YLOW1+DY/2.0D0
      IF(YLOW1.GE.YTOPU1) THEN
          YLOW1=YLOW+DY/4.0D0
      END IF
      YP(K)=YLOW1
      XP(K)=XLEFT+DX/4.0D0
      CP(K)=100.0D0
!----(2) PARTICLE EXCEEDS LEFT
BOUNDARY=>>MOVE TO RIGHT
      ELSE IF(XP(K).LT.XLEFT) THEN
          YLOW2=YLOW2+DY/2.0D0

```

```

IF(YLOW2.GE.YTOPU2) THEN
  YLOW2=YLOW+DY/4.0D0
END IF
  YP(K)=YLOW2
  XP(K)=XRIGHT-DX/4.0D0
  CP(K)=0.0D0
ELSE
END IF
!----(3) PARTICLE EXCEEDS TOP
BOUNDARY=>MOVE TO LEFT
IF(YP(K).GE.YTOPU) THEN
  YLOW1=YLOW1+DY/2.0D0
IF(YLOW1.GE.YTOPU1) THEN
  YLOW1=YLOW+DY/4.0D0
END IF
  YP(K)=YLOW1
  XP(K)=XLEFT+DX/4.0D0
  CP(K)=100.0D0
!----(4) PARTICLE EXCEEDSD BOTTOM=>MOVE
TO LEFT
ELSE IF(YP(K).LT.YLOW) THEN
  YLOW1=YLOW1+DY/2.0D0
IF(YLOW1.GE.YTOPU1) THEN
  YLOW1=YLOW+DY/4.0D0
END IF
  YP(K)=YLOW1
  XP(K)=XLEFT+DX/4.0D0
  CP(K)=100.0D0
ELSE
END IF
!****DECIDE THE GRID *****
!----(1) X-AXIS
IF(XP(K).LT.XX(IMIN)) THEN
  IK=IMIN
  KGRID(K,1)=IK
ELSE IF(XP(K).GE.XX(IMAX)) THEN
  IK=IMAX
  KGRID(K,1)=IK
ELSE
DO I=IMIN,IMAX-1
  X1=XP(K)-XX(I)
  X2=XP(K)-XX(I+1)
  X3=X1*X2
  X4=DX/2.0D0
IF(X1.GE.0.0D0.AND.X2.LT.0.0D0.AND.X3.LE.0.0D0)
THEN
  IF(X1.GE.X4) THEN
    IK=I+1
  ELSE
    IK=I
  END IF
END IF
END DO
  KGRID(K,1)=IK
END IF
!----(2)Y-AXIS
  J0=YP(K)/DY+1.0
  YPOINT=(J0-1)*DY+DY/2.0D0
IF(YP(K).GE.YPOINT) THEN
  JK=J0+1
ELSE
  JK=J0
END IF
  KGRID(K,2)=JK
!****DECIDE NUMBER OF PARTICLE IN A GRID
*****
IF(KPKOSU(IK,JK).GE.PMAX)THEN
ELSE
  KPKOSU(IK,JK)=KPKOSU(IK,JK)+1
  PK=KPKOSU(IK,JK)
IF(PK.GT.PKMAX) THEN
  PKMAX=PK
END IF
  KPRYUSI(IK,JK,PK)=K
END IF

```



```

END DO
RETURN
END
!*****
*****
!* SUBROUTINE HOKAN (INTERPOLATION OF
PARTICLE CONCENTRATION)      *
!*****
*****

SUBROUTINE
HOKAN(C,XP,YP,DX,DY,XX,KGRID,CP,KOSU,KDIM
,IMIN,IMAX,JGL,NS1)

PARAMETER (ILIMIT=500,JLIMIT=500)
IMPLICIT REAL*8(A-H,O-Z)
DIMENSION
C(ILIMIT,ILIMIT),XP(KDIM),YP(KDIM),CP(KDIM)
DIMENSION XX(ILIMIT)
DIMENSION
KGRID(KDIM,2),NS1(ILIMIT,JLIMIT)
REAL JGL(ILIMIT)

XLR=XX(IMIN)
XRL=XX(IMAX)
XLEFT=XX(IMIN)-DX/2.0D0
XRIGHT=XX(IMAX)+DX/2.0D0
YLOW=0.0
DO 10 K=1,KOSU
  IK=KGRID(K,1)
  JK=KGRID(K,2)
  DCP=0.0D0
  YTOP=(JGL(IK)-1)*DY
  YTOPU=(JGL(IK)-1)*DY+DY/2.0
  IF(YP(K).LT.YLOW) GO TO 10
  IF(YP(K).GE.YTOPU) GO TO 10
  IF(XP(K).LT.XLEFT.OR.XP(K).GE.XRIGHT) GO
TO 10
  IF(IK.LE.0.OR.JK.LE.0) THEN

```

```

!====DISPLAY:18=====
=
WRITE(* ,743) IK,JK,K,XP(K),YP(K)
743 FORMAT(3X,'ERROR IN SUB-HOKAN:
',3I6,2F14.2)
!=====
=====

WRITE(* ,*) 'CONTINUE???'
READ(* ,*) CODE
STOP
ELSE
END IF

IF(XP(K).LT.XLR.AND.YP(K).LT.YTOPU) GO
TO 10
IF(XP(K).GE.XRL.AND.YP(K).LT.YTOPU) GO
TO 10
IF((XP(K).GE.XLR.AND.XP(K).LT.XRL).AND.YP(K).
GE.YTOP) THEN
  GO TO 10
END IF
IF (IK.EQ.IMIN) THEN
  IK2=IK+1
  IK0=IK
ELSE IF (IK.EQ.IMAX) THEN
  IK2=IK
  IK0=IK-1
ELSE
IF(NS1(IK,JK).EQ.3)THEN
  IK2=IK+1
  IK0=IK
ELSE IF(NS1(IK,JK).EQ.1)THEN
  IK2=IK+1
  IK0=IK-1
END IF
END IF
XPOINT=XX(IK)

```

```

YPOINT=(JK-1)*DY
DXP=XP(K)-XPOINT
DYP=YP(K)-YPOINT
IF(DXP.LT.0.0D0) THEN
  IF(DYP.LT.0.0D0) THEN
    DCP=C(IK,JK)+(C(IK,JK)-
C(IK0,JK))*DXP/DX+(C(IK,JK)-C(IK,JK-
1))*DYP/DY !NO3
  ELSE
    DCP=C(IK,JK)+(C(IK,JK)-
C(IK0,JK))*DXP/DX+(C(IK,JK+1)-
C(IK,JK))*DYP/DY !NO2
  END IF
ELSE
  IF(DYP.LT.0.0D0) THEN
    DCP=C(IK,JK)+(C(IK2,JK)-
C(IK,JK))*DXP/DX+(C(IK,JK)-C(IK,JK-
1))*DYP/DY !NO4
  ELSE
    DCP=C(IK,JK)+(C(IK2,JK)-
C(IK,JK))*DXP/DX+(C(IK,JK+1)-
C(IK,JK))*DYP/DY !NO1
  END IF
END IF
CP(K)=CP(K)+DCP
IF(CP(K).GE.100.0D0) THEN
  CP(K)=100.0D0
ELSE IF(CP(K).LE.0.0D0) THEN
  CP(K)=0.0D0
END IF
10 CONTINUE
RETURN
END
!*****
*****
!* SUBROUTINE WELLREMOVE (REMOVAL OF
PARTICLE WITHIN THE WELLS) *

```

```

!*****
*****
SUBROUTINE
WELLREMOVE(CP,XP,YP,DX,DY,KOSU,XLEFT,XRI
GHT,ISMIN,ISMAX,KDIM,XX,YLOW,KAI,XE1,XE1L
,XE1R,YE1,YE1B,YE1T,IE1,IE1L,IE1R,JE1,JE1B,JE1T
,XE2,XE2L,XE2R,YE2,YE2B,YE2T,IE2,IE2L,IE2R,JE2
,JE2B,JE2T)
PARAMETER (ILIMIT=500, JLIMIT=500)
IMPLICIT REAL*8(A-H,O-Z)
DIMENSION XX(ILIMIT), YY(JLIMIT)
DIMENSION CP(KDIM), XP(KDIM), YP(KDIM)
!----BOUNDARY AREA
XXL1=XX(IE1L)-DX/2.0
XXL2=XX(IE1R)+DX/2.0
YYL1=(JE1B-1)*DY-DY/2.0
YYL2=(JE1T-1)*DY+DY/2.0
XXT1=XX(IE2L)-DX/2.0
XXT2=XX(IE2R)+DX/2.0
YYT1=(JE2B-1)*DY-DY/2.0
YYT2=(JE2T-1)*DY+DY/2.0
!----WELL POINT (WELL 1)
XLEFTS=XX(ISMIN-1)-DX/2.0
XRIGHTS=XX(ISMAX)-DX/2.0
DO K=1, KDIM
  IF(KAI.EQ.2.OR.KAI.EQ.4)THEN
    !
IF((XP(K).GE.XXL1).AND.(XP(K).LE.XE1L))THEN
!LEFT OF BOUNDARY OF WELL 1
    ! IF(XP(K).GE.XXL1.AND.XP(K).LE.XE1)THEN
    !
IF((YP(K).GT.YYL1).AND.(YP(K).LT.YYL2))THEN
    ! XP(K)=XLEFT+DX/4.0
    ! YP(K)=YP(K)
    ! CP(K)=100.0D0
    ! END IF

```

```

! END IF
!
IF((XP(K).GE.XE1R).AND.(XP(K).LE.XXL2))THEN
!RIGHT OF BOUNDARY OF WELL 1
! !IF(XP(K).GT.XE1.AND.XP(K).LE.XXL2)THEN
!
IF((YP(K).GT.YYL1).AND.(YP(K).LT.YYL2))THEN
! XP(K)=XRIGHT-DX/4.0
! YP(K)=YLOW+DX/4.0
! CP(K)=0.0D0
! END IF
! END IF

IF((XP(K).GE.XE1L).AND.(XP(K).LE.XE1R))THEN

IF((YP(K).GT.YYL1).AND.(YP(K).LT.YYL2))THEN
XP(K)=XRIGHTS-DX/4.0
YP(K)=YLOW+DX/4.0
CP(K)=0.0D0
END IF
END IF
ELSE IF(KA1.EQ.3)THEN
!
IF((XP(K).GE.XXL1).AND.(XP(K).LE.XE1L))THEN
!LEFT OF BOUNDARY OF WELL 1
!
!
IF((YP(K).GT.YYL1).AND.(YP(K).LT.YYL2))THEN
! XP(K)=XLEFT+DX/4.0
! YP(K)=YP(K)
! CP(K)=100.0D0
! END IF
! END IF
!
IF((XP(K).GE.XE1R).AND.(XP(K).LE.XXL2))THEN
!RIGHT OF BOUNDARY OF WELL 1
!
!
IF((YP(K).GT.YYL1).AND.(YP(K).LT.YYL2))THEN
! XP(K)=XRIGHT-DX/4.0

```

```

! YP(K)=YLOW+DX/4.0
! CP(K)=0.0D0
! END IF
! END IF

IF((XP(K).GT.XE1L).AND.(XP(K).LT.XE1R))THEN
!AT WELL1 POSITION

IF((YP(K).GT.YYL1).AND.(YP(K).LT.YYL2))THEN
XP(K)=XRIGHTS-DX/4.0
YP(K)=YP(K)
CP(K)=0.0D0
END IF
END IF
!
IF((XP(K).GE.XXT1).AND.(XP(K).LE.XE2L))THEN
!LEFT OF BOUNDARY OF WELL 2
!
!
IF((YP(K).GT.YYT1).AND.(YP(K).LT.YYT2))THEN
! XP(K)=XLEFT+DX/4.0
! YP(K)=YP(K)
! CP(K)=100.0D0
! END IF
! END IF
!
IF((XP(K).GE.XE2R).AND.(XP(K).LE.XXT2))THEN
!RIGHT OF BOUNDARY OF WELL 2
!
!
IF((YP(K).GT.YYT1).AND.(YP(K).LT.YYT2))THEN
! XP(K)=XRIGHT-DX/4.0
! YP(K)=YLOW+DX/4.0
! CP(K)=0.0D0
! END IF
! END IF

IF((XP(K).GT.XE2L).AND.(XP(K).LT.XE2R))THEN
!AT WELL1 POSITION

```

IF((YP(K).GT.YYT1).AND.(YP(K).LT.YYT2))**THEN**

XP(K)=XLEFTS-DX/4.0

YP(K)=YLOW+DX/4.0

CP(K)=100.0D0

END IF

END IF

END IF

END DO

RETURN

END

!*****

!* SUBROUTINE RESULTS (WRITE RESULTS)

*

!*****

SUBROUTINE

RESULTS(DX,DY,XX,YY,IMIN,ISMIN,ISMAX,IMAX,
JMIN,JMAX)

PARAMETER (ILIMIT=500,JLIMIT=500)

IMPLICIT REAL*8(A-H,O-Z)

DIMENSION

XX(ILIMIT),YY(JLIMIT),XX2(ILIMIT)

DIMENSION

CRESULT(ILIMIT,JLIMIT,50),CTOE(JLIMIT,50),CTO

E100(JLIMIT,50),CTOEI(ILIMIT,50)

INTEGER TIMER(50)

DO I=IMIN,IMAX

IF(I.EQ.IMIN) **THEN**

XX(I)=0.0D0

ELSE

XX(I)=XX(I-1)+DX

END IF

END DO

DO J=JMIN,JMAX

IF(J.EQ.JMIN)**THEN**

YY(J)=0.0D0

ELSE

YY(J)=YY(J-1)+DY

END IF

END DO

!---TIME-----

-----!

DO K=1,35

IF(K.EQ.1)**THEN**

TIMER(K)=1

ELSE IF(K.GE.2.AND.K.LE.5)**THEN**

TIMER(K)=TIMER(K-1)+1

ELSE IF(K.EQ.6)**THEN**

TIMER(K)=10

ELSE IF(K.GE.7)**THEN**

TIMER(K)=TIMER(K-1)+10

END IF

END DO

!---DETERMINE KMAX VALUE-----

-----!

READ(50,*) KFT

IF(KFT.EQ.60.0D0)**THEN**

KMAX=1

ELSE IF(KFT.EQ.120.0D0)**THEN**

KMAX=2

ELSE IF(KFT.EQ.180.0D0)**THEN**

KMAX=3

ELSE IF(KFT.EQ.240.0D0)**THEN**

KMAX=4

ELSE IF(KFT.EQ.300.0D0)**THEN**

KMAX=5

ELSE IF(KFT.EQ.600.0D0)**THEN**

KMAX=6

ELSE IF(KFT.EQ.1200.0D0)**THEN**

KMAX=7

ELSE IF(KFT.EQ.1800.0D0)**THEN**

KMAX=8

```

ELSE IF(KFT.EQ.2400.0D0)THEN
  KMAX=9
ELSE IF(KFT.EQ.3000.0D0)THEN
  KMAX=10
ELSE IF(KFT.EQ.3600.0D0)THEN
  KMAX=11
ELSE IF(KFT.EQ.4200.0D0)THEN
  KMAX=12
ELSE IF(KFT.EQ.4800.0D0)THEN
  KMAX=13
ELSE IF(KFT.EQ.5400.0D0)THEN
  KMAX=14
ELSE IF(KFT.EQ.6000.0D0)THEN
  KMAX=15
ELSE IF(KFT.EQ.6600.0D0)THEN
  KMAX=16
ELSE IF(KFT.EQ.7200.0D0)THEN
  KMAX=17
ELSE IF(KFT.EQ.7800.0D0)THEN
  KMAX=18
ELSE IF(KFT.EQ.8400.0D0)THEN
  KMAX=19
ELSE IF(KFT.EQ.9000.0D0)THEN
  KMAX=20
ELSE IF(KFT.EQ.9600.0D0)THEN
  KMAX=21
ELSE IF(KFT.EQ.10200.0D0)THEN
  KMAX=22
ELSE IF(KFT.EQ.10800.0D0)THEN
  KMAX=23
ELSE IF(KFT.EQ.11400.0D0)THEN
  KMAX=24
ELSE IF(KFT.EQ.12000.0D0)THEN
  KMAX=25
ELSE IF(KFT.EQ.12600.0D0)THEN
  KMAX=26
ELSE IF(KFT.EQ.13200.0D0)THEN
  KMAX=27

```

```

ELSE IF(KFT.EQ.13800.0D0)THEN
  KMAX=28
ELSE IF(KFT.EQ.14400.0D0)THEN
  KMAX=29
ELSE IF(KFT.EQ.15000.0D0)THEN
  KMAX=30
END IF
!---READ-----
-----
-!
DO K=1,KMAX
  READ(50,*) ISTEP,TIME
  DO J=JMAX,,JMIN,-1
    READ(50,*) (CRESULT(I,J,K),I=IMIN,IMAX)
  END DO
END DO
!---COMPARE THE POSITION OF TOE-----
-----
-----!
DO K=1,KMAX
  DO I=IMIN,IMAX
    DO J=JMIN,JMAX
      IF(I.GT.ISMIN.AND.I.LE.ISMAX)THEN
        IF(CRESULT(I,J,K).GT.0.0D0.AND.CRESULT(I+1,J,K)
          ).EQ.0.0D0)THEN
          CTOE(J,K)=XX(I)-11.0D0
        END IF
      IF(J.GE.60)THEN
        CTOE(J,K)=0.0D0
      END IF
    END IF
  END DO
END DO
END DO
!---COMPARE THE POSITION OF
CONCENTRATIONI OF 100 %-----
-----!

```

```

DO K=1,KMAX
  DO I=IMIN,IMAX
    DO J=JMIN,JMAX
      IF(I.GT.ISMIN.AND.I.LE.ISMAX)THEN
        IF(CRESULT(I,J,K).EQ.100.0D0.AND.CRESULT(I+1,J
,K).NE.100.0D0)THEN
          CTOE100(J,K)=XX(I)-11.0D0
        END IF
        IF(J.GE.60)THEN
          CTOE100(J,K)=0.0D0
        END IF
      END IF
    END DO
  END DO
END DO
!--COMPARE VERTICAL
DO K=1,KMAX
  DO I=ISMIN,ISMAX
    DO J=JMIN,JMAX
      IF(CRESULT(I,J,K).GT.0.0D0.AND.CRESULT(I,J+1,K
).EQ.0.0D0.AND.CRESULT(I,J+2,K).EQ.0.0D0)THEN
        CTOEI(I,K)=YY(J)
        GO TO 3433
      ELSE
        CTOEI(I,K)=0.0D0
      END IF
    END DO
  3433 CONTINUE
END DO
END DO
!--WRITE-----
-----
-!
DO K=1,KMAX
  WRITE(95,1195)TIMER(K)
  1195 FORMAT(I6,'min')

```

```

DO J=JMAX,JMIN,-1
  WRITE(95,1095)CTOE(J,K),YY(J)
  1095 FORMAT(F6.2,1X,F6.2)
END DO
WRITE(96,1195)TIMER(K)
DO J=JMAX,JMIN,-1
  WRITE(96,1096)CTOE100(J,K),YY(J)
  1096 FORMAT(F6.2,1X,F6.2)
END DO
WRITE(94,1195)TIMER(K)
DO I=ISMIN,ISMAX
  XX2(I)=XX(I)-11.0
  WRITE(94,1094) XX2(I),CTOEI(I,K)
  1094 FORMAT(F7.2,1X,F7.2)
END DO
WRITE(93,1195)TIMER(K)
DO I=ISMIN,ISMAX,2
  XX2(I)=XX(I)-11.0
  WRITE(93,1094) XX2(I),CTOEI(I,K)
END DO
END DO
RETURN
END

```

```

!-----
-----
-----

```